IDENTIFICATION AND CHARACTERIZATION OF TWO ENDOPLASMIC RETICULUM PROTEIN ISOFORMS ENCODED BY SENESCENCE-ASSOCIATED FAM134B GENE

A THESIS SUBMITTED TO
THE DEPARTMENT OF MOLECULAR BIOLOGY AND GENETICS
AND THE INSTITUTE OF ENGINEERING AND SCIENCE OF
BILKENT UNIVERSITY
IN PARTIAL FULFILLMENT OF THE REQUIREMENTS
FOR THE DEGREE OF
MASTER OF SCIENCE

BY
NİLGÜN TAŞDEMİR
JULY 2008

I certify that I have read this thesis and that in my opinion it is fully adequate, in scope and in quality, as a thesis for the degree of Master of Science.

Prof. Dr. Mehmet Öztürk

I certify that I have read this thesis and that in my opinion it is fully adequate, in scope and in quality, as a thesis for the degree of Master of Science.

Assoc. Prof. Dr. Rengül Atalay

I certify that I have read this thesis and that in my opinion it is fully adequate, in scope and in quality, as a thesis for the degree of Master of Science.

Assoc. Prof. Dr. Çetin Kocaefe

I certify that I have read this thesis and that in my opinion it is fully adequate, in scope and in quality, as a thesis for the degree of Master of Science.

Assist. Prof. Dr. Ali Osmay Güre

Approved for the Institute of Engineering and Science

Director of Institute of Engineering and Science
Prof. Dr. Mehmet Baray

ABSTRACT

IDENTIFICATION AND CHARACTERISATION OF TWO ENDOPLASMIC RETICULUM PROTEIN ISOFORMS ENCODED BY SENESCENCE-ASSOCIATED FAM134B GENE

Nilgün Taşdemir
MSc. in Molecular Biology and Genetics
Supervisor: Prof. Dr. Mehmet Öztürk
July 2008, 112 Pages

Liver cancer is the fifth most common cancer in the world. Until recently, tumor cells were known to have the capacity to proliferate indefinitely. In a previous study, we showed the spontaneous induction of replicative senescence in p53- and p16INK4a-deficient HCC (hepatocellular carcinoma) cells. In a follow-up study, we have analyzed the Affymetrix expression profiling of the senescent and immortal HCC clones that we had established. Among the genes with differential expression pattern, in this study, we have focused on a novel gene, FAM134B (family with sequence similarity 134, member B), which is significantly up-regulated (p-value=1.097E-06) in our senescent clones with respect to their immortal counterparts. FAM134B gene is located on human chromosome 5p15.1 near a LOH region, and its protein product has not yet been characterized. To begin with, we confirmed the up-regulation of FAM134B in our senescent clones as compared to our immortal clones by RT-PCR analysis. As a next step, meta-analysis of HCC microarray data indicated that the expression of FAM134B gene is progressively down-regulated in non-metastatic and metastatic HCC as compared to normal liver. Thus, we decided to characterize the protein product of this gene. Two known forms of transcripts were used to construct FLAG-tagged expression plasmids (encoding two isoforms with predicted molecular weights of 30 and 55 kDa). Immuno-staining experiments performed after transient ectopic expression indicated that both short and long isoforms of FAM134B-encoded protein localize to the endoplasmic reticulum (ER). Both protein isoforms co-localized with calnexin, a well known ER-chaperon. Thus, it appears that senescent cells over-express FAM134B-encoded ER protein isoforms, while cancer cells are deficient in their expression. We have also performed gain-of-function studies by stable ectopic expression of these two protein isoforms in an HCC cell line and addressed the potential role(s) of these isoforms in senescence and ER-stress. Our studies indicated that over-expression of these proteins did not have a ‘causative’ role in induction of senescence and did not affect the rate of cell proliferation. We also did not observe any changes in the responses of cells over-expressing these two protein isoforms to ER-stress induced via tunicamycin treatment. Therefore, FAM134B gene may be performing a yet unidentified function in senescent cells. All in all, we have identified two FAM134B-encoded proteins that localize to the ER, the function and the senescence association of which need further investigation.

ÖZET

HÜCRE YAŞLANMASIYLA İLİNTLİ FAM134B GENİ TARAFINDAN KODLANAN İKİ ENDOPLASMİK RETİKULUM PROTEİN İZOFORMUNUN BELİRLENMESİ VE KARAKTERİZASYONU

Nilgün Taşdemir
Moleküler Biyoloji ve Genetik Yüksek Lisansı
Tez Yöneticisi: Prof. Dr. Mehmet Öztürk
Temmuz 2008, 112 Sayfa

Karaciğer kanseri dünyada beşinci sıklıkla görülen kanser türüdür. Yakın bir zamana kadar, tümör hücrelerinin sonsuz bölünebilme kapasitesine sahip olduğu düşünülmekteydi. Önceki çalışmalarımızın birinde, p53 ve p16INK4a proteinlerinden yoksun olan karaciğer kanseri hücre hatlarında kendiliğinden gelişen hücre yaşlanmasını gösterdik. Bunu takip eden bir çalışmada, elde etmiş olduğumuz senesant ve ölümsüz klonlarin Affymetrix gen ifade profillerini inceledik. Klonlarda ifadesi fark gösteren genler arasından, bu çalışmada, yeni bir gen olan ve senesant klonlarda ölümsüz klonlara göre ifadesi istatistiksel olarak anlamlı artış gösteren (p-değeri=1.097E-06) FAM134B geni üzerinde yoğunlaştık. FAM134B geni beşinci insan kromozomunun p15.1 bölgesi üzerinde yer almaktadır ve kodladığı protein ürünü henüz karakterize edilmemiştir. Başlangıç olarak, revers transkriptaz polimeraz zincir reaksiyonu kullanarak FAM134B geninin senesant klonlarda ölümsüz klonlara göre ifade artışını doğruladık. Bir sonraki adımda, hepatosellüler karsinoma mikro-dizinlerinin meta-analizi, FAM134B geninin ifadesinin normal karaciğer dokusuna göre metastatik olmayan ve metastatik hepatosellüler karsinomada dereceli olarak azaldığını gösterdi. Bu nedenle, bu genin protein ürününü karakterize etmeye karar verdik. Bilinen iki transkript formu kullanılarak (tahmini moleküler ağırlıkları 30 ve 50 kDa olan iki izofomu kodlayan) FLAG-işaretli ifade vektörleri oluşturuldu. Hücrelerde bu vektörlerin geçici ifadesi sonrasında yapılan immüno-boyama deneyleri, hem uzun hem kisa FAM134B protein izoformlarının endoplazmik retikuluma lokalize olduğunu gösterdi. Her iki protein izoformu, iyi bilinen bir endoplozmik retikulum şaperonu olan kalneksin proteini ile ortak lokalizasyon gösterdi. Buradan anlaşıldığı gibi, senesant hücrelerde endoplazmik retikuluma lokalize olan FAM134B protein izoformlarınn ifadesi artarken, kanser hücreleri bu izoformlarin ifadesinden yoksundular. Ayrica, bu iki protein izoformunun bir karaciğer kanseri hücre hattında sürekli ifadesi yoluyla işlev-kazanım deneyleri yaptık. bu protein izoformlarının senesansta ve endoplazmik retikulum stresindeki potansiyel rol veya rollerini sorguladık. Çalışmalarımızın sonuçları, bu protein izoformlarinin hücrelerde yüksek seviyedeki ifadesinin senesans indüklenmesine yol açacak bir rol oynamadığı ve hücrelerin bölünme hızını değiştirmediği yönünde bilgi verdi. Ayrica bu iki izoformu yüksek seviyede ifade eden hücrelerin tunikamisin ile indükenen endoplazmik retikulum stresine karşı yanıtlarında bir değişiklik gözlemlemedik. Dolayısıyla, FAM134B geninin senesansa girmiş olan hücrelerde henüz tanımlayamadığımız bir işlevi söz konusu olabilir. Sonuç

olarak, FAM134B tarafından kodlanan ve endoplazmik retikuluma lokalize olan iki protein izoformu belirledik ve bu izoformların hücre içindeki görevleri ve senesansla olan bağlarının ilerki çalışmalarla ortaya koyulması gerekmektedir.

TO MY FAMILY

ACKNOWLEDGEMENTS

It is a pleasure for me to thank the many people who made this thesis possible.

First and foremost, I would like to thank my thesis advisor Prof. Dr. Mehmet Öztürk for his supervision and guidance throughout this study. I am grateful for his patience, motivation, enthusiasm, and immense knowledge in molecular biology that, taken together, make him a great mentor.

This thesis would simply not have been possible if it weren't for Dr. Hani Alotaibi. He has provided assistance in numerous ways during my experiments, for which I shall always remember him as my 'troubleshooter'. Not to mention that he has been a great friend outside the laboratory.

I would like to thank the entire past and present MBG faculty. I am especially grateful to Assist. Prof. Tamer Yağcı, Assist. Prof. Uygar H. Tazebay and Assoc. Prof. Rengül Çetin-Atalay for providing me with experimental support and inspiration.

I would also like to thank all the past and present members of the MBG lab, especially to Tolga Acun, Kutay Karatepe and Tamer Kahraman. My deepest thanks to all the members of the Molecular Oncology Group, especially to Şerif Şentürk, Ayça Arslan Ergül, Mine Mumcuoğlu, Sevgi Bağışlar, Haluk Yüzügüllü and Pelin Gülay who have always been so much more than just lab colleagues and of course, to Dr. Nuri Öztürk, who is long gone but never forgotten…

I was delighted to interact with Füsun Elvan, Sevim Baran, Abdullah Ünnü, Bilge Kılıçoğlu, Pelin Telkoparan and Burcu Cingöz during my research at Bilkent University. I am indebted to them for their help, be it in or outside the lab.

Lastly but not leastly, my deepest gratitude goes to my family for their unconditional love and support throughout my life; I dedicate this dissertation to them.

This work was supported by the KANILTEK project from State Planning Office (coordinator M. Ozturk), and partially by a grant from TUBITAK (project no: 106S151/SBAG-3399; project leader: M. Ozturk). Additionally, during my MSc research, I was personally supported by TÜBİTAK with scholarship 2210.

TABLE OF CONTENTS

LIST OF TABLES

LIST OF FIGURES

CHAPTER 1. INTRODUCTION

1.1 Hepatocellular Carcinoma

Liver cancer comprises diverse, histologically distinct primary hepatic neoplasms, which include hepatocellular carcinoma (HCC), intrahepatic bile duct carcinoma (cholangiocarcinoma), hepatoblastoma, bile duct cystadenocarcinoma, haemangiosarcoma and epitheliod haemangioendothelioma (Anthony P. *et al*., 2002). Among these, HCC is the most common type of liver cancer, representing 83% of all cases (American Cancer Society, 2005). It is also one of the most lethal cancers, and affects many of the world's populations (Farazi PA. and DePinho RA., 2006).

HCCs are phenotypically (morphology and microscopy) and genetically heterogenous tumors, possibly reflecting in part the heterogeneity of etiologic factors implicated in HCC development, the complexity of hepatocyte functions and the late stage at which HCCs usually become clinically symptomatic and detectable. Malignant transformation of hepatocytes may occur regardless of the etiologic agent through a pathway of increased liver cell turnover, induced by chronic liver injury and regeneration in a context of inflammation, immune response, and oxidative DNA damage. This may result in genetic alterations, such as activation of cellular oncogenes, inactivation of tumor suppressor genes, possibly in cooperation with genomic instability, including DNA mismatch repair defects and impaired chromosomal segregation, over-expression of growth and angiogenic factors, and telomerase activation (Ozturk M. *et al.*, 1999; Bergsland EK. *et al.*, 2001; Thorgeirsson SS. and Grisham JW., 2002; Block TM. *et al.*, 2003; Brechot C. *et al.*, 2004; Satyanarayana A. *et al.*, 2004; Suriawinata A. and Xu R., 2004; Yu MC. and Yuan JM., 2004; Blum Hubert E. *et al.*, 2005).

1.2 Pathogenesis of hepatocellular carcinoma

The neoplastic evolution of HCC proceeds through a multi-step histological process that is less well defined than that of other cancer types (Figure 1.1). Diverse HCC-inducing aetiologies provoke continuous rounds of hepatocyte damage and regeneration, culminating in chronic liver disease. As a next step, hepatocyte proliferative arrest leads to liver cirrhosis. Cirrhosis of the liver is a premalignant state and a major histopathological risk factor for HCC development, since more than 80 percent of HCC in the western world develop in a cirrhotic liver (Edmondson HA., Peters RL., 1983). Abnormal liver nodules of the cirrhotic liver go on to develop into hyperplastic nodules. Hyperplastic nodules of regenerating hepatocytes have normal cytological features, and represent a potential first step towards HCC.

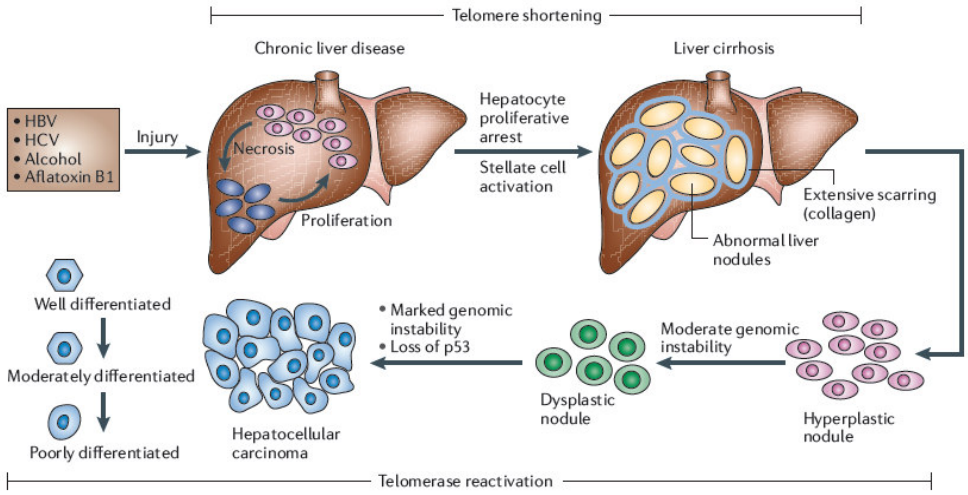

Farazi PA. and DePinho RA., 2006

Figure 1.1: Histopathological progression and molecular features of HCC. After hepatic injury incurred by any one of several factors (HBV, HCV, alcohol and aflatoxin B1), there is necrosis followed by hepatocyte proliferation. Continuous cycles of this destructive–regenerative process foster a chronic liver disease condition that culminates in liver cirrhosis. Subsequently, hyperplastic nodules are observed, followed by dysplastic nodules and ultimately hepatocellular carcinoma (HCC) Telomere shortening, loss and/or mutation of p53 and genomic instability also characterize hepatocarcinogenesis. (Farazi PA. and DePinho RA., 2006).

These lesions can progress to pre-malignant dysplastic nodules, which have abnormal cytological features including clear cell changes and nuclear crowding, and these lesions are associated with the increased thickening of the trabeculae, which indicates abnormal liver architecture (Farazi PA. and DePinho RA., 2006). These dysplastic nodules can evolve to frank HCC which, in addition to all the aforementioned abnormal features, is endowed with the capacity to invade the surrounding fibrous stroma and vessels, and occasionally has metastatic potential (Okuda K. *et al.*, 2000).

1.3 Aetiologies of hepatocellular carcinoma

The most prominent factors associated with HCC include chronic hepatitis B and C viral infection, chronic alcohol consumption, aflatoxin-B1-contaminated food and virtually all cirrhosis-inducing conditions (Badvie S., 2000). In addition, gender can also influence the risk and behaviour of HCC, with males accounting for a larger fraction of cases (Sherman M., 2005). The suspected mechanisms of hepatocarcinogenesis for the various risk factors are summarized in Figure 1.2.

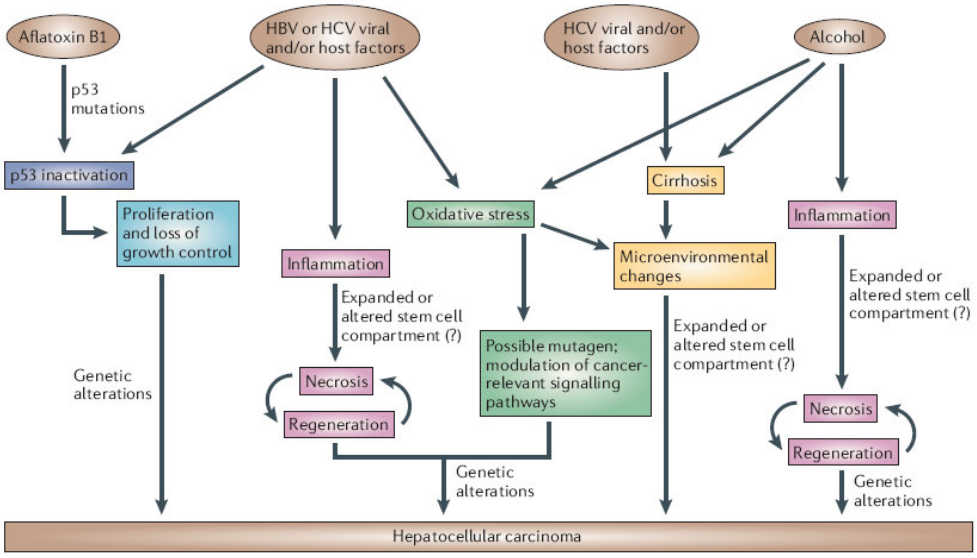

Farazi PA. and DePinho RA., 2006

Figure 1.2: Mechanisms of hepatocarcinogenesis. The suspected mechanisms of hepatocarcinogenesis for the various risk factors are shown. Commonalities are indicated using the same colour. In addition to these mechanisms, hepatitis B virus (HBV) and aflatoxin B1 share the characteristic of affecting the genome — HBV can integrate into the host genome and aflatoxin B1 is a mutagen. HCV, hepatitis C virus (Farazi PA. and DePinho RA., 2006).

1.3.1 Viral-induced hepatocarcinogenesis

There are two main hepatitis viruses associated with the development of HCC: Hepatitis B virus (HBV) and Hepatitis C virus (HCV). Approximately 30–50% of HBV-related deaths are attributable to HCC (Lavanchy D., 2004). HBV-induced hepatocarcinogenesis can involve an array of processes, including host–viral interactions, sustained cycles of necrosis–inflammation–regeneration, viral–endoplasmic-reticulum interactions (induction of oxidative stress), viral integration into the host genome (and associated host DNA deletions) and the targeted activation of oncogenic pathways by various viral proteins (Farazi PA. and DePinho RA., 2006). Hepatitis C virus (HCV) infects approximately 170 million individuals worldwide (Chisari F. V., 2005). Approximately 20% of chronic HCV cases develop liver cirrhosis, and 2.5% develop HCC (Bowen DG. and Walker CM., 2005). HCV-induced hepatocarcinogenesis also provokes similar biological processes to that of HBV, but is associated with a propensity of HCV to evade the host's immune responses and to promote cirrhosis (Farazi PA. and DePinho RA., 2006).

1.3.2 Alcohol-induced hepatocarcinogenesis

Alcohol-induced hepatocarcinogenesis is associated with the induction of inflammation and, consequently, cycles of hepatocyte necrosis and regeneration, oxidative stress and cirrhosis (Farazi PA. and DePinho RA., 2006). Ethanol-induced oxidative stress might have an effect on HCC-relevant signalling pathways (Osna NA. *et al.*, 2005). Oxidative stress might also cause the accumulation of oncogenic mutations, for example, mutations in p53 (Marrogi AJ. *et al.*, 2001).

1.3.3 Aflatoxin-induced hepatocarcinogenesis

Aflatoxin B1 is a toxin with mutagenic properties that is produced as a secondary metabolite by the fungus *Aspergillus flavus*, which can contaminate many food products such as nuts, spices and oilseeds (Farazi PA. and DePinho

RA., 2006). Ingestion of this fungal toxin poses an increased risk for the development of HCC. Aflatoxin B1 seems to function as a mutagen, and is associated with a specific p53 mutation (Bressac B. *et al.*, 1991; Hsu IC. *et al.*, 1991; Ozturk M., 1991; Aguilar F., 1994; Ozturk M., 1999). specifically, Aflatoxin B1 has been shown to target the third base of codon 249 of the p53 gene, which underwent a G to C mutaton in a liver-specific manner (Puisieux A. *et al.*, 1991).

1.3.4 Other aetiological factors associated with HCC

In addition to the most common aetiological factors presented in this review, other factors have been proposed to have a role in hepatocellular carcinoma (HCC) with a lower frequency, including:

• Long-term oral contraceptive use in women, although a definitive connection to the development of HCC will require an expanded study (Thorgeirsson SS. and Grisham JW., 2002).

• Certain metabolic disorders such as: hereditary haemochromatosis, which is associated with increased iron absorption by liver cells and hepatocellular damage (Badvie S., 2000; Limdi JK. and Crampton JR., 2004); porphyria cutanea tarda, which is also characterized by increased iron uptake in the liver, and in some cases is associated with increased inflammation, necrosis and fibrosis (Badvie S., 2000; Sarkany RP., 2001); α1-antitrypsin deficiency, which involves the increased appearance of antitrypsin polymers in hepatocytes, provoking hepatocyte death and cirrhosis (Badvie S., 2000; Parfrey H. *et al.*, 2003); and hereditary tyrosinaemia, which involves defects in tyrosine metabolism that result in toxic metabolites in the liver with potential mutagenic properties (Tanguay RM. *et al.*, 1996; Badvie S., 2000).

• Diabetes: a higher incidence of HCC has been described in diabetic patients with no previous history of liver disease associated with other factors (El-Serag HB. *et al.*, 2004). This predisposition might relate to insulin resistance and associated increased free fatty acids in the liver and the accumulation of

hepatic triglycerides (fatty liver disease). Such intrahepatic accumulation of lipids can lead to hepatocellular injury, hepatocyte apoptosis, cytokine induction, and oxygen radical generation due to fatty acid oxidation, and ultimately the development of fibrosis (Farrell GC. and Larter CZ., 2006).

• Non-alcoholic fatty liver disorders (NAFLD) and non-alcoholic steatohepatitis contribute to the development of fibrosis and cirrhosis, and therefore might also contribute to HCC development (Adams LA. and Angulo P., 2005; Farrell GC. and Larter CZ., 2006).

1.4 Liver and ER stress

The ER provides an optimal environment for the synthesis, folding, and assembly of membrane and secreted proteins. The accumulation of unfolded or misfolded proteins in the ER under conditions of "ER stress" threatens the normal functioning of eukaryotic cells (Kokame K. *et al.*, 2001). Although the physiological conditions inducing ER stress are not fully understood, the cellular response to the stress is essential for homeostasis (Kaufman RJ., 1999). The ER-stress responses are currently categorized to three mechanisms: transcriptional induction, translational attenuation, and degradation (Mori K., 2000). In addition, ER stress activates c-Jun Nterminal kinases (Urano F. *et al.*, 2000) and induces caspase-12-mediated apoptosis (Nakagawa T. *et al.*, 2000). This stress response system, called the unfolded protein response (UPR) or the ER stress response, is thought to be conserved from yeast to mammals (McMillan DR. *et al.*, 1994; Shamu C. *et al.*, 1994).

Hepatocytes contain abundant endoplasmic reticulum (ER) which is essential for protein metabolism and stress signaling. Hepatic viral infections, metabolic disorders, mutations of genes encoding ER-resident proteins, and abuse of alcohol or drugs can induce ER stress. Liver cells cope with ER stress by an adaptive protective response termed unfolded protein response (UPR), which includes enhancing protein folding and degradation in the ER and down-regulating overall protein synthesis. When the UPR adaptation to ER stress is insufficient, the ER stress response unleashes pathological consequences

including hepatic fat accumulation, inflammation and cell death which can lead to liver disease or worsen underlying causes of liver injury, such as viral or diabetes-obesity-related liver disease (Ji C. and Kaplowitz N., 2006).

For experimental induction of ER-stress in mammalian cells, a variety of chemical agent are used, the most common of which are thapsigargin, tunicamycin, brefeldin A. Of these chemical agents, the one with the most direct effect on the ER is tunicamycin. Tunicamycin is a mixture of homologous antibiotics. It is an inhibitor of bacterial and eukaryote N-acetylglucosamine transferases; preventing formation of N-acetylglucosamine lipid intermediates and glycosylation of newly synthesized glycoproteins (Dawson RMC. *et al.*, 1986). It blocks the formation of protein N-glycosidic linkages by inhibiting the transfer of N-acetylglycosamine 1-phosphate to dolichylmonophosphate (Heifetz A. *et al.*, 1979). It has been shown that tunicamycin induced a programmed cell death in plant cells (Crosti P. *et al.*, 2001) and in mammalian cells via stimulation of ER stress (Fujita E. *et al.*, 2002).

1. 5 Liver cirrhosis and senescence

Liver cirrhosis a pathological condition characterized by abnormal liver nodule formation and fibrotic scarring of the liver caused by excessive collagen deposition after chronic liver disease or damage (Farazi PA. and DePinho RA., 2006). Cirrhosis is considered a major clinical and histopathological risk factor for HCC development (Libbrecht L. *et al.*, 2005). Hepatocyte telomere shortening and senescence are general markers of human liver cirrhosis, and correlates with progression of fibrosis in cirrhosis samples (Wiemann SU. *et al.*, 2002).

1.5.1 Cellular senescence

Cellular senescence was initially defined as the loss of proliferative capacity of cells in culture and it results in the inability of the population to increase in cell number, typically after cultures have been passaged 50 or more

times (Sherwood SW. *et al.*, 1988). Cellular senescence, the state of stable cell cycle arrest, can be provoked by a variety of potentially oncogenic stimuli, such as telomere shortening, DNA damage or activation of certain oncogenes (Ben-Porath I. and Weinberg RA., 2004; Campisi J., 2005; Herbig U. and Sedivy JM., 2006). Senescence is associated with a number of gross cellular changes including cell-cycle arrest (Collado M. *et al.*, 2005; Herbig U. and Sedivy JM., 2006), increase in cell size and size heterogeneity , and increase in the frequency of cells with chromosomal aberrations, including polyploidy (Sherwood SW. *et al.*, 1988). Senescent cells display SABG (Senescent Associated B-galactosidase) activity at pH 6.0 and this activity can be used as a marker for identifying senescent cells. Cellular senescence appears to be acting as a barrier to cancer, preventing damaged cells from undergoing aberrant proliferation (Braig M. *et al*., 2005; Campisi J., 2005; Chen Z. *et al.*, 2005; Collado M. *et al.*, 2005; Michaloglou C. *et al*., 2005; Narita M., Lowe SW., 2005; Sharpless NE. and DePinho RA., 2005). Two well established tumor suppressor proteins, pRb and p53, have been shown to play key roles in cellular senescence (Ben-Porath I. and Weinberg RA., 2004; Campisi J., 2005; Herbig U. and Sedivy JM., 2006).

1.5.2 Replicative senescence and telomere shortening

Telomeres progressively shorten with age in somatic cells in culture and in vivo because DNA replication results in the loss of sequences at the 5' ends of double-stranded DNA. Whereas somatic cells do not express the enzyme, telomerase, which adds repeated telomere sequences to chromosome ends, telomerase activity is detected in immortalized and tumour cells in vitro and in primary tumour tissues. This represents an important difference between normal cells and cancer cells, suggesting that telomere shortening causes cellular senescence (Oshimure M. and Barrett JC., 1997). There is accumulating evidence that when only a few telomeres are short, they form end-associations, leading to a DNA damage signal resulting in replicative senescence (Shay JW. and Wright Woodring E., 2004). This DNA damage signal leads to the activation of cell cycle checkpoint pathways involving p53, p16INK4a, and/or retinoblastoma (pRb) proteins (Campisi J., 2005; Dimri GP., 2005). It is known

that cells acquire replicative immortality by inactivation of p53 and p16INK4a genes (Shay JW. and Bacchetti S., 1997) and reactivation of hTERT gene expression (Sherr CJ. and McCormick F.; 2002), as depicted in Figure 1.3.

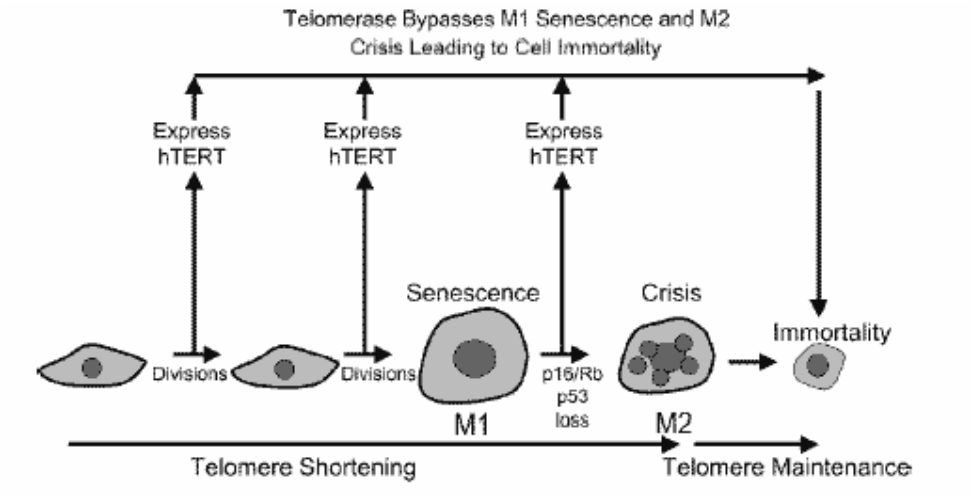

Shay JW. and Wright WE., 2005

Figure 1.3: Senescence and immortalization: role of telomeres and telomerase. The ectopic expression of the catalytic subunit of hTERT results in immortalization of human cells. Telomeres are thus important in both senescence (M1) and crisis (M2) as hTERT introduction either before M1 or after M1 results in cell immortalization. (Shay JW. and Wright WE., 2005)

1.6 Reprogramming of immortal cell lines for replicative senescence

Until recently, it was not known whether the immortality feature exhibited by cancer cells was a reversible or an irreversible feature. Ozturk N. *et al.* (2005), however, showed that cancer cells with replicative immortality can be reprogrammed for replicative senescence.

1.6.1 Induction of Spontaneous Replicative Senescence in HCC-derived stable cell lines

In their work, Ozturk N. *et al.* (2005) expanded different Huh7-derived clones in long-term culture and examined their potential to undergo replicative senescence. Through this method, the researchers established two sets of clones:

C1/C3-Early/C3-Late and G11/G12-Early/G12-Late clones. The C3 clone performed only 80 PD (Population doublings) and was fully SABG positive, whereas C1 clone replicated over 150 PD. Early passage C3 (PD 57) cells, like the C1 clone, displayed normal morphology with heterogeneous SABG staining. Growth-arrested C3 cells displayed very low BrdU staining, in contrast to early passage C3 and late passage C1 cells. Similar results were obtained with G11/G12 clones. This work showed that replicative immortality, after all, was not an irreversible phenomenon and that cancer cells could spontaneously generate senescent progeny.

1.6.2 Mechanism of Spontaneous Replicative Senescence in HCC-derived stable cell lines

The immortal C1 clone in the work of Ozturk N. *et al.* (2005) displayed hTERT activity and thus maintained its telomere length, whereas the senescent C3 clone displayed no detectable hTERT activity and thus had prominently shortened telomeres. Going through the known regulators of hTERT expression, the researchers found a perfect reverse correlation between the expression of hTERT and that of *SIP1* gene (Zinc finger homeobox 1B; *ZFHX1B*). SIP1 encodes a transcriptional repressor protein that interacts with SMAD proteins of the TGF-B signaling pathway and CtBP co-repressor (Verschueren K. *et al.*, 1999; Postigo A.A., 2003). The involvement of SIP1 protein as a key regulator in this senescence mechanism was further verified by the demonstration of bypass of senescence arrest after functional inactivation of SIP expression by shRNA in senescence-programmed C3 clonal cells.

1.7 Gene Expression Changes Between Senescent and Immortal Huh7 clones

1.7.1 Gene Expression Profiling of Senescent and Immortal Huh7 clones

In attempt to better understand the differences between the immortal and the senescent Huh7 clones, Ozturk M. *et al.* took a follow-up approach on the

work of Ozturk N. *et al.* (2005). Affymetix gene expression profiling was performed on the C1 Immortal/C3 Early Senescent/C3 Late Senescent clones and G11 Immortal /G12 Early Senescent/G12 Late Senescent clones and the results of this profiling are yet not published. Briefly, 3 copies of each clone were grown in a 175cm^2 flask and RNA was extracted separately from each clone. In this way, no RNA pooling was done and the data could be processed as triplicate. For RNA isolation, Promega SV RNA Isolation Kit was employed. The samples were treated extensively with DNAse and the obtained RNA samples were subjected to quality-assessment using Agilent 2100 bioanalyzer and Agilent RNA 6000 Nano LabChip® kit. RNA integrity was found to be around 100%, reflecting almost no RNA degradation. cDNA and eventually cRNA was synthesized from the RNA samples using the One Cycle cDNA Synthesis Kit from Affymetrix. 5 ug of cRNA from each clone was hybridized for 16 hours to Affymetrix HGU133Plus2 Chips (18 chips in total) and the signals were detected according to the manufacturer's protocol.

1.7.2 Analysis of Genes Differentially Expressed Between Senescent and Immortal Clones

After the signals received from the chips were detected, they were automatically saved as .CEL files by the Affymetrix Scanner. These .CEL files were accessed and processed using 'R' software. This tool allowed the intensities of the signals received from the chips to be converted into numeric expression values of genes. Background correction was performed on this expression data using 'Bioconductor Packages' in 'R' software and normalization was performed through 'RMA' method . The data was then subjected to T-test analysis (two-tailed, unpaired, unequal variance) where the p-value limit was set to 0.05 ($p<0.05$). Hierarchical clustering of genes was done with GenePattern-software. Finally significant gene lists were obtained that contained the names of genes differentially expressed between the early senescent, late senescent and immortal clones at a statistically significant level. The HGU133Plus2 chip used in this microarray study contains 54675 probes corresponding to a total of 47000 transcripts and variants that represent

approximately 39000 human genes. In the generation of the significant gene lists, the early senescent clones were named as 'Revertant' and the late senescent clones were named as 'Senescent'. The final Senescent*vs.*Immortal significant gene list contained 3073 genes represented by 3872 probes, the Revertant*vs.* Immortal significant gene list contained 2149 genes represented by 2552 probes and the Senescent*vs.*Revertant significant gene list contained 2023 genes represented by 2388 probes . In total, there were 8812 probes corresponding to 7245 genes with significantly differential expression (Ozturk M. *et al.*, unpublished data).

1.7.3 Identification of FAM134B as a Senescence-Associated Gene

The Immortal vs. Senescent, Immortal vs. Pre-Senescent and Senescent vs. Pre-Senescent significant gene lists were analyzed for genes that were the most significantly differentially expressed by looking at the p-value calculated for each probe. Some of these genes were already well-known and extensively studied, while others were genes the protein products of which were previously uncharacterized. Of this latter group, the focus of this study is directed towards a gene named FAM134B. FAM134B gene was represented by two probes in the gene expression profiling study. According to the probe number 218532_s_at, this gene was up-regulated in the senescent clones with respect to the immortal clones with a fold change of 6.5 and up-regulated in the senescent clones with respect to the revertant clones with a fold change of 2.6. According to the probe number 218510_x_at, this gene was up-regulated in the senescent clones with respect to the immortal clones with a fold change of 4.9 and up-regulated in the senescent clones with respect to the revertant clones with a fold change of 2.8. Apparently, FL20152 gene was progressively up-regulated as cells reverted from immortality to senescence and was one of the genes that differed the most significantly between the three sample types with a p-value of 1.097E-06. Being supposedly a senescence-associated gene which hadn't previously been studied in depth, we chose to focus on the characterization of the protein product of this gene in this study.

CHAPTER 2. OBJECTIVES AND RATIONALE

Hepatocellular carcinoma is among the most lethal and prevalent cancers in the human population. Despite its significance, there is only an elemental understanding of the molecular, cellular and environmental mechanisms that drive disease pathogenesis, and there are only limited therapeutic options, many with negligible clinical benefit (Farazi PA. and DePinho RA., 2006). Therefore, it is of ultimate importance to come up with new approaches that could open up the way to novel therapeutic applications. One finding of the work of Ozturk N. *et al.* (2005) on the reprogramming of immortal cancer cells into replicatively senescent progeny is crucial in this respect. In their study, Ozturk *et al.* (2005) injected cells from the immortal C1 clone into one side of a nude mouse and cells from the senescent C3 clone into the other side. As expected, it was observed that the C1 cells formed readily observable tumors at the site of injection. Interestingly, however, the C3 cells failed to form any such tumors, indicating that somewhere along the path to replicative senescence program they had lost their tumorigenic potential. This observation brought along the question of whether it would be possible to design therapies that could revert the immortal cancer cells residing in tumors into replicatively arrested senescent cells and stop, or at least slow down, liver tumor progression.

In order to be able to design such smart therapies, one needs to thoroughly understand the differences underlying between the immortal and the senescent Huh7 clones. In an attempt to assess this difference at the level of transcript repertoire, gene expression profiling was performed on immortal and senescent clones and a set of genes were identified which are differentially expressed between them. Of this significant gene list, in this study we decided to focus on a novel gene named FAM134B which is significantly up-regulated in the senescent clone with respect to its immortal counterpart. The high fold change of this gene suggested that it could be important for the onset of the senescent phenotype. This gene was further queried in several HCC arrays (which will be further discussed in detail in the 'Results' chapter) and it was observed that whereas it is a constituent of normal liver, its expression is

significantly lost in liver tumors, suggesting a possible 'tumor-suppression' function. Thus we hypothesized that this gene could be encoding a senescence-inducing protein product and that, if such was the case, the expression of this gene could be manipulated in immortal cells as to drive them into senescence. Being a novel gene with an uncharacterized gene product, cloning, localization and functional studies were directed towards FAM134B, the results of which will be presented in the next section.

CHAPTER 3. MATERIALS AND METHODS

3.1 MATERIALS

3.1.1 Reagents

All laboratory chemicals were analytical grade from Sigma-Aldrich (St. Louis, MO, U.S.A), Farmitalia Carlo Erba (Milano, Italy) and Merck (Schucdarf, Germany) with the following exceptions: Ethanol and methanol were from Riedel-de Haën (Germany). Nucleospin Plasmid mini-prep kit (for small scale DNA isolation) was from Macherey-Nagel (Duren, Germany). Qiagen Plasmid Maxi-prep kit (for large-scale DNA isolation) and QiaQuick Gel Extraction Kit (for recovery and extraction of DNA from agarose gel) were from Qiagen (Chatsworth, CA, U.S.A). PureYield Plasmid Midi-prep System kit was from Promega (Madison, WI, USA). Agar, tryptone and yeast extract were obtained from Gibco (Carlsbad, CA,USA), BRL Life Technology Inc. (Gaithersburgs, MD, U.S.A). Bradford Ready-made Reagent was purchased from Sigma-Aldrich (St.Louis, MO,USA). X-gal and IPTG were purchased from MBI Fermentas GmbH (Germany).

3.1.2 Bacterial Strains

The bacterial strain used in this work was: *E. coli*: DH5α

3.1.3 Enzymes

Restriction endonucleases used for gene cloning were purchased from MBI Fermentas GmbH (Germany). T4 DNA ligase was purchased from Promega (Madison, WI, USA).

3.1.4 PCR and cDNA synthesis reagents

For cDNA synthesis, RevertAid First Strand cDNA synthesis kit was used (MBI Fermantas, Germany). The reagents used in Polymerase Chain Reaction (PCR): Taq DNA Polymerase, 2 mM dNTP, 25 mM $MgCl_2$, 10X Taq DNA Polymerase Buffer were purchased from MBI Fermentas GmbH (Germany).

3.1.5 Nucleic acids

DNA molecular weight standard and ultrapure deoxyribonucleotides were purchased from MBI Fermentas GmbH (Germany). pCMV10-3XFLAG and pCMV14-3XFLAG plasmids were purchased from Sigma-Aldrich (St. Louis, MO, U.S.A). pGEMT-Easy plasmid was purchased from Promega (Madison, WI, USA). pEGFPN1 plasmid was purchased from Clontech.

3.1.6 Oligonucleotides

The primers used in polymerase chain reactions (PCR) for cloning of FAM134B isoforms and the oligonucleotides used in the reverse-transcription polymerase chain reactions (RT-PCR) of FAM134B in human cell lines and in a mouse tissue cDNA panel were purchased from Metabion International AG (Martiensried, Germany). The sequencing-primers used for sequence-verification of engineered constructs and the oligonucleotides used in reverse-transcription polymerase chain reactions (RT-PCR) of human and mouse GAPDH (*glyceraldehyde-3-phosphate dehydrogenase)* were synthesized by İONTEK (Istanbul, Turkey). The sequencing primers CMV24, CMV30 were purchased from Sigma-Aldrich (St.Louis, MO, USA) and T7 and SP6 primers were purchased from Promega (Madison, WI, USA). The sequences of the primers are given in Table 3.1.

Primer ID	Sequence (5' → 3')
FAM134B_1F (Fwd)	C CTCGAGAAGCTTATGGCGAGCCCGGCGCCTCC
FAM134B_2F (Fwd)	CTCGAGAAGCTTATGCCTGAAGGTGAAGACTT
FAM134B_NTR (Rev)	GAATTCGGATCC*TTA*ATGGCCTCCCAGCAGAT
FAM134B_CTR (Rev)	GAATTCGGATCCATGGCCTCCCAGCAGATTTG
FAM134B_FWD1 (Fwd)	GCTGTTCTGGTTCCTTGCAT
FAM134B_FWD2 (Fwd)	TCTCCTGGTCTGTAGTGTGT
FAM134B_FWD3 (Fwd)	TCTCAGAGGTATCCTGGACT
FAM134B_FWD4(Fwd)	CTTCCTCTGAACAGTGACCA
FAM134B_REV1 (Rev)	ACCAGCTGCTGATTGCGTCT
FAM134B_REV2 (Rev)	CCGTGAGGCTAATCTTAGGA
FAM134B_REV3 (Rev)	CACTACAGACCAGGAGACAA
FAM134B_REV4 (Rev)	CCATGGAGTCAATGCAAGGA
CMV30 (Fwd)	AATGTCGTAATAACCCCGCCCCGTTGACGC
CMV24 (Rev)	TATTAGGACAAGGCTGGTGGGCAC
T7 (Fwd)	TAATACGACTCACTATAGGG
SP6 (Rev)	ATTTAGGTGACACTATAG

Table 3.1: The sequences of primers used for cloning and sequencing. Underlined sequences represent restriction enzymes sites, italic sequences represent stop codons. Fwd: Forward Rev: Reverse

3.1.7 Electrophoresis, photography and spectrophotometer

Electrophoresis grade agarose was obtained from Sigma Biosciences Chemical Company Ltd. (St. Louis, MO, USA). Horizontal electrophoresis apparatuses were from E-C Apparatus Corporation (Florida, USA). The power supply Power-PAC300 and Power-PAC200 was from Bio Rad Laboratories (CA, USA). The Molecular Analyst software used in agarose gel profile visualizing was from Vilber Lourmat (France). Beckman Spectrophotometer Du640 was purchased from Beckman Instruments Inc. (CA. USA) and Nanodrop ND-1000 Full-spectrum UV/Vis Spectrophotometer was purchased from Thermo Fisher Scientific (Wilmington, DE, USA).

3.1.8 Tissue culture reagents and cell lines

Dulbecco's modified Eagle's medium (DMEM) and trypsin were obtained from BIOCHROM (Berlin, Germany) and HyClone (South Logan, UT, USA), fetal calf serum was obtained from BIOCHROM AG (Berlin, Germany). Penicillin/Streptomycin mixture was from Biological Industries (Haemel, Israel). Tissue culture flasks, petri dishes, 15 ml polycarbonate centrifuge tubes with lids and cryotubes were purchased from Costar Corp. (Cambridge, England). Geneticin-G418 sulfate was purchased from GibcoBRL (Carlsbad, CA, USA), Life tech (USA). Tunicamycin was purchased from Sigma-Aldrich (St.Louis, MO,USA).

3.1.9 Antibodies and chemiluminescence

FLAG M2 Mouse Monoclonal Antibody used at a dilution of 1:1000 in western-blotting (immuno-blotting) and 1:200/1:1500 in immuno-fluorescence was obtained from Sigma-Aldrich (St. Louis, MO, U.S.A). Calnexin Rabbit Polyclonal Antibody used at a dilution of 1:200 in immuno-fluorescence was obtained from Sigma-Aldrich (St. Louis, MO, U.S.A). BrdU Mouse Monoclonal Antibody, used at a dilution of 1:500 in BrdU incorporation assay, was purchased from DAKO (Glostrup, Denmark). ECL Western Blotting detection

kit was purchased from Amersham Pharmacia Biotech Ltd. (Buckinghamshire, UK). Anti-mouse TRITC secondary antibody was purchased from Sigma-Aldrich (St.Louis, MO,USA). AlexaFluor Red 568 anti-mouse and AlexaFluor Green 488 anti-rabbit secondary antibodies were purchased from Invitrogen, Carlsbad, CA, USA) .

3.1.10 Immuno-peroxidase Staining

The DAKO EnVision™+ System used in peroxidase staining was purchased from DAKO (Glostrup, Denmark).

3.2 SOLUTIONS AND MEDIA

3.2.1 General solutions

50X Tris-acetic acid-EDTA (TAE):	2 M Tris-acetate, 50 mM EDTA pH 8.5. Diluted to 1X for working solution.
Ethidium bromide:	10 mg/ml in water (stock solution), 30 ng/ml (working solution)
6X Gel loading dye solution:	10mM Tris-HCl (pH 7.6), 0.03% bromophenol blue, 0.03% xylene cyanol**,** 60% glycerol, 60mM EDTA (0.5M pH8.0)

3.2.2 Microbiological media, reagents and antibiotics

Luria-Bertani medium (LB)	*Per liter:* 10 g bacto-tryptone, 5 g bacto- yeast extract, 10 g NaCl. For LB agar plates, add 15 g/L bacto agar.
Glycerol stock solution	A final concentration of 25% glycerol in LB was added to bacterial culture
Ampicillin	100 mg/ml solution in double-distilled water, sterilized by filtration and stored at -20°C (stock solution).100 µg/ml (working solution)
Kanamycin	300 mg/ml solution in double-distilled water sterilized by filtration and stored at -20°C (stock solution). Working solution was 30 µg/ml.
0.1 M IPTG	1.41 g IPTG in 50 ml double-distilled water, sterilized by filtration and stored at-20^{o}C.

Luria-Bertani medium (LB)	*Per liter:* 10 g bacto-tryptone, 5 g bactoyeast extract, 10 g NaCl. For LB agar plates, 15 g/L bacto agar was added.
SOB medium:	*Per liter:* 20 g tryptone (2%), 5 g yeast extract (0.5%), 0.584 gr NaCl (10 mM), 0.1864 g KCl (2.5 mM) autoclaved to sterilize. Then, 2.46 g MgSO4 and 2.03 g $MgCl_2$ (10 mM) are added.
SOC medium:	SOB + 20 mM glucose from filter sterilized 1M glucose stock solution in ddH2O.
Transformation Buffer (TB):	10 mM K.PIPES, 55 mM $MnCl_2$, 15 mM $CaCl_2$, 250 mM KCl. Filter sterilized and stored at 4^oC.

3.2.3 Tissue culture solutions

DMEM/RPMI working medium	10% FBS, 1% penicillin / streptomycin, 1% non-essential amino acid were added and stored at 4^oC.
10X Phosphate-buffered saline (PBS)	*Per liter:* 80 g NaCl, 2 g KCl,

	14.4 g Na_2HPO_4, 2.4 g KH_2PO_4, pH 7.4

Antibiotics

Geneticin-G418 Sulfate)	500 mg/ml solution in double-distilled water. Sterilized by filtration and stored at -20°C (stock solution). 500 µg/ml (working solution for stable cell line selection and maintenance)
Tunicamycin	5mg/ml solution in DMSO. Sterilized by filtration and stored -20°C (stock solution).

3.2.4 SDS (Sodium Deodecyl Sulfate)-PAGE (Polyacrylamide Gel Electrophoresis)

solutions

30% Acrylamide mix (1:29)	*Per 100 ml*: 29 g acrylamide, 1 g bisacrylamide in double-distilled water, filtered, degassed, and stored at 4°C (stock solution).
5X SDS gel-loading buffer	3.8 ml double-distilled water, 1 ml of 0.5 M Tris-HCl, 0.8 ml glycerol, 1.6 ml of 10% SDS, o.4 ml of 0.05% bromophenol-blue. Before use, β-mercaptoethanol was freshly added to a final

	concentration of 5% to reach 1% when mixed with protein samples.
10X Towbin SDS-electrophoresis buffer	*Per liter:* 30.3 g Tris base, 144.0 g Glycine, 10.0 g SDS. Diluted to 1X for working solution. Stored up to 1 month at 4°C.
10% Ammonium persulfate (APS)	0.1 g/ml solution in double distilled water (Prepared freshly).
1.5 M Tris-HCl, pH 8.8	54.45 g Tris base (18.15 g/100 ml) ~150 ml distilled water. Adjust to pH 8.8 with 1 N HCl. Completed to 300 ml with distilled water and stored at 4° C.
1 M Tris-HCl, pH 6.8	12.14 g Tris base ~ 60 ml distilled water. Adjust to pH 6.8 with 1 N HCl. Completed to 100 ml with distilled water and store at 4° C.
Coomassie brilliant blue solution	*Per Liter:* 100mg Coomassie brilliant blue G-250, 50ml 95% ethanol, 100ml 85%

	phosphoric acid. Filtered through whatman paper and stored at 4°C.

3.2.5 Immuno-blotting solutions

Semi-dry transfer buffer	*Per liter*: 48 mM Tris-base, 39 mM glycine, 0.037% SDS, 20% methanol.
10X Tris-buffer saline (TBS)	*Per liter:* 100 mM Tris-base, 1.5 M NaCl, pH 7.6 in double distilled water.
TBS-Tween (TBS-T)	0.5% Tween-20 solution in TBS. (Prepared freshly)
Blocking solution	5% (w/v) non-fat milk, 0.5% Tween-20 in TBS. (Prepared freshly).

3.2.6 Immuno-fluorescence and immuno-peroxidase solutions

H33258 fluorochrome dye	1 mg/ml solution in double-distilled water and stored at -20 °C. Working solution:1µg/ml

DAPI (4', 6-diamidino-2-phenylindole)	0.1-1 μg/ml (working solution in PBS).
Blocking solution	5% BSA (bovine serum albumin) in 1X PBS

3.2.7 BrdU incorporation assay solutions

BrdU stock solution	10 mg/ml BrdU in ddH2O
2N HCl	8.62 ml of 37% HCl, 16.36 ml dH2O
PBS-TritonX-100 (PBS-T)	0.1 TritonX-100 in PBS.

3.2.8 SABG assay solutions

SABG buffer	40mM citric acid/sodium phosphate buffer (pH 6.0), 5mM potassium ferrocyanide, 5mM potassium ferricyanide, 150mM NaCl, 2mM $MgCl_2$, 1mg/ml X-gal

3.3 METHODS

3.3.1 General Methods

3.3.1.1 Transformation of *E .coli*

Transformation of plasmid DNA into *E. coli* was achieved by using calcium chloride method. Competent *E. Coli* was prepared by two different methods as described below.

3.3.1.2 Preparation of competent cells: Conventional "calcium chloride" method

5 ml LB was inoculated with a single colony from a freshly grown plate of *E. coli* strain (*DH5*α) and incubated for approximately 2.5 hours at 37^{o}C, shaking at 200 rpm to an optical density 0.6 at 590 nm (OD 590). Then, 1.5 ml of growing cells was centrifuged at 13,000 rpm for 1 minute in a bench-top centrifuge. Excess LB was removed away. The cells were resuspended in 0.5 ml of 50 mM $CaCl_2$ by gently vortexing, before being placed on ice for 30 minutes. The cells were harvested by centrifugation for 1 minute at 13,000 rpm and the supernatant was discarded. The pellet was resuspended in 0.1 ml of 50 mM $CaCl_2$ by gently vortexing. At this stage, bacterial cells were competent, and transformed as described in 3.3.1.3.1.

3.3.1.3 Conventional "calcium chloride" transformation

This method was used for transformation of plasmids.20 ng plasmid was added to competent cells in 0.1 ml of 50 mM $CaCl_2$ and incubated on ice for 30 minutes. Then, cells were incubated for 60-90 seconds at 42^{o}C (heat-shock), and placed on ice for 2 minutes. 800 µl of pre-warmed LB was added onto cells.

Cells were cultured for 1 hour at 37°C with vigorous shaking (200 rpm). After 1 hour incubation, samples were centrifuged at 13,000 rpm for 30 seconds, and excess LB was discarded but leaving approximately 100 µl of LB. The pellet was resuspended in the remaining LB. Resuspended bacteria cells were plated out on LB-agars with selection agents ampicillin, kanamycin or ampicillin/kanamycin) and incubated overnight at 37°C without shaking to allow the growth of the transformants.

3.3.1.4 Long term storage of bacterial strains

To keep bacterial cells including plasmid in it or as empty for future experiments and to have a stock of strain in a laboratory is necessary. The most frequently used method is "Glycerol-Stock" method. A single colony picked from either an agar plate or a loop-full of bacterial stock was inoculated into 5 ml LB (with a selective agent if necessary) in 15 ml screw capped tubes. Tubes were incubated overnight at 37°C and at 200 rpm. For glycerol stock, 500 µl of saturated culture was added into 700 ul of 50% glycerol v/v. This mix was frozen/stored at –70 or -80°C.

3.3.1.5 Purification of plasmids

3.3.1.5.1 Purification of plasmid DNA using MN (Macherey-Nagel) miniprep kit

This method was preferred for isolation of plasmids in order to use in sequencing or cloning procedures. 5 ml of saturated culture was used for isolation of plasmid DNA by using "MN miniprep plasmid DNA purification kit" (MN Macherey-Nagel, Duren, Germany) following manufacture's

instructions. The quality of miniprep was checked by loading about 100ng of final yields on agarose gel and visualizing under U.V.

3.3.1.5.2 Large-scale plasmid DNA purification (midi-prep)

This method was used for isolation of plasmids in order to use in sequencing or mammalian cell transfection procedures by using "Promega PureYield Midi-Prep Plasmid System" following manufacture's instructions. The quality of midiprep was checked by loading about 100ng of final yields on agarose gel and visualizing under U.V.

3.3.1.5.3 Large-scale plasmid DNA purification (maxi-prep)

This method was used for isolation of plasmids in order to use in sequencing or mammalian cell transfection procedures by using "Qiagen large-scale plasmid DNA purification kit" following manufacture's instructions. The quality of maxiprep was checked by loading about 100ng of final yields on agarose gel and visualizing under U.V.

3.3.1.6 Preparation of genomic DNA from cultured cells

Cultured cells were grown in 100mm tissue culture dishes to 70-80% confluency, trypsinized, and washed with 1X PBS. Genomic DNA was isolated by using "Zymogen DNA isolation kit" following manufacturer's instructions.

3.3.1.7 Quantification and qualification of nucleic acids and proteins

Concentration and purity of the double stranded nucleic acids (plasmid and genomic DNAs) and total RNAs were determined by using the ds DNA and RNA methods on Nanodrop ND-1000 Full-spectrum UV/Vis Spectrophotometer (Thermo Fisher Scientific, Wilmington, DE, USA). Concentration and purity of

proteins were determined by using the Beckman Instruments Du Series 600 Spectrophotometer software programs on the Beckman Spectrophotometer Du640 (Beckman Instruments Inc. CA. USA).

3.3.1.8 Restriction enzyme digestion of DNA

Restriction enzyme digestions were routinely performed in 20 µl or 50 ul reaction volumes and typically 5-10 µg DNA was used. Reactions were carried out with the appropriate reaction buffer and conditions according to the manufacturer's recommendations. Digestion of DNA with two different restriction enzymes was also performed in the appropriate common reaction buffer and conditions recommended by the manufacturer.

3.3.1.9 Gel electrophoresis of nucleic acids

DNA fragments were fractionated by horizontal electrophoresis by using standard buffers and solutions. DNA fragments less than 1 kb were generally separated on 1.0% or 2.0 % agarose gel, those greater than 1 kb (up to 11 kb) were separated on 1 % agarose gels. Agarose gels were prepared by completely dissolving agarose in 1x TAE electrophoresis buffer to required percentage in microwave and ethidium bromide was added to final concentration of 30 µg/ml. The DNA samples were mixed with 5X DNA loading buffer and loaded onto gels. The gel was run in 1x TAE at different voltage and time depending on the size of the fragments at room temperature. Nucleic acids were visualized under ultraviolet light (long wave, 340 nm) and GeneRuler (MBI Fermentas) DNA size markers was used to estimate the fragment sizes.1 kb DNA ladder was loaded for products sizes of over 1kb and 100 bp ladder for product sizes of below 1kb.

3.3.2 Computer analyses

The sequences of the cloned FAM134B isoforms and of their mouse homologues were obtained from NCBI (National Center for Biotechnology Information) and UCSC (University of California, Santa Cruz) Genome Browser. The exon-intron information of these genes was derived using Ensembl Genome Browser at *http://www.ensembl.org*. Restriction endonuclease maps of the plasmid DNAs were analyzed by using the Clone.exe program. Primers were designed by using Primer.exe program provided by Whitehead Institute for Biomedical Research. The results of the DNA sequencing of engineered constructs were visualized using Finch TV 1.4 available for download at *http://www.geospiza.com/finchtv.html*. The alignments of nucleic acids or protein sequence were performed by using the NCBI Blast2Sequences algorithm available at the web page http://www.ncbi.nlm.nih.gov/BLAST/ , BIOEDIT Sequence Alignment Editor software publicly available at *http://www.mbio.ncsu.edu/BioEdit/BioEdit.html* and ClustalW algorithm provided by EMBL-EBI at *http://www.ebi.ac.uk/Tools/clustalw2/index.html* (Thompson JD., Higgins DG., Gibson TJ., 1997).

For querying FAM134B in HCC microarrays, two databases were used. Oncomine- Cancer Profiling Database (Rhodes DR. *et al.,* 2004) can be accessed after a free 'academic' or 'non-profit' registration. FAM134B was queried through the 'Gene Search' tool on the Oncomine homepage. On the return page, clicking on the term matched 'FAM134B' takes the user to a new page where information on this gene is listed under 5 categories: Summary, Annotation, Diff/Ex, C0/Ex and Outlier. For the purposes of this study, 'Diff/Ex' was clicked and the returned results were filtered by 'tissue'. Selecting 'liver' as tissue and viewing 'differentially-expressed' genes took the user to a list of 19 liver microarrays in which FAM134B displayed differential expression.

Another database used in this study is OncoDB.HCC- Oncogenomic Databas of Hepatocellular Carcinoma (Jou *et al.,* 2007). For querying FAM134B, 'FLJ20152' (which is an alias of FAM134) was typed in the 'Gene description' section of 'Display queried gene and reginal data' query tool and 'region around gene option' on the left side of the query tool was left as default,

+/- 10 Mb (megabases). On the return page, there are two types of data stored. Clicking on 'display region' gives information on the mapped human markers and LOH (loss of heterozygosity) regions around the queried gene. It also lists syntenic regions on rat and mouse chromosomes and CGH (comparative genomic hybridization) results. Clicking on 'display data' gives information on differential expression of FAM134B in Stanford HCC microarray data.

3.3.3 Vector construction

NT-3XFLAG-FAM134B-1 (N-terminal or amino-terminal FLAG tagged) and NT-3XFLAG-FAM134B-2 (N-terminal or amino-terminal FLAG tagged) vectors were generated by cloning the translated region of the mRNA sequence of human FAM134B isoform1 and human FAM134B isoform2 into the HindIII-BamHI digested p3XFLAG-CMV10 plasmid respectively. CT-3XFLAG-FAM134B-iso1 (C-terminal or carboxy-terminal FLAG tagged) and CT-3XFLAG-FAM134B-iso2 (C-terminal or carboxy-terminal FLAG tagged) vectors were generated by cloning the translated mRNA sequence of human FAM134B isoform1 and human FAM134B isoform2 into the HindIII-BamHI digested p3XFLAG-CMV14 plasmid respectively. All plasmids were sequence-verified.

3.3.4 Tissue culture techniques

3.3.4.1 Cell lines and stable clones

14 HCC derived cell lines (Huh7, FOCUS, Mahlavu, Hep40, Hep3B, HepG2, PLC/PRF/5, SK-Hep1, Snu182, Snu387, Snu398, Snu423, Snu449 and Snu475) were used in this study, and cultured as described in previously (Cagatay T. and Ozturk M., 2002). Breast cancer cell lines MCF-7, MDA-MB-231, MDA-MB-468, ZR-75-1, MDA-MB-453, CAMA1, SkBR3, MCF12A, HCC1937, MDA-157, T-47D (ATCC) and BT-474 (ATCC) and cervical cancer

cell line HeLa were cultivated in DMEM. Huh7-derived isogenic clones were obtained by G-418 selection after transfection with p3X-FLAG-CMV10 or p3X-FLAG-CMV10 plasmids. Cells were transfected using Fugene6 Transfection Reagent. 48 hours following transfection, cells were trypsinized and re-plated at lower density into 100cm plates. Cells were cultivated in the presence of geneticin G-418 sulfate (500 μg/ml; GIBCO, Carlsbad, CA, USA) for 30 days and isolated single cell-derived colonies were picked up with the help of a micropipette tip under microscope light and expanded in the presence of 500 μg/ml geneticin G-418 sulfate. For experiments where a defined number of cells were to be seeded, cell counting was performed. Following trypsinization, cells were resuspended in culture medium and counted manually with a hemocytometer.

3.3.4.2 Thawing cell lines

One vial of the frozen cell line from the liquid nitrogen tank was taken and immediately put into ice. The vial was left 1 minute on the bench to allow excess nitrogen to evaporate and then placed into 37^{o}C water bath until the external part of the cell solution was thawed (takes approximately 1-2 minutes). The cells were resuspended gently using a pipette and transferred immediately into a 15 ml. sterile tube containing 10 ml cold fresh medium. The cells were centrifuged at 1500 rpm at 4^{o}C for 5 minutes. Supernatant was discarded and the pellet was resuspended in 10 ml 37^{o}C culture medium to be plated into 100 mm dish. After overnight incubation in a humidified incubator at 37°supplied with 5% CO2, culture mediums were refreshed.

3.3.5.3 Growth conditions of cells

Dulbecco's modified Eagle's medium (DMEM) or RPMI 1640 supplemented 10% FCS and penicillin and streptomycin (50 mg/ml), and 1% NEAA was used to culture the HCC cell lines. The cells were incubated in at 37°C in an incubator with an atmosphere of 5% CO2 in air. Empty vector and

3X-FLAG-FAM134B expression vector transfected stable clones were cultured in parental cell line's culture medium + 500 μg/ml geneticin G-418 sulfate. The cells were passaged before reaching confluence. The growth medium was aspirated and the cells were washed once with calcium and phosphate-free PBS. Trypsin was added to the flask to remove the monolayer cells from the surface. The fresh medium was added and the suspension was pipetted gently to disperse the cells. The cells were transferred to either fresh petri dishes or fresh flasks using different dilutions (from 1:2 to 1:10) depending on requirements. All media and solutions used for culture were kept at 4°C (except stock solutions) and warmed to 37°C before use.

3.3.4.4 Cryopreservation of cell lines

Exponentially growing cells were harvested by trypsinization and neutralized with growth medium. The cells were counted and precipitated at 1500 rpm for 5 min. The pellet was suspended in a freezing solution (10% DMSO, 20% FCS and 70% DMEM for adherent cells) at a concentration of 4x106cells/ml. 1 ml of this solution was placed into 1 ml screw capped-cryotubes. The tubes were left at -70°C overnight. The next day, the tubes were transferred into the liquid nitrogen storage tank.

3.3.4.5 Transient transfection of eukaryotic cells using Fugene 6 transfection reagent

Transfection was performed with Fugene6 Transfection Reagent reagent (Invitrogen, Carlsbad, CA, USA) following manufacturer's instructions.

3.3.5 Extraction of total RNA from tissue culture cells and tissue samples

Total RNAs were isolated from cultured cells using the NucleoSpin RNA II Kit (MN Macherey-Nagel, Duren, Germany) according to the manufacturer's protocol.

3.3.6 First strand cDNA synthesis

First strand cDNA synthesis from total RNA was performed using RevertAid First Strand cDNA synthesis kit (MBI Fermantas, Germany). The RevertAid kit relies on genetically engineered version of Moloney Murine Leukemia Virus reverse transcriptase (RevertAid M-MuLV RT) with low RNase H activity. This allows the synthesis of full-length cDNA from long templates. The first strand reactions were primed with oligo(dT)18 primer to specifically amplified mRNA population with 3'-poly(A) tails. As the reaction conditions and components of this kit and those of conventional PCR are compatible, first strand synthesized with this system can be used as a template for PCR. 1 to 5 µg total RNA was used to synthesize the first stand cDNA following the manufacturer's instruction. After 1:1 dilution of total reaction products in DEPC-treated water, 2 µl of diluted first strand cDNA was used for PCR.

3.3.7 Primer design for expression analysis by semi-quantitative PCR

The primer pairs that have been used in expression profile analyses were designed carefully. Forward and reverse primer were positioned on different exons of the gene of interest, so that the primer pair was either be able to produce a longer amplicon from genomic DNA or not be able to amplify from the covered genomic DNA region in a given PCR condition (critical parameter was extension time). Primers used for expression analysis have been designed strictly considering these criteria, and listed in Table 3.2.

Genes	Primer pairs (5'→3') (upper: forward; lower: reverse)	Tm, (°C)	Number of cycles
hFAM134B isoform1	CAAGAGGTGCACAGTTGTGGAGAA	58	35
	GCAACCGTGAGGCTAATCTTAGGA		
hFAM134B isoform2	CTCGAGAAGCTTATGCCTGAAGGTGAAGACTT	58	35
	GCAACCGTGAGGCTAATCTTAGGA		
hGAPDH	GGCTGAGAACGGGAAGCTTGTCAT	60	19
	CAGCCTTCTCCATGGTGGTGAAGA		
Riken cDNA 1810015C04 isoform1*	CTCCTTGGAGAGTGTATCACCTCA	60	30
	GTCCAAGAGACTTCTGACAC		
Riken cDNA 1810015C04 isoform2*	TGTGGACAAGACAGCATTCTCTGG	60	30
	GTCCAAGAGACTTCTGACAC		
mGAPDH	ACCACAGTCCATGCCATCAC	55	20
	TCCACCACCCTGTTGCTGTA		

Table 3.2: RT-PCR primer list. m: mouse h:human * mouse homolog of human FAM134B

3.3.8 Fidelity and DNA contamination control in first strand cDNAs

The fidelity and genomic DNA contamination of first strand cDNAs were checked before performing expression analyses. 2µl of diluted first strand cDNA was used for cold-PCR amplification of the *glyceraldehyde-3-phosphate dehydrogenase (GAPDH)* transcript. *GAPDH* primer pair for this analysis was designed to produce a 151 bp fragment from cDNA and 250 bp fragment from genomic DNA.

3.3.9 Expression analysis of a gene by semi-quantitative PCR

Determination of optimal cycle of a gene for semi-quantitative PCR

Using equal amount of templates for PCR amplifications of a gene of interest give comparable results at a certain number of PCR cycles. The number of optimal PCR cycle was determined by an initial study for each gene by performing 35-cycle PCR during which PCR amplicon samples were collected by 2-cycle intervals. Agarose gel analysis of samples from 20th, 23rd, 26th, 29th, 32nd, 35th, 36th 39th, 41st, 43rd, 45th cycles of PCR with an equal load defined the minimum number of cycle to visualize the product on agarose gel and the saturation cycle. Agarose gels were analyzed by Densitometric Fluorescence-Chemiluminescence image analyzer and The Molecular Analyst software (BioRad, Hercules,CA,USA). The determined cycle number was used for amplification of the gene of interest.

GAPDH normalization

Equal volume (2µl) of all first strand cDNA samples was used for cold-PCR amplification of *GAPDH* transcript using the pre-determined optimal cycle number for GAPDH. Then an equal volume of each sample was loaded onto agarose gel and intensity of each band was analyzed by Densitometric Fluorescence-Chemiluminescence image analyzer and The Molecular Analyst software. After intensities were determined, intensity of sample with the highest densitometric reading and 2 µl loading volume were used as reference points for normalization of input loading volume of other samples for expression analysis of both *GAPDH* and gene of interest by cold PCR amplification. Amplification products were analyzed in computer.

3.3.10 Crude total protein extraction

Adherent monolayer cells (both stable and parental cells) were grown to 70% confluency in growth medium lacking selective antibiotic. After removal of growth medium, cells were washed twice with ice-cold PBS to remove any serum residue. 400 µl of RIPA lysis-buffer (150 mM NaCl, 50 mM Tris-HCl pH 8.0, 0.5% sodium deoxycholate, 1 % NP-40, 0.1% SDS and 1X Complete Protein Inhibitor mix (Roche, Basel, Switzerland)) was added into 10 cm tissue culture petri dish, and cells were scraped with rubber scrapper. Complete lysis was achieved by pipetting of crude cell lysates several times and by incubating the lysates on ice for 30 min, and then centrifuged at 13.000 G for 30 minutes. Total cell protein was collected as supernatant.

3.3.11 Western blotting

The conventional Bradford protein assay was employed to quantity the protein in the lysates obtained from either Crude total. After protein quantification, protein lysates were aliquoted into fresh tubes and, stored at –80°C. 10% resolving gel and 5% stacking gel was used in SDSPAGE analysis of protein lysates. EC-120 (E-C Apparatus Corp., Holbrook, NY, USA) and ProteanII-xi (BioRad, Hercules,CA, USA) vertical Gel system was set up according to manufacturer's instructions. The standard SDS-electrophoresis buffer system was used. Equal amounts of cell lysates were solubilized in 5X SDS gel-loading buffer, denatured at 100°C for 5 min and incubated on ice for 2 min. After a quick spin, samples were loaded onto SDS-polyacrylamide gel. After electrophoresis at 80 V for 20 minutes followed by 120 V for 1-2 hours, proteins were transferred onto PVDF western blotting membrane (Roche, Basel, Switzerland) by using Transblot-Semi Dry (BioRad, Hercules, CA, USA) electroblotting apparatus according to the manufacturer's instructions at 12V for 45 min for EC-120 gel. Membrane was immediately treated for an hour in blocking solution at room temperature and probed with primary antibody either for an hour at room temperature or overnight at 4°C. After washing 4 times for (5 min, 15 min, 5 min, 5 min) in TBS-T solution at room temperature, the

membrane was incubated with appropriate HRP73 conjugated secondary antibody for 1 hr. The membrane was washed 3 times for 5 min in TBS-T solution at room temperature. After final wash, the blot was exposed to ECL western blot detection kit (Amersham, Buckinghamshire, UK) according to manufacturer's instructions. The chemiluminescence emitted was captured on X-ray film within 30 sec. to 5 min. exposure times.

3.3.12 Immuno-fluorescence

Autoclaved-sterilized coverslips were placed into the well of 6-multiwell plates. 6x104 cells were seeded onto each coverslip and grown overnight in 1 ml growth medium. Cells were washed with PBS and fixed in 1 ml of cold methanol for 5 minutes. After fixation cells were blocked in 1 ml blocking solution (5% BSA in 1X PBS) for 1 hour at room temperature. Coverslips were probed with primary antibody in appropriate dilution for 1 hr at room temperature. After washing cells twice with 1X PBS, either appropriate TRITC-conjugated or AlexaFluor Red/Green secondary antibody was applied for 1 hour at room temperature. Cells were washed 2 times with 1X PBS and DNA counter staining was performed by with DAPI for 3 minutes. After DAPI was aspirated, destaining was done in double-distilled water for 5 minutes. Immediately after coverslips were taken out from the well and excess water removed by tissue paper, coverslips were mounted onto slides containing DAKO Fluorescent Mounting Medium. All steps after the addition of TRITC-conjugated secondary antibody or AlexaFluor Red/Green secondary antibody were performed in the dark. Stained cells were examined under fluorescence microscope (ZEISS) and pictures were captured in a digital ZEISS AxioCam MRc5 camera.

3.3.13 Immuno-peroxidase staining

Autoclaved-sterilized coverslips were placed into the well of 6-multiwell plates. 6x104 cells were seeded onto each coverslip and grown overnight in 1 ml growth medium. Cells were washed with PBS and fixed in 1 ml of cold methanol

for 5 minutes. After fixation cells were blocked in 1 ml blocking solution (5% BSA in 1X PBS) for 1 hour at room temperature. Coverslips were probed with primary antibody in appropriate dilution for 1 hr at room temperature. After washing cells twice with PBS, DAKO-DAB secondary antibody was applied for 30 min at room temperature. Cells were washed 2 times with PBS and incubated with DAB Chromogen Substrate for 1 min. DNA counter staining was performed with Hematoxylene for 1 minute. Hematoxylene was aspirated and destaining was done in double-distilled water for 5 minutes. Immediately after coverslips were taken out from the well and excess water removed by tissue paper, coverslips were mounted onto slides containing DAKO Fluorescent Mounting Medium. Stained cells were examined under microscope (ZEISS) and pictures were captured in a digital ZEISS AxioCam MRc5 camera.

3.3.14 BrdU incorporation assay

Sub-confluent cells were labeled with the thymidine analogue BrdU (5-bromo-2-deoxyuridine) for 4 hours in freshly added culture medium and tested as described (Erdal E. *et al.*, 2005). Briefly, cells were washed twice with 1X PBS, fixed with 70% ice-cold methanol and washed for 10 minutes with 1X PBS. Then the cells were incubated in 2 N HCl for 20 minutes and washed three times for 5 minutes with 1X PBS. Following blocking with PBS-T plus 3% BSA for 15 minutes, anti-BrdU antibody (Dako) incubation was performed for an hour, followed by DAB-ENVISION secondary antibody treatment for 30 minutes. Following this, cells were incubated with DAB Chromogen substrate for visualization.

3.3.15 SABG assay

SABG activity was detected by using a described protocol (Dimri GP. *et al.*, 1995). Briefly, ~20000 cells were seeded in 6-well plates on coverslips. After 24 hours, cells were subjected to 5min formaldehyde fixation, followed by overnight β-gal buffer incubation at 37ºC. Where B-gal/FLAG immuno-

peroxidase co-staining was performed, cells were permeabilized with 10 min 0.25% TRITON-X-100, blocked for 1hour with 5%BSA in 1X PBS. Then immuno-peroxidase staining method was employed using α-Flag mouse monoclonal antibody. After hematoxylene counterstaining, SABG positive and negative cells were identified and counted.

3.3.16 ER-stress experiments

In ER-stress experiments, 10000 or 20000 cells were seeded in 24 well-plates. After 24 hours, cells were treated with various concentration of tunicamycin (0-12 ug/ml) in DMEM containing 0.2% FCS for an additional 24 hours. On the next day, cells were washed twice with PBS, fixed with ice-cold methanol for 5 minutes and stained with Coomassie Brilliant Blue solution for 5 minutes. Then cells were washed with PBS, photograpahed using a Nikon digital camera and counted under the light of a microscope.

3.3.17 Sulforhodamine B (SRB) colorimetric assay for cytotoxicity screening

The sulforhodamine B (SRB) assay is used for cell density determination, based on the measurement of cellular protein content. In this study, this method is employed for the toxicity screening of tunicamycin to adherent cells in a 96-well format. Following 24 hours of tunicamycin incubation period, cell monolayers are fixed with 50% (wt/vol) trichloroacetic acid and stained for 60 min at 4°C, after which the excess dye is removed by washing repeatedly with 1% (vol/vol) acetic acid. Following air drying of plates, the protein-bound dye is dissolved in 10 mM Tris base solution for OD determination at 515 nm using a microplate reader. The results are linear over a 20-fold range of cell numbers and the sensitivity is comparable to those of fluorometric methods (Vichai V. and Kirtikara K., 2006).

CHAPTER 4. RESULTS

4.1 FAM134B

4.1.1 Nucleotide and gene information

The section cites the information on FAM134B in NCBI (National Center for Biotechnology Information)'s 'Nucleotide' and 'Gene' query databases. The name FAM134B stands short for 'family with sequence similarity 134, member B'. Other aliases for this gene are FLJ20152, FLJ22155, and FLJ22179. Its NCBI GeneID is 54463. FAM134B nucleotide sequence has been determined as part the Human Genome Project (International Human Genome Sequencing Consortium, 2004) and also as part of a comparative analysis of human chromosome 5 (Schmutz J. *et al*., 2004). The locus in which FAM134B gene resides is named NC_000005 and it corresponds to a 143972 bp linear DNA molecule. It has been mapped to the minus strand of the p arm of human chromosome 5 and its exact chromosomal location is 5p15.1, with ZNF622 gene in the upstream and MYO10 gene in the downstream genomic neighbourhood. The following image from the NCBI webpage illustrates the genomic context in which FAM134B resides:

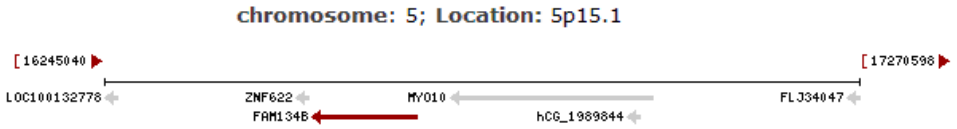

Figure 4.1: Genomic Context of FAM134B gene.

FAM134B gene has been classified as a protein-encoding gene. It encodes two transcripts: NM_001034850 (gil77917616) is transcript variant # 1, which has a linear full-length mRNA of 3259 bps (basepairs). NM_019000 (gil77917615) is transcript variant # 2, which has a linear full-length mRNA of 3108 bps. The translated region of transcript variant 1 is from base pair number 39 to 1532, corresponding to a translated mRNA length of 1494 bp . The

translated region of transcript variant 2 is from base pair number 311 to 1308, corresponding to a translated mRNA length of 998 bp. The two transcripts are produced by alternative splicing of exons. Transcript variant 1 consists of 9 exons of which the first three are unique to this variant. Transcript variant 2 consists of 7 exons of which the first is unique to this variant. Therefore, the two variants have alternatively spliced unique exons in the 5' region and are 100% identical in the 6 exons at the 3' region. The two variants are depicted as follows at NCBI 'Gene' webpage:

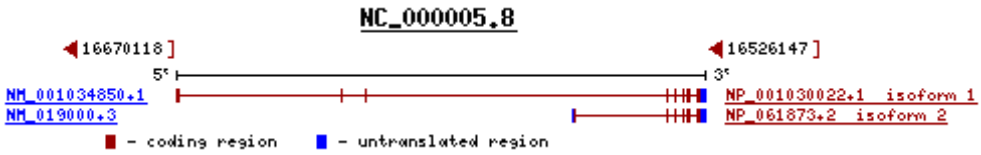

Figure 4.2: Genomic regions, transcripts, and products of FAM134B gene.

4.1.2 Protein information

4.1.2.1 General information

The protein encoded by FAM134B gene is designated as either 'protein FAM134B' or 'hypothetical protein LOC54463'. This actually corresponds to two protein isoforms translated from the two alternatively-spliced mRNA variants, as depicted in the above image. At the beginning of this section, information stored on FAM134B protein in the SWISS-PROT Database (Bairoch A. and Apweiler R., 1998) will be presented, which will be followed by analyses of FAM134B using protein database prediction tools. FAM134B protein isoform 1 is represented in SWISSPROT database by Q9H6L5 symbol and it consists of 497 aminoacids, corresponding to a molecular weight of 54680 Daltons and a theoretical isoelectric point (pI) of 4.53. Protein isoform 2 is represented by Q9H6L5-2 symbol and it consists of 356 aminoacids, corresponding to a molecular weight of 39317 Daltons and a theoretical isoelectric point (pI) of 4.39. The isoelectric point, the pH value at which the

protein molecule does not migrate, is in the range of pH 5 to 7 for many proteins (*Encyclopædia Britannica*, 2008). The low isoelectric points of these two protein isoforms indicate that both are unusually acidic proteins, reflecting a high composition of negatively charged residues (over 65 percent).

The two protein isoforms differ at the N-terminus and are entirely identical at the C-terminus. By similarity, the protein belongs to a family named 'FAM134B' family which is a protein family comprised of members belonging to species as diverse as human, mouse, rat, zebra fish, cow and African frog. According to SWISS-PROT protein database, evidence for the existence of these protein isoforms is only at the transcriptional level and so far, these proteins have not been detected or visualized at the translational level. According to protein database searches, this protein doesn't show homology to any known functional protein.

4.1.2.2 Protein domain and motif predictions

In terms of its sub-cellular localization, FAM134B has been classified as a 'potential' multi-pass transmembrane protein in many protein databases such as SWISS-PROT or HPRD (Human Protein Reference Database, Mishra G. *et al.*, 2006). This classification reflects only the 'potential' localization as it has been inferred through non-experimental evidence, mainly based on results from protein sequence analysis tools and on the presence of alternating hydrophobic and hydrophilic amino acid patches along the protein sequence. Furthermore, it is not known whether FAM134B potentially localizes to the plasma membrane or an organelle membrane. The same databases classify this protein as a 'modified' protein, pointing to a few phospho-specific residues that could be targeted by possible phosphorylation events. SwissProt database emphasizes serine #276 in isoform1 (corresponding to serine #135 in isoform 2) as such a possible phospho-specific residue, as inferred 'by similarity to other members in the protein family'. HPRD predicts serine #211 and tyrosine #218 in isoform 1 (corresponding to serine #80 and tyrosine #87 in isoform 2) as possible sites of phosphorylation based on the idea that there is some logical or conclusive

evidence that the given annotation could apply. The exact serine or tyrosine kinases that could be recruited to these sites are also not known but are predicted by HPRD and SWISSPROT to be Casein Kinase II, PKC (Protein Kinase C), PKB (Protein Kinase B) and others. Figure 4.3a and Figure 4.3b illustrate the potential transmembrane domains and phospho-residues of both FAM134B isoforms as predicted by SWISSPROT's MotifScan database.

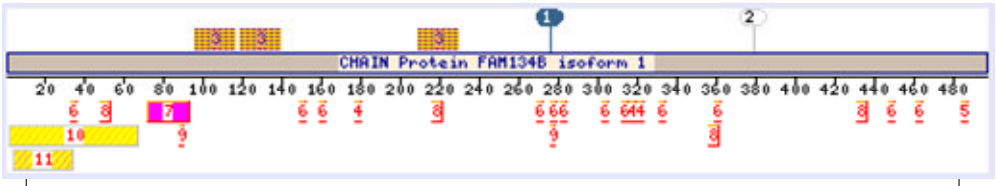

Legend:
1. PHOSPHO-SERINE (By similarity): Serine residue at position 276
2. VARIANT Q -> E (in dbSNP:rs34432513): non-synonymous SNP at position 379
3. POTENTIAL TRANSMEMBRANE DOMAIN: 96-116, 119-139, 209-229
4*. N-GLYCOSYLATION SITE: 177-180, 316-319, 320-323
5*. cAMP- AND cGMP-DEPENDENT PROTEIN KINASE PHOSPHORYLATION SITE: 484-487
6*. CASEIN KINASE II PHOSPHORYLATION SITE: 33-36, 149-152, 159-162, 269-272, 276-279, 281-284, 302-305, 312-315, 331-334, 359-362, 447-450, 461-464
7*. POTENTIAL LEUCINE ZIPPER: 72-93
8*. N-MYRISTOYLATION SITE: 48-53, 216-221, 356-361, 431-436
9*.PROTEIN KINASE C PHOSPHORYLATION SITE: 88-90, 276-278
10*.ALANINE-RICH REGION: 2-67
11*.PROLINE-RICH REGION: 4-34

Figure 4.3a: MotifScan Results of FAM134B isoform 1. * indicates motifs frequently found in proteins. The numbers next to each site/domain/region in the legend indicate its position on the protein in terms of amino acid numbers.

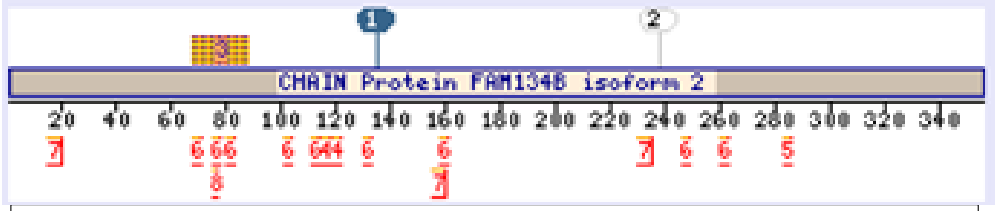

Legend:
1. PHOSPHO-SERINE (By similarity): Serine residue at position 135
2. VARIANT Q -> E (in dbSNP:rs34432513): non-synonymous SNP at position 238
3. POTENTIAL TRANSMEMBRANE DOMAIN: 68-88
4*. N-GLYCOSYLATION SITE: 115-118, 119-122
5*. cAMP- AND cGMP-DEPENDENT PROTEIN KINASE PHOSPHORYLATION SITE: 283-286
6*. CASEIN KINASE II PHOSPHORYLATION SITE: 68-71, 75-78, 80-83, 101-104, 111-114, 130-133, 158-161, 246-249, 260-263
7*. N-MYRISTOYLATION SITE: 230-235
8*. PROTEIN KINASE C PHOSPHORYLATION SITE: 75-77

Figure4.3b: MotifScan Results of FAM134B isoform 2. * indicates motifs frequently found in proteins.The numbers next to each site/domain/region in the legend indicate its position on the protein in terms of amino acid numbers.

Apart from these predicted transmembrane domains and phospho-specific residues mentioned above, there are no apparent functional or structural domains in FAM134B protein. SWISSPROT's MotifScan and ScanProsite prediction tools return a list of motifs that could possibly be found on this protein. However, these motifs are those that occur frequently in all proteins and thus may not have specificity for FAM134B protein. These motifs include glycosylation or myristoylation sites, alanine or proline-rich regions and leucine zipper motif. These predicted motifs are also illsutrated for each isoform in Figure 4.3a and Figure 4.3b. From these predictions, both FAM134B isoforms appear to be potential transmembrane proteins that could be subject to post-translational modifications. The hydrophobic leucine zipper predicted in isoform 1 could be employed in dimerization of this protein.

4.1.2.3 SNPs and protein structure of FAM134B

Ten SNP (Single Nucleotide Polymorphism)s have so far been reported in GeneCards database (Rebhan M. *et al*., 1997) for FAM134B gene. Of these ten SNPs, two are intronic, five are in the UTR regions, two are synonymous and only one SNP is non-synonymous. This non-synonymous SNP is a Q (Glutamine) to E (Glutamic Acid) aminoacid change at aminoacid position 379 in isoform 1 (corresponding to position 238 in isoform 2). The minor allele frequency of this SNP, according to GeneCards database, is 0.02. The exact location of this SNP on FAM134B isoforms has been depicted in Figure 4.3a and Figure 4.3b.

The secondary-structure information of FAM134B isoforms was obtained by querying at NPS (Network Protein Sequence Analysis) database using PHD (Rost B. *et al.*, 1994), DSC (King RD. and Stenberg MJ., 1996) and MLRC on GOR4, SIMPA96 and SOPMA (Guermeur Y. *et al.*, 1999) prediction methods. The consensus secondary structure from these three prediction methods indicates that FAM134B protein isofroms are predominantly folded into alpha-helices with random coils in between and occasionally into extended strands, as depicted in Figure 4.4a and 4.4b.

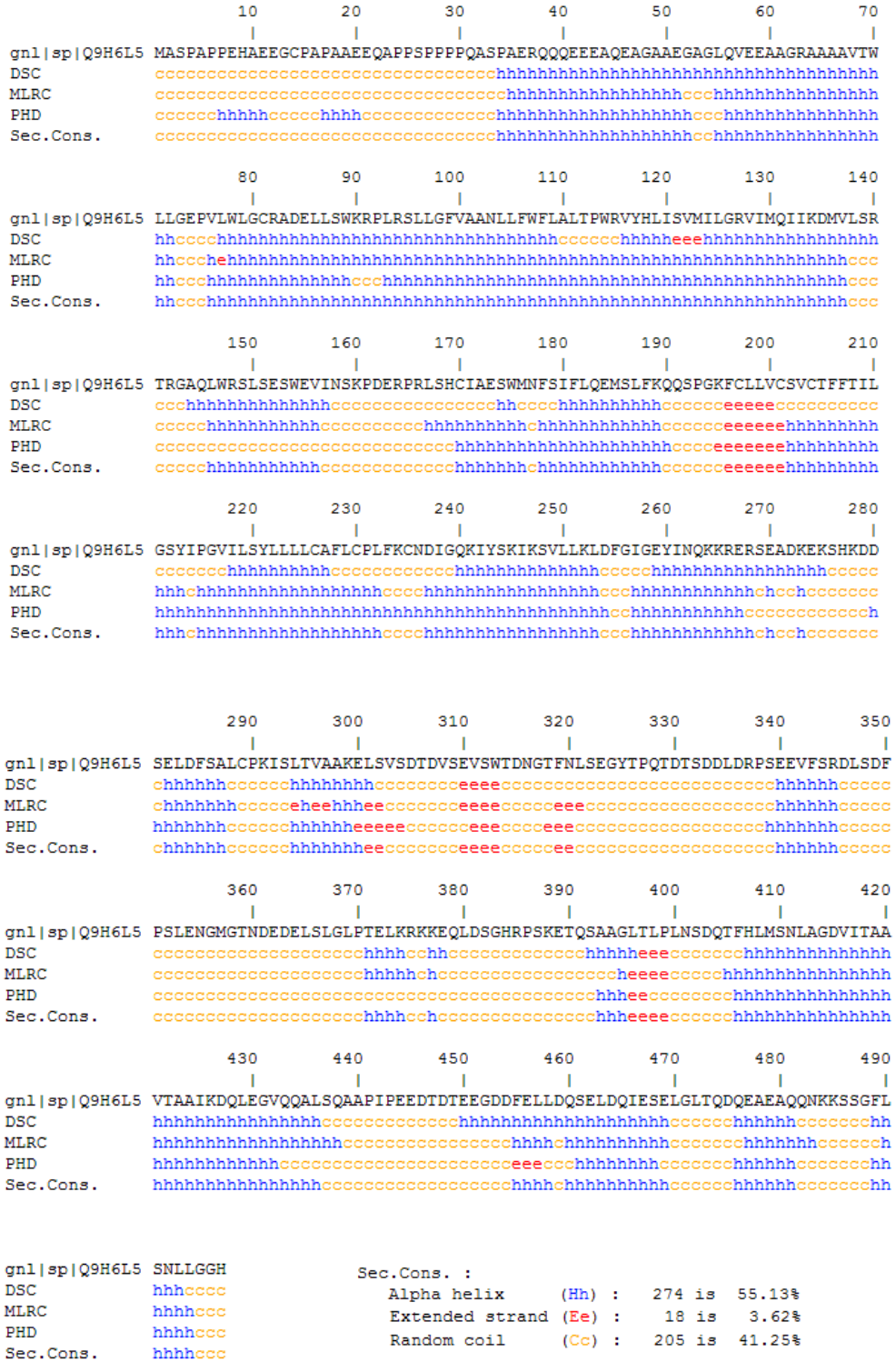

Figure 4.4a: Consensus secondary (Sec. Cons.) structure prediction of FAM134B isoform 1

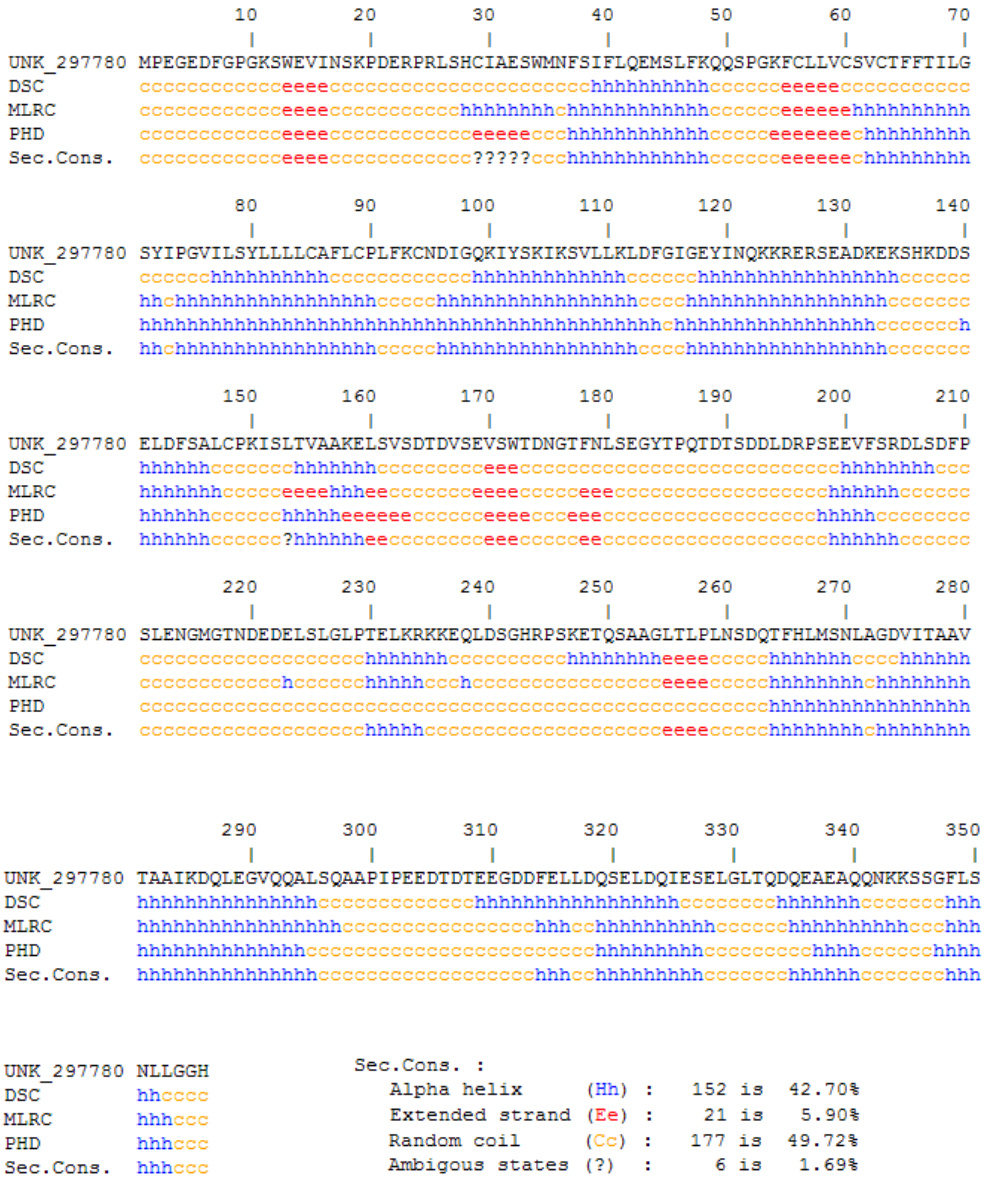

Figure 4.4b: Consensus secondary (Sec. Cons.) structure prediction of FAM134B isoform 2

As for the 3-D structure of FAM134B protein, protein modelling tools fail to produce a 3-D structure for FAM134B due to the lack of a homolog with an established 3-D structure that can be used as a template by these modelling tools.

4.1.3 Gene Homologs and Protein Sequence Conservation

4.1.3.1 Orthologs of FAM134B

According to HomoloGene Database of NCBI, orthologs of FAM134B gene exist in four other species. For FAM134B isoform 1, genes identified as putative orthologs of one another and proteins used in sequence comparisons and their conserved domain architectures are:

FAM134B, *Homo sapiens* family with sequence similarity 134, member B	NP_001030022.1 497 aa
LOC479382, *Canis lupus familiaris* hypothetical LOC479382	XP_536520.2 574 aa
1810015C04Rik, *Mus musculus* RIKEN cDNA 1810015C04 gene	NP_001030023.1 480 aa
LOC619558, *Rattus norvegicus* hypothetical protein LOC619558	NP_001030084.1 480 aa
LOC100003524, *Danio rerio* hypothetical protein LOC100003524	XP_001343062.1 460 aa

Table 4.1a: Genes identified as putative orthologs one another during the construction of HomoloGene for FAM134B isoform 1.

Table 4.1b: Corresponding orthologous of proteins of FAM134B isoform 1 and their of conserved domain architectures.

The multiple sequence alignment of the protein sequences of these orthologs, generated using ClustalW 2.0.8 (Thompson JD., Higgins DG., Gibson TJ., 1997) and showing conserved residues, is given below. The sequnces aligned from top to bottom belong to Homo sapiens (human), Rattus norvegicus (rat), Mus musculus (mouse), Canis lupus familiaris (dog) and Danio rerio (zebrafish) respectively.

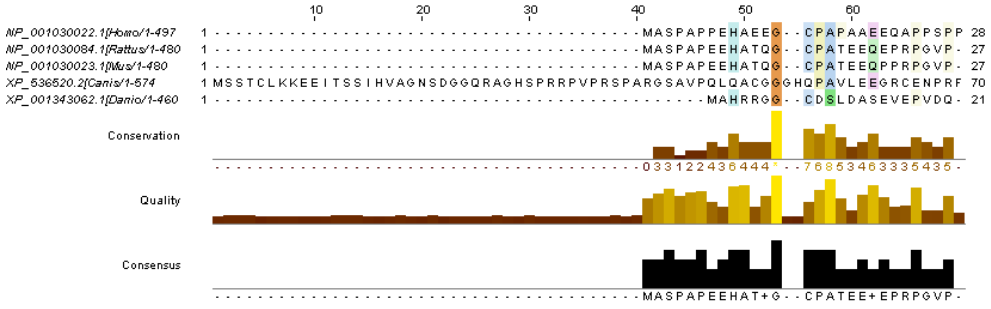

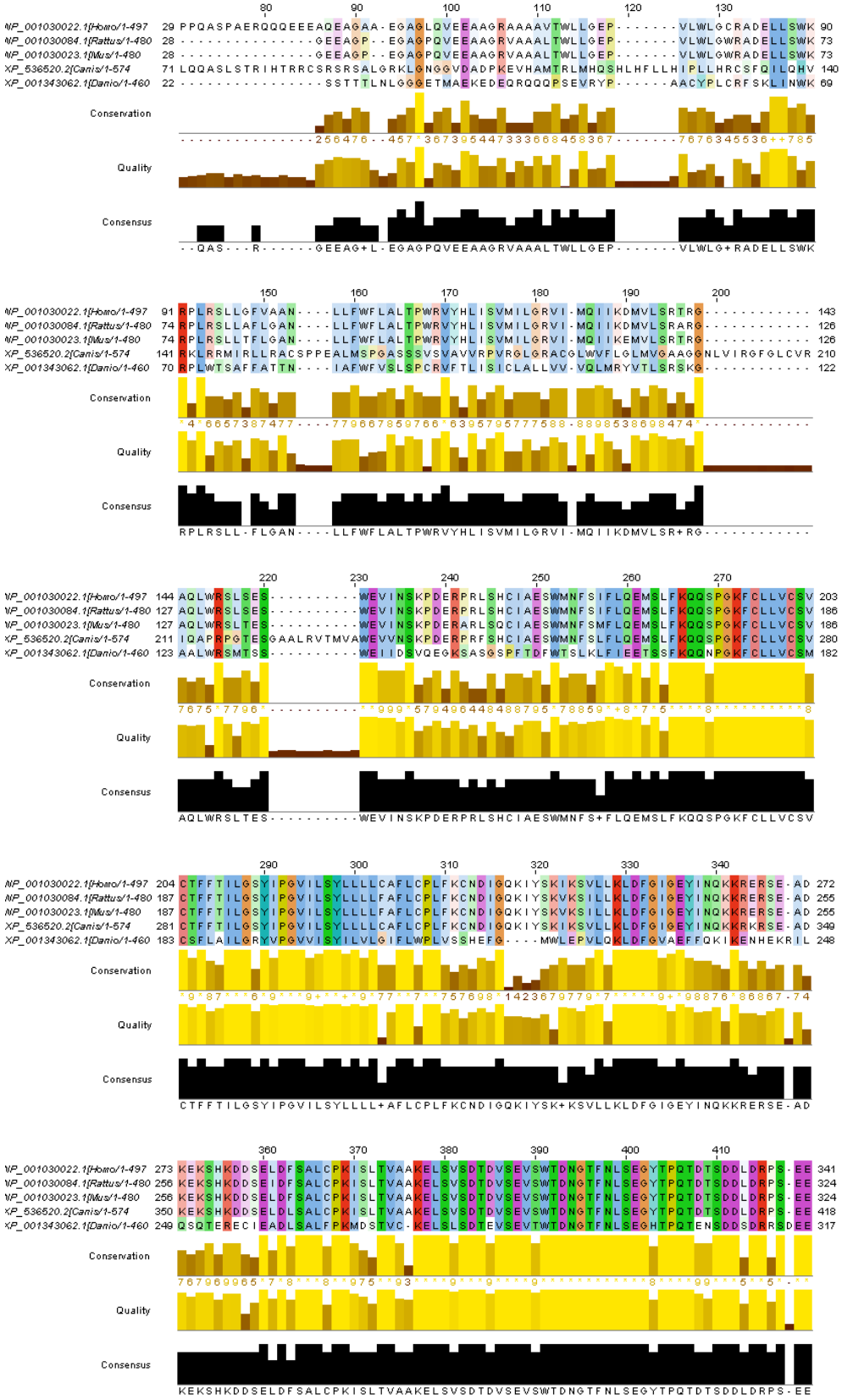
NP_001030022.1[Homo/1-497
NP_001030084.1[Rattus/1-480
NP_001030023.1[Mus/1-480
XP_536520.2[Canis/1-574
XP_001343062.1[Danio/1-460
Conservation
Quality
Consensus

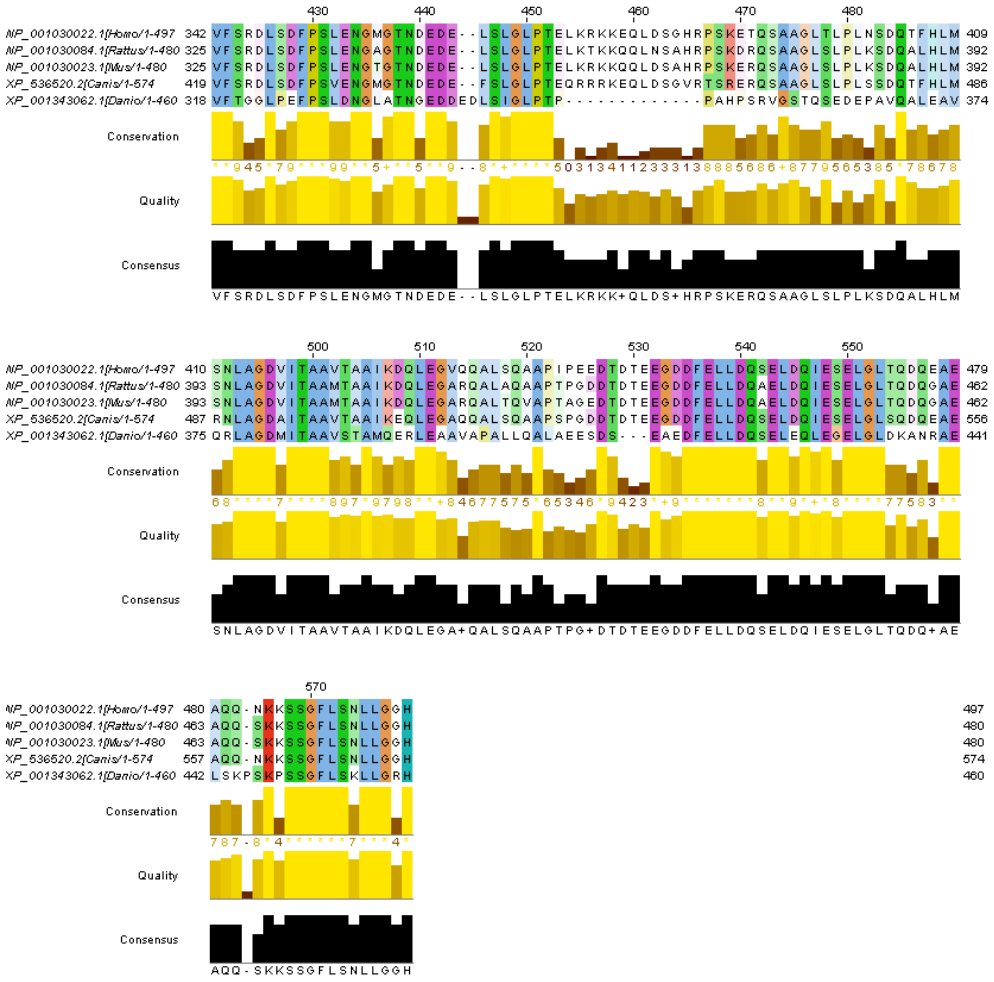

Figure 4.5: The ClustalW 2.0.8 multiple sequence alignment of FAM13B isoform 1 orthologs.

The alignment scores revealed by this multiple alignment are given below:

SeqA	Name	Len(aa)	SeqB	Name	Len(aa)	Score
1	NP_001030022.1	427	2	XP_536520.2	574	76%
1	NP_001030022.1	427	3	NP_001030023.1	480	92%
1	NP_001030022.1	427	4	NP_001030084.1	480	92%
1	NP_001030022.1	427	5	XP_001343062.1	460	44%

Table 4.2: FAM134B isoform 1 orthologs multiple alignment pair-wise similarity scores

This alignment indicates that the human FAM134B isoform 1 protein sequence is 76 % similar to its dog ortholog, 92% similar to its mouse and rat orthologs and 44% similar to its zebrafish ortholog. Of the transmembrane domains predicted for FAM134B isoform 1 in MotifScan, the domains between amino acid numbers 96-116 and 119-139 are fairly conserved between the five

species. The domain between amino acid numbers 209-229 is very highly conserved. The Serine residue at position 276, which was proposed as a possible phosphorylation site based on predictions of SWISSPROT database, appears as a highly conserved residue which is present in 4 of the 5 species analyzed. In zebrafish, this residue has been changed to threonine, another residue that can be targeted for phosphorylation by kinases.

According to UniGene database of NCBI, orthologs of FAM134B isoform 2 exist in three other species. Genes identified as putative orthologs of one another and proteins used in sequence comparisons and their conserved domain architectures are:

FAM134B, *Homo sapiens* family with sequence similarity 134, member B	NP_061873.2 356 aa
1810015C04Rik, *Mus musculus* RIKEN cDNA 1810015C04 gene	NP_079735.2 356 aa
Bt.28690, *Bos taurus* Hypothetical protein FLJ20152	NP_001015672.1 355 aa
Str.70704, *Xenopus tropicalis* Transcribed locus, weakly similar to NP_001030022.1 hypothetical protein LOC...	NP_001120447.1 350 aa

Table 4.3a: Genes identified as putative orthologs of one another during the construction of HomoloGene for FAM134B isoform 2.

Table 4.1b: Corresponding orthologous proteins of FAM134B isoform 2 and their conserved domain architectures.

The multiple sequence alignment of these orthologs, generated using ClustalW 2.0.8 (Thompson JD., Higgins DG., Gibson TJ., 1997) and showing conserved residues, is given below. The sequnces aligned from top to bottom belong to Homo sapiens (human), Bos taurus (domestic cow), Mus musculus (mouse) and Xenopus tropicalis (western clawed frog) respectively.

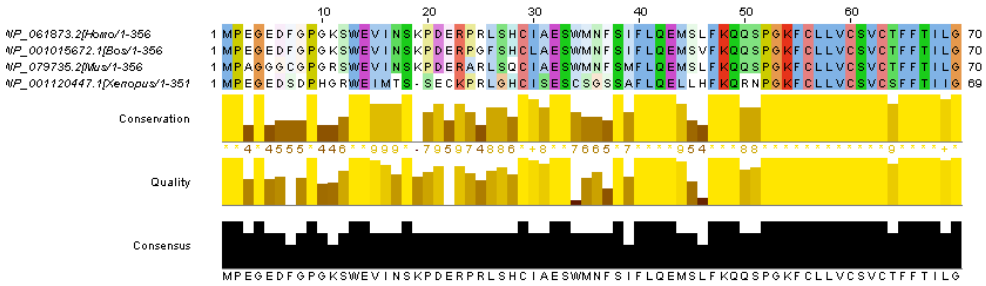

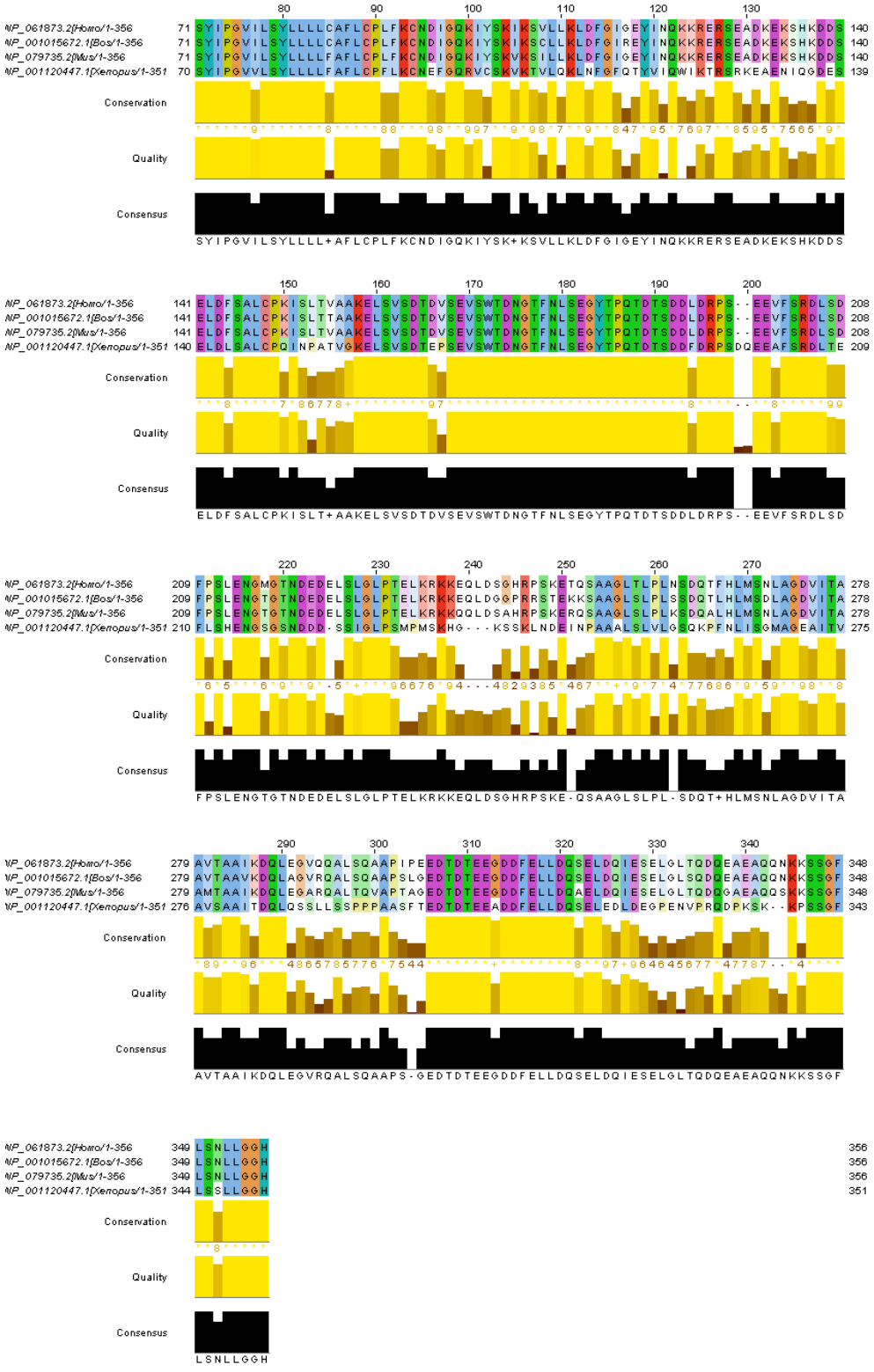

Figure 4.6: The ClustalW 2.0.8 multiple sequence alignment of FAM13B isoform 2 orthologs.

The alignment scores revealed by this multiple alignment are given below:

SeqA	Name	Len(aa)	SeqB	Name	Len(aa)	Score
1	NP_061873.2	356	2	NP_079735.2	356	91%
1	NP_061873.2	356	3	NP_001015672.1	356	92%
1	NP_061873.2	356	4	NP_001120447.1	351	58%

Table 4.4: FAM134B isoform 2 orthologs multiple alignment pair-wise similarity scores

This alignment indicates that the human FAM134B isoform 2 protein sequence is 91% similar to its mouse ortholog, 92% similar to its bovine ortholog and 58% similar to its African frog ortholog. The transmembrane domain predicted for FAM134B isoform 2 in MotifScan, which lies between amino acid numbers 68-88 is very highly conserved between the four species. The Serine residue at position 135, which was proposed as a possible phosphorylation site based on predictions of SWISSPROT database, appears as a highly conserved residue which is present in 3 of the 4 species analyzed. In Xenopus tropicalis, this residue has been changed to isoleucine.

4.1.3.2 Paralogs of FAM134B

FAM134B protein belongs to a protein family named 'family with sequence similarity 134'. There isn't any data on this family except for a list of proteins that belong to this family. Among the human paralogs identified for FAM134B by KEGG (Kyoto Encyclopedia of Genes and Genomes) database (Kanehisa M. *et al.*, 2004), two are FAM134B family members . These paralogs are FAM134A (family with sequence similarity 134, member A) and FAM13C (family with sequence similarity 134, member C). Both genes encode single isoform, hypothetical proteins. The multiple sequence alignment of the protein sequences of these paralogs generated using CLUSTALW 2.0.8 is given below:

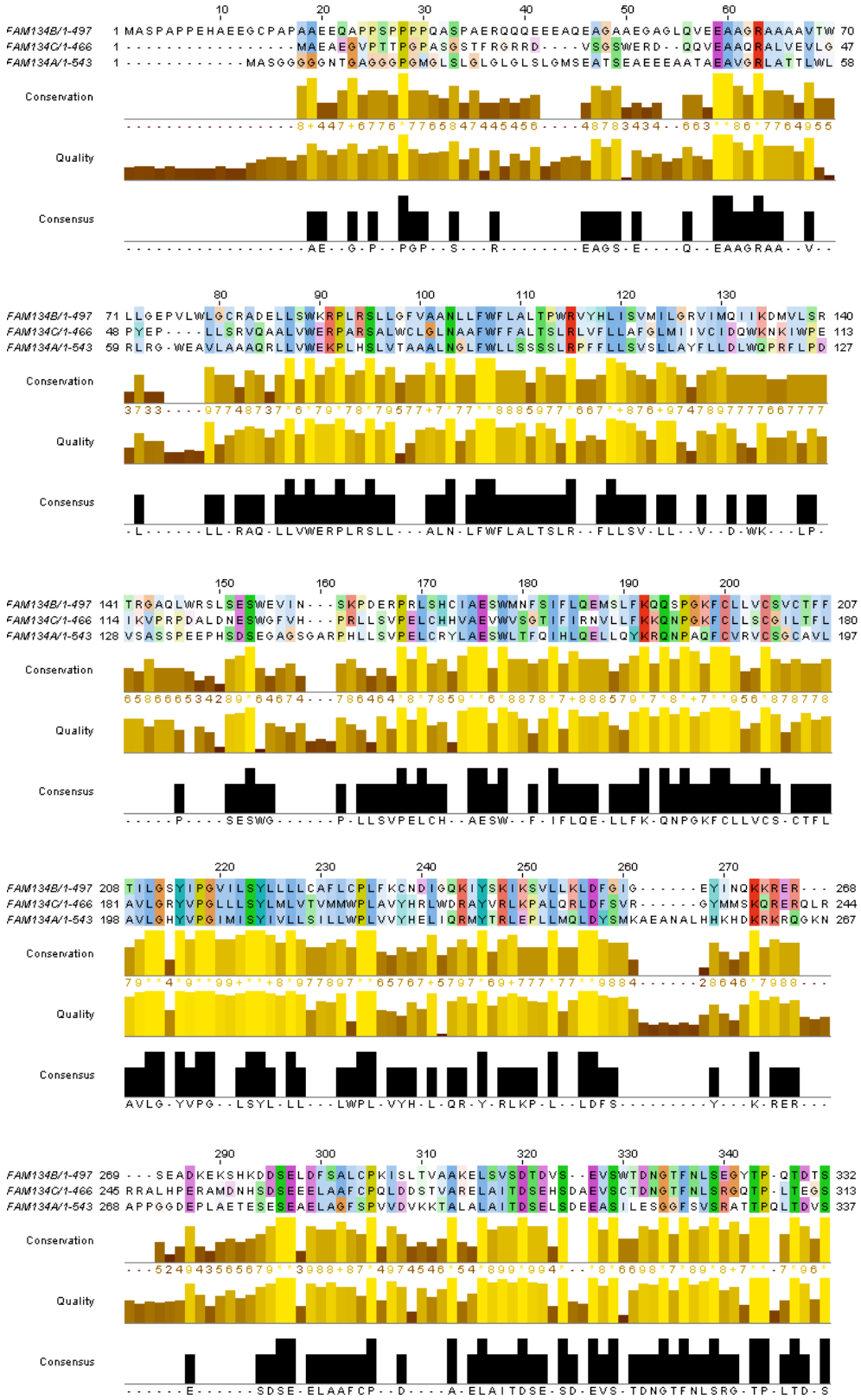
FAM134B/1-497
FAM134C/1-466
FAM134A/1-543
Conservation
Quality
Consensus

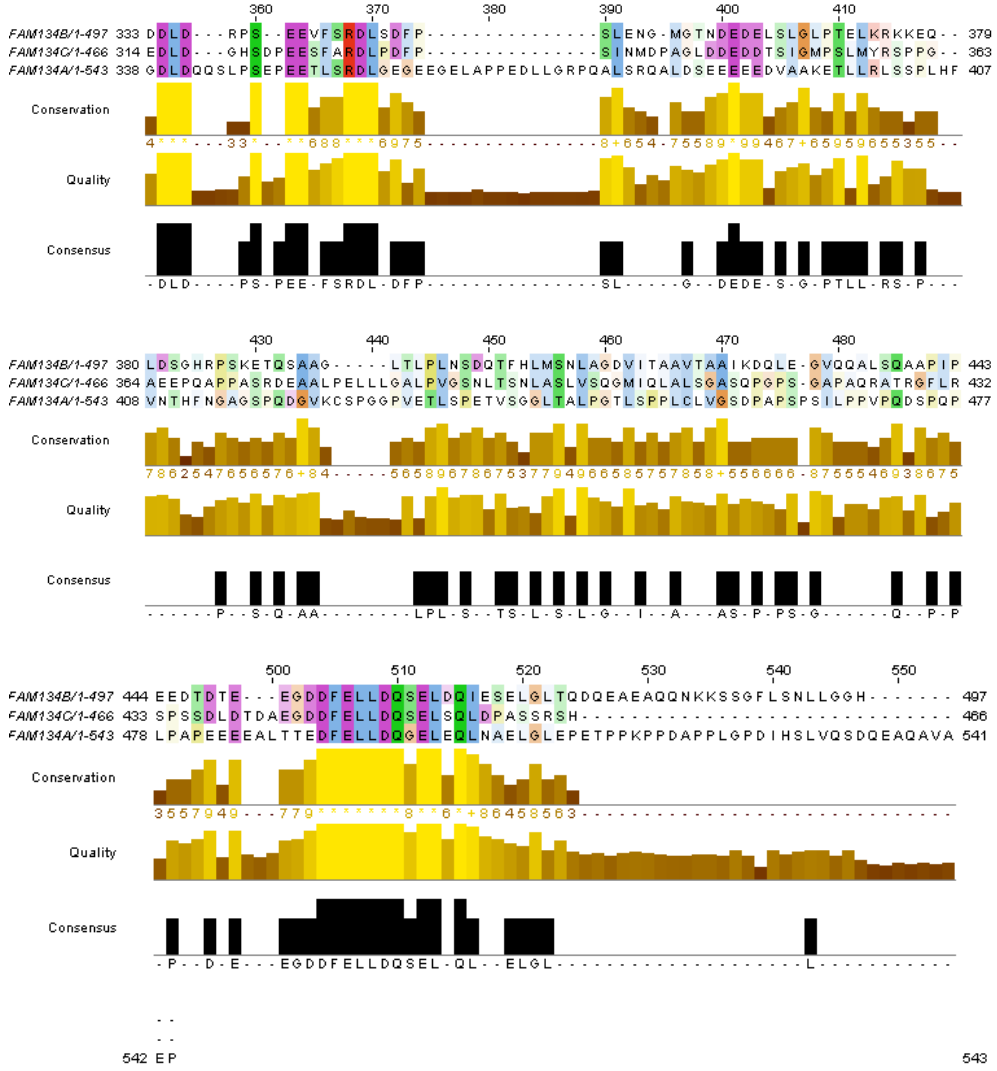

Figure 4.7: The ClustalW 2.0.8 multiple sequence alignment of FAM13B paralogs.

The alignment scores revealed by this multiple alignment are given below:

SeqA	Name	Len(aa)	SeqB	Name	Len(aa)	Score
1	FAM134B	497	2	FAM134C	466	33%
1	FAM134B	497	3	FAM134A	543	26%

Table 4.5: FAM134B paralogs multiple alignment pair-wise similarity scores.

This alignment reveals that there is 26% percent similarity between FAM134B and FAM134A and 33% percent similarity between FAM134B and FAM134C. The predicted transmembrane domains display a high degree of conservation between the paralogs. The serine residue at amino acid position

276, predicted to be phosphorylated, does not show conservation among the paralogs.

And here is the phylogenetic tree of the FAM134 gene family according to HOVERGEN database (Duret L. *et al.*, 1999), showing the divergence of the gene in vertebrates throughout time:

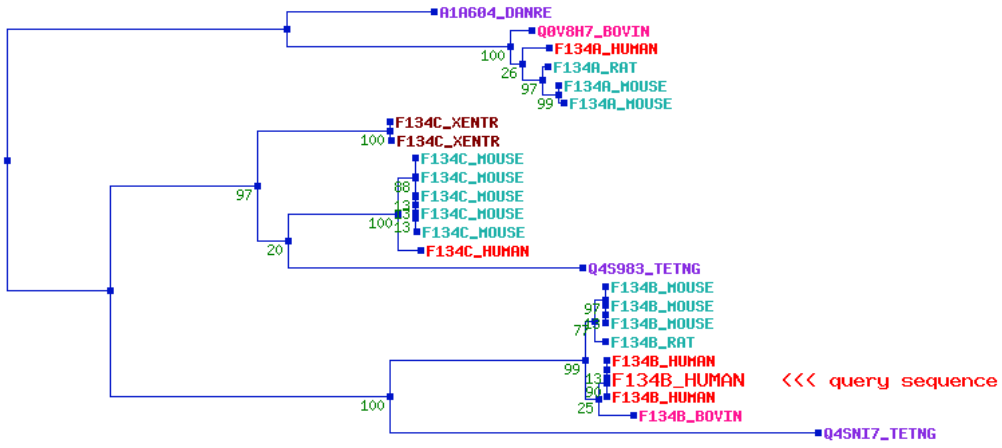

Figure 4.8: Phylogenetic tree of the FAM134 gene family
MOUSE: *Mus musculus,* **RAT:** *Rattus norvegicus*
XENTR: *Xenopus tropicalis,* **DANRE:** *Danio rerio*
BOVIN: *Bos taurus,* **TETNG:** *tetraodon negrovidis*

The closest orthologs of human FAM134B gene, according to this phylogenetic tree, are bovine, mouse and rat FAM134B genes. The FAM134B orthologous genes appear to have diverged from a common ancestor after a speciation event and have probably retained the same function in the course of evolution. FAM134A and FAM134C, which are the paralogs of FAM134B, are also depicted on the phylogenetic tree. These paralogs have little similarity to each other, as shown by the above alignment. Thus they are positioned on different branches of the phyogenetic tree in Figure 4.8. They appear to have diverged from a common ancestor after a gene duplication event and have probably evolved new functions, even if these are related to the original one.

4.1.4 FAM134B in Literature

Since FAM134B is a gene with an uncharacterized protein product, there are no research articles listed in 'PubMed' and only four research articles listed in 'PubMed Central' for FAM134B. The first one is an article named 'Classification of ductal carcinoma *in situ (DCIS)* by gene expression profiling' (Hannemann J. *et al.*, 2006). In this article, the authors have studied differences in gene expression between different types of DCIS and between DCIS and invasive breast carcinomas. In their study, FAM134B is ranked 19 in the list of 43 genes that are able to discriminate between well- and poorly differentiated DCIS. In another article titled 'Gene expression patterns in blood leukocytes discriminate patients with acute infections' (Ramilo O. *et al.*, 2007), FAM134B appears in the list of the 30 classifier genes distinguishing S. aureus from E. coli infections. In yet another article named 'Meta-analysis of human cancer microarrays reveals GATA3 is integral to the estrogen receptor alpha pathway' (Wilson BJ. and Giguère V., 2008), FAM134B is referred as a gene that has binding sites in its promoter region for ER-alpha but not far GATA3 transcription factor. Finally, in 'Aging impacts transcriptomes but not genomes of hormone-dependent breast cancers' article (Yau C. *et al.*, 2007), FAM134B appears in the list of differentially expressed genes between matched estrogen receptor (ER)-positive sporadic breast cancers diagnosed in younger (age $\leq$ 45 years) and older (age $\geq$ 70 years) Caucasian women.

4.1.4.1 Transforming capacity of FAM134B

The physiological role of FAM134B is yet not known. The only report focusing on any functional aspect of FAM134B is an article titled 'Oncogenic properties of a novel gene JK-I located in chromosome 5p and its over-expression in human esophageal squamous cell carcinoma'. This report concentrates only on FAM134B isoform 2, and not isoform 1, and refers to isoform 2 as 'JK-1', a name that has previously not been designated for this gene in any database. The results of this study have shown that of the thirteen ESCC cell lines and 30 surgical specimens of ESCC (esophageal squamous cell

carcinoma) studied, *JK-I* was over-expressed in 9 (69%) of the ESCC cell lines and 9 (30%) of the ESCC patient cases. Both NIH 3T3 and HEK 293 cells are reported to have acquired the properties of anchorage-dependent and -independent growth in response to JK-1 was over-expression. Furthermore, the researchers observed the formation of subcutaneous sarcomas in all (3/3) the athymic nude mice following the subcutaneous injection of NIH 3T3 cells over-expressing JK-1. The researchers claim that their results indicate that JK-1 is commonly over-expressed in ESCC and has a prominent capacity to transform normal cells. They emphasize this work as being the first evidence that the over-expression of JK-1 and its transforming capacity in normal cells may play a critical role in the molecular pathogenesis of ESCC (Tang WK. *et al.*, 2007).

4.1.4.2 FAM134B in Gene Expression Profiling Microarrays

In one microarray study, titled 'Using a xenograft model of human breast cancer metastasis to find genes associated with clinically aggressive disease' (Kluger HM. *et al.*, 2005), FAM134B was identified as a gene with a significantly down-regulated expression in a metastatic breast cancer cell line with respect to its non-metastatic counterpart, indicating a reverse correlation between FAM134B expression and the metastatic process.

In another study named 'Anti-proliferative effect of estrogen in breast cancer cells that re-express ER (Estrogen Receptor) alpha is mediated by aberrant regulation of cell cycle genes' (Moggs JG. *et al.*, 2005), the expression of FAM134B was shown to be significantly up-regulated in response to estradiol in MDA-MB-231 cells that have been engineered to re-express ER-alpha. Furthermore, through *in silico* analysis, three putative ERE (Estrogen Response Element) motifs were identified in the promoter of FAM134B.

In yet another study named 'Gene expression in human neural stem cells: effects of leukemia inhibitory factor (LIF) (Wright LS. *et al.*, 2004)', the researchers used LIF as an agent to prevent the senescence observed when human neural stem cells are passaged extensively and they observed an increase in the expression of FAM134B in these cells in response to LIF treatment.

In the study 'Expression profiling reveals novel pathways in the transformation of melanocytes to melanomas' (Hoek K. *et al.*, 2004), FAM134B was reported to exhibit increased expression as cells transformed from melanocytes to melanomas.

Finally, in the research article titled 'Discovery of novel methylation biomarkers in cervical carcinoma by global demethylation and microarray analysis' (Sova P. *et al.*, 2006), the expression of FAM134B was shown to re-activated in invasive cervical cancer cell lines in response to treatment with 5-aza-2'-deoxycytidine and trichostatin A, indicating a possible epigenetic control mechanism of FAM134B expression in this system.

4.1.5 Expression Data

On the UCSC (University of California, Santa Cruz) Genome Browser website, the expression data of FAM134B is gathered from several microarray studies. The data gathered from the GNF Expression Atlas 1 human data on Affy U95 chips (Su AI. *et al.*, 2002) , where red represents high expression level and green represents low expression level, is as follows:

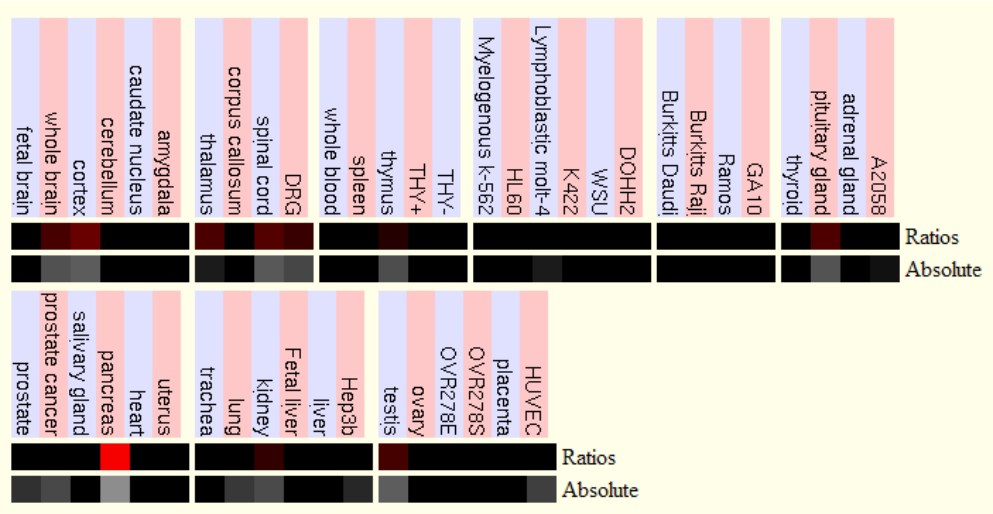

Figure 4.9: Expression data of FAM134B based on the GNF Expression Atlas 1 Human Data on Affy U95 Chips

According to this human expression data, high expression of FAM134B is observed in the central nervous system and testis, as wells as in thymus, kidney and notably in pancreas. In either adult or fetal liver, there isn't any apparent FAM134B expression.

The data gathered from the GNF Expression Atlas 2 data from U133A and GNF1H chips (Su AI. *et al.*, 2004), where red represents high expression level and green represents low expression level, is as follows:

Figure 4.10: Expression data of FAM134B based on the GNF Expression Atlas 2 Data from U133A and GNF1H Chips

According to this human expression data, FAM134B shows high expression levels in the central nervous system, T-cells, adipocytes, skeletal muscle, pancreas and testis cells. On the other hand, low levels of FAM134B have been detected in bone marrow, whole blood, lung, kidney, liver and ovary.

4.2 Confirmation of the association of FAM134B gene expression with replicative senescence in the Huh7 cell line model system

Prior to any functional or localization studies, the first step taken was the confirmation of the FAM134B gene expression data gathered from the gene expression profiling study. For this purpose, RT-PCR was performed on cDNA samples prepared from Huh7 C1 immortal, C3 late senescent clones to amplify the expressed FAM134B transcripts. The result of this RT-PCR is shown in Figure 4.11.

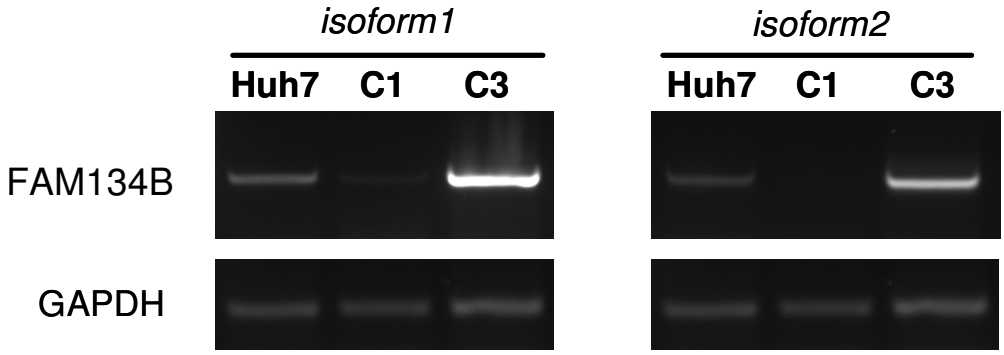

Figure 4.11: FAM134B is up-regulated in senescent clones of Huh7 when compared to their immortal counterparts. cDNA representing transcriptome of Huh7 (parental HCC cell line), C1 (immortal clone) and C3 (senescent clone) were prepared from freshly extracted RNA (1 µg) and were used for semi-quantitative RT-PCR experiments. GAPDH: Glyceraldehyde-3-phosphate dehydrogenase was used as an internal control.

According to the Figure 4.11, the expression of FAM134B gene is down-regulated in the C1 immortal clone compared to the parental Huh7 cell line. The expression level of the transcript variant 2 is much less than that of transcript variant 1 in the C1 immortal clone. In the C3 senescent clone, in contrast, the expression of both variants is up-regulated with respect to the parental Huh7 cell line, with transcript variant1 displaying a higher expression level than that of

transcript variant 2. All in all, these results clearly demonstrate the up-regulation of FAM134B in the senescent clones compared to immortal clones.

4.3 FAM134B Expression is down-regulated in liver cancer

4.3.1 FAM134B in Oncomine database

Oncomine database is an online cancer gene expression analysis platform dedicated to the academic and non-profit research community. It contains cancer microarray data obtained using several tissues (Rhodes DR. *et al.,* 2004). We were specifically interested in expression changes of FAM134B in liver arrays and according to this database, there are 17 liver arrays in which FAM134B is differentially expressed. Of these 17 arrays, FAM134B displays very significant (p-value ≤ 0.05) differential expression in one of them. In this study (Chen X. *et al.*, 2002), tumor and adjacent non-tumor tissues were collected from HCC patients and gene expression profiling was performed on these two sets of samples. As shown in Figure 4.12 ,the expression of FAM134B is significantly down-regulated (p-value=1.6E-16) in HCC as compared to non-tumor liver.

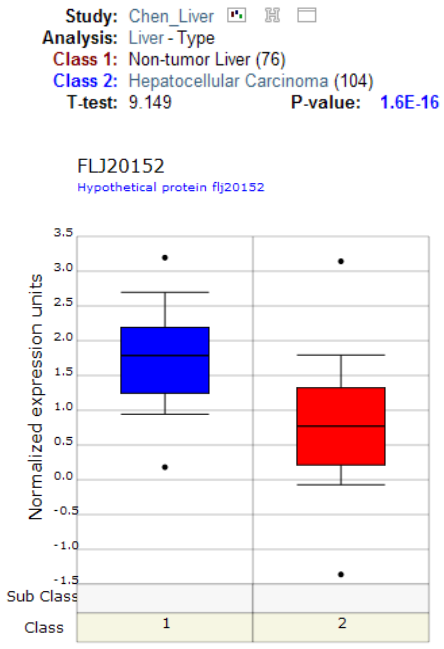

Chen X. *et al.* (2002)

Figure 4.12: Box plot images from Oncomine database displaying progressive down-regulation of FAM134B in liver cancer.

4.3.2 FAM134B in OncoDB HCC Database

'OncoDB.HCC' is a comprehensive oncogenomic database of hepatocellular carcinoma (Jou *et al.*, 2007). According to this database, FAM134B gene is listed as an HCC-significant gene, as it displays at least 2 folds expression change in 72% of patients in reprocessed Stanford microarray database, deposited here from again the study of Chen X. *et al.* (2002). Figure 4.13 illustrates this data, where the gene expression levels have been given in log base 2:

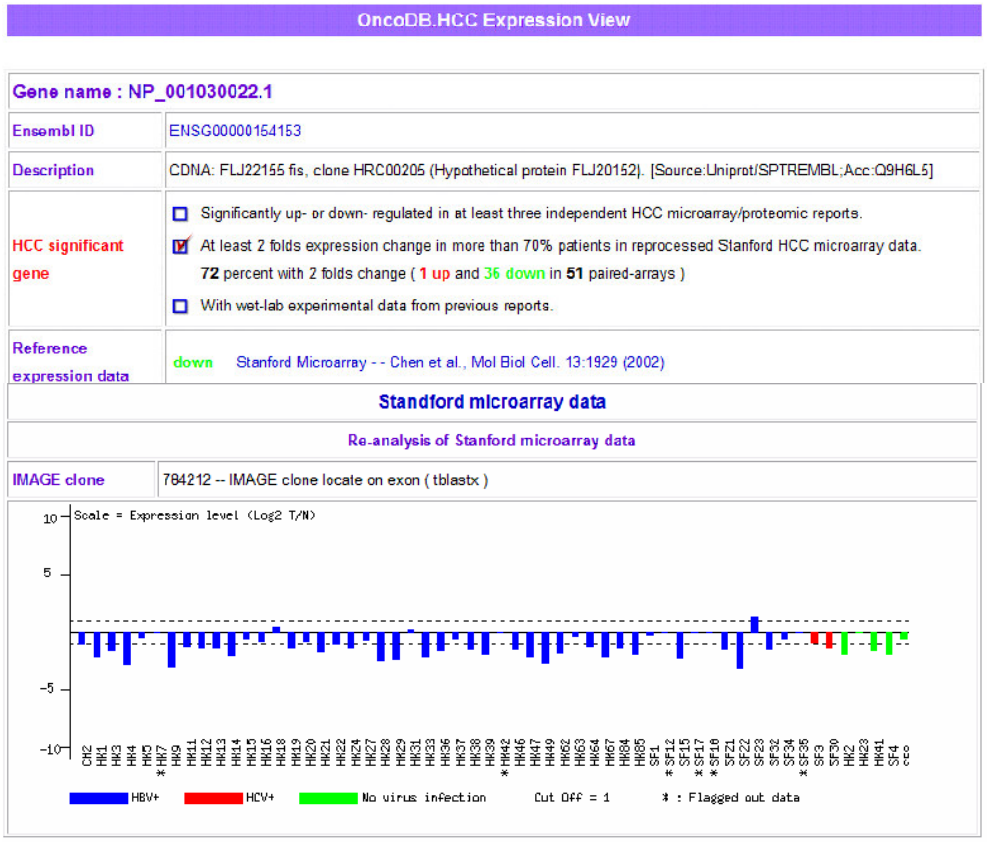

Figure 4.13: Down-regulated expression of FAM134B in Stanford HCC microarrays. Of the 51-paired arrays listed in the Standford HCC microarray database, FAM134B displays down-regulation in 36 of these microarray studies.

The majority of the down-regulation cases occur in HBV+ background, with a few displaying down-regulation in HCV+ background or with no virus infection at all. Also according to this database, FAM134B gene is located on the p arm of human chromosome 5 near a LOH (Loss of Heterozygosity) region. These data indicate that whereas normal liver cells express FAM134B protein,

its expression is lost in liver cancer cells and this loss of expression can be the result of loss of heterozygosity at the region around FAM134B gene . It's important to mention that these two features are characteristic of tumor suppressor genes.

4.3.3 FAM134B in Wurmbach Microarray Data

In 2007, Wurmbach *et al.* published a research article that aimed to characterize the molecular events of the hepatocarcinogenic process, and to identify new biomarkers for early HCC. In their study, the gene expression profiles of 75 tissue samples were analyzed representing the stepwise carcinogenic process from preneoplastic lesions (cirrhosis and dysplasia) to HCC, including 4 neoplastic stages (very early HCC to metastatic tumors) from patients with HCV infection. To have an idea of how the expression of FAM134B gene changes in the stepwise hepatocarcinogenic process, we queried FAM134B gene in the microarray data of Wurmbach *et al.*. The mean expression values were calculated for the two probes representing FAM134B in each disease stage. Furthermore, the different disease stages were merged as to end up with a total of five stages. The resulting expression values in log2 for different HCC stages are given in Figure 4.14:

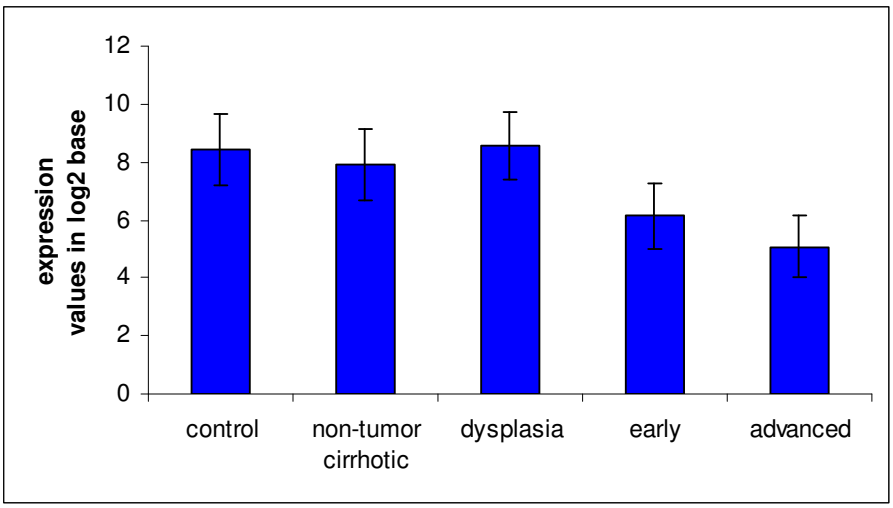

Figure 4.14: FAM134B expression in different HCC stages

In addition, hierarchical supervised clustering was performed on the data of Wurmbach. Following normalization with JustRMA method, the two probes representing FAM134B were chosen and hierarchical supervised clustering of genes was performed using Average Linkage and One Minus Correlation and the following image was obtained:

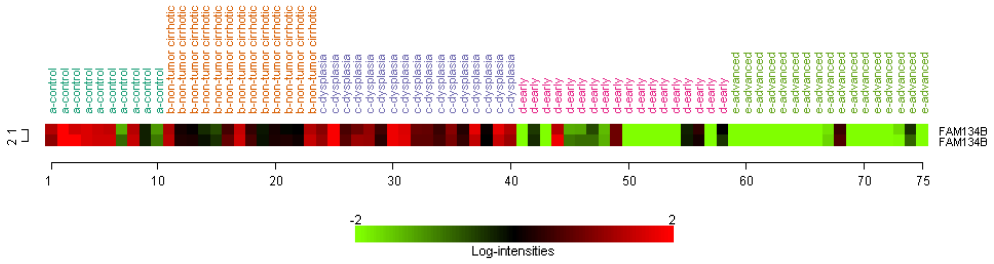

Figure 4.15: Hierarchical supervised clustering of FAM134B expression in Wurmbach data

It is clear from the graph displaying the expression values and from the hierarchical clustering image above that FAM134B gene expression is progressively down-regulated as liver disease progresses from cirrhosis to very advanced HCC.

4.4 Expression Data of FAM134B

4.4.1 Expression in Mouse Tissues

Of our initial interest was the tissue distribution of FAM134B gene throughout the body. This spatial expression information was gathered by RT-PCRs that checked the expression of the mouse homolog of FAM134B gene in a mouse tissue cDNA panel. The mouse homolog is called Riken cDNA 1810015C04 gene and like its human counterpart, it encodes two transcript variants. Again, like their human counterparts, these two variants are generated from a common mRNA by alternative splicing. Therefore, the two variants differ in their 5' exons and are 100% identical in the 6 exons at the 3' region.

The results of the PCR reactions displaying the tissue distribution of Riken cDNA 1810015C04 isoforms is given in Figure 4.16:

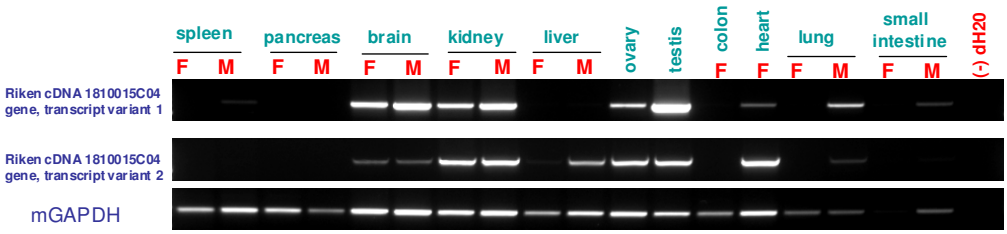

Figure 4.8: Riken cDNA 1810015C04 gene expression in mouse tissues mGAPDH: Mouse glyceraldehyde 3- phosphate dehydrogenase was used as an internal control. One male and one female mouse were sacrificed to generate duplicate data. The tissues were homogenized using a Downs homogenizer and subjected to RNA extraction, followed by cDNA synthesis. Some tissue samples yielded high quality RNA products, while others suffered from RNA degradation to some extent. Where possible, duplicate PCR reactions were carried out in pairs from the male and the female mouse cDNA samples.

According to the above data, the highest expression of the mouse homolog of FAM134B is observed in brain, kidney and testis. No expression of FAM134B isoform 1 and a low level of expression of FAM134B isoform 2 were observed in liver tissue.

4.4.3 Expression in Human Liver and Breast Cancer Cell Lines

Next, an expression study was carried out where the expression of both transcript variants of FAM134B gene were checked in a panel of human liver cancer cell lines by RT-PCR. Figure 14 displays this expression data, along with the corresponding GAPDH expression levels used for normalization.

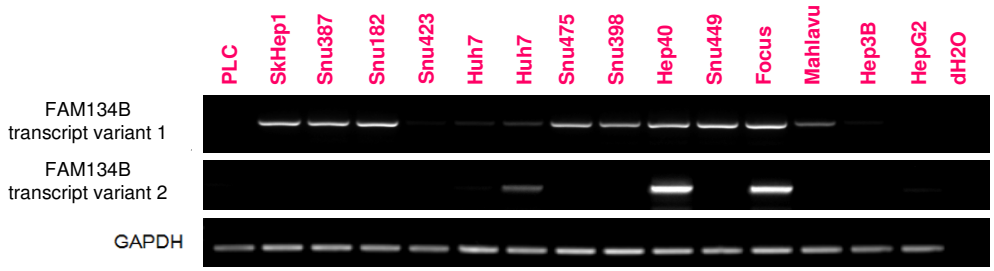

Figure 4.17: FAM134B expression in human liver cancer cell lines. GAPDH: Glyceraldehyde-3-phosphate dehydrogenase was used as an internal control.

The same expression study was performed also in a panel of human breast cancer cell lines. The results of this RT-PCRs are as below:

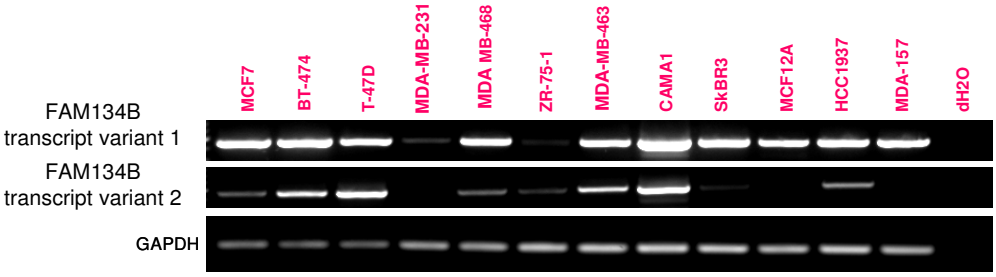

Figure 4.18: FAM134B expression in human breast cancer cell lines.
GAPDH: Glyceraldehyde-3- phosphate dehydrogenase was used as an internal control.

These expression results show that FAM134B transcript variant 1 is apparently more widely expressed among the HCC cell lines analyzed when compared to transcript variant 2. The same also holds true for the breast cancer cell lines analyzed. Both transcripts show heterogenous expression in HCC and breast cancer cell lines.

4.5 Transient ectopic over-expression of FAM134B isoforms

4.5.1 Transient transfection experiments with vectors encoding FAM134B isoforms

As already mentioned in the Methods chapter, four vectors encoding FAM134B isoforms were generated. These vectors are:

- NT-3XFLAG-FAM134B-1 (N-terminal FLAG tagged FAM134B isoform
- NT-3XFLAG-FAM134B-2 (N-terminal FLAG tagged FAM134B isoform 2)
- CT-3XFLAG-FAM134B-1 (C-terminal FLAG tagged FAM134B isoform 1
- CT-3XFLAG-FAM134B-2 (C-terminal FLAG tagged FAM134B isoform 2)

Using these circular vectors, along with the circular p3XFLAG-CMV10 (N-terminal FLAG empty control plasmid) and circular p3XFLAG-CMV14 (N-terminal FLAG empty control plasmid) vectors, transient transfections were performed in Huh7 cells grown on coverslips using Fugene6 transfection

reagent. In addition, HeLa cells were transiently transfected with NT-3XFLAG-FAM134B-2 vector using the same transfection reagent.

4.5.2 Immuno-blotting of FAM134B isoforms in transiently transfected Huh7 cells

Prior to sub-cellular localization experiments, we wanted to verify the FAM134B over-expression vectors that we had constructed. Therefore, we performed a FLAG immuno-bloting experiment. 48 hours following transfection, Huh7 cells transiently transfected with FLAG-tagged FAM134B encoding vectors were pelleted and lysed. 30ug of each cell lysate was loaded to a gel and blotted with FLAG mouse monoclonal antibody. The result of this immuno-staining is given in Figure 4.19:

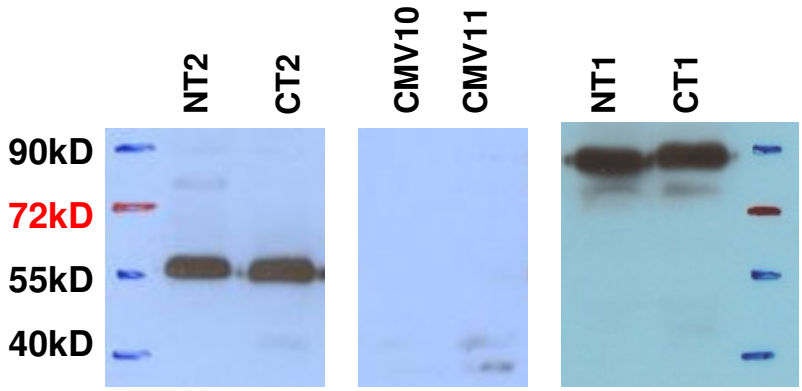

Figure 4.19: Immuno-blotting results of FLAG-tagged FAM134B isoforms.

*NT2: NT-3XFLAG-FAM134B-2 vector (N-terminal FLAG tagged FAM134B isoform 2) *CT2: CT-3XFLAG-FAM134B-2 vector (C-terminal FLAG tagged FAM134B isoform 2) *NT1: NT-3XFLAG-FAM134B-1 vector (N-terminal FLAG tagged FAM134B isoform 1)*CT1: CT-3XFLAG-FAM134B-1 vector (C-terminal FLAG tagged FAM134B isoform 1) *CMV10: p3XFLAG-CMV10 vector *CMV11: p3XFLAG-CMV14 vector

The FLAG antibody produced a single major band for each isoform, indicating that it recognized a specific protein. This immuno-blotting data also revealed an unexpected result. Whereas the predicted molecular weight of FAM134B isoform 1 is 55kD, the band it produced in the western blot represents (by comparison to the pre-stained molecular weight marker) a molecular weight of over 80 kDa (kilo daltons). Likewise, FAM134B isoform 2 appeared to have a

molecular weight of around 60 kDa, whereas its predicted molecular weight is only 39kDa. The empty control vectors did not produce any bands, as expected.

4.6 Sub-cellular localization studies of FAM134B protein

4.6.1 FAM134B protein localizes to the ER (Endoplasmic Reticulum)

After waiting for 48 hours to allow time for protein expression, immuno-fluorescence staining was performed on HeLa cells transfected, as outlined in section 4.4.2, with NT-3XFLAG-FAM134B-2 and pEGFPN1 vectors (to mark transfected cells) and this allowed the tracking of N-terminal FLAG tagged FAM134B isoform 2 using anti-FLAG mouse monoclonal antibody and DAPI for counterstaining. The images obtained at the end of this staining, along with the staining from the cells transfected with the empty control vector, are given below:

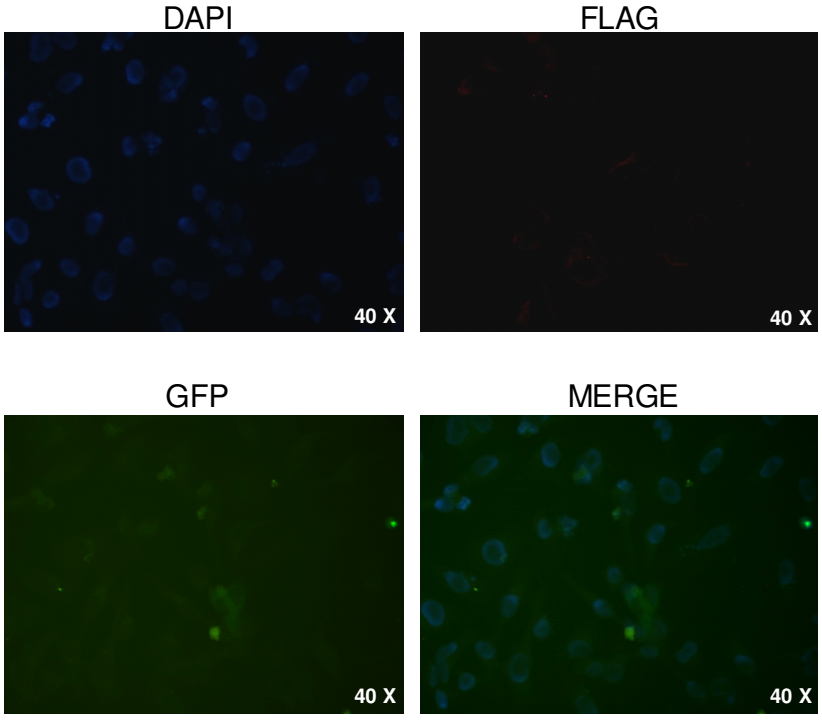

Figure 4.20a: Immuno-fluorescence staining results performed on HeLa cells transiently transfected with p3XFLAG-CMV10 empty vector (used to detect the background signal from anti-FLAG primary antibody) **and pEGFP-N1 vector** (to mark transfected cells) **using anti-FLAG mouse monoclonal antibody.**

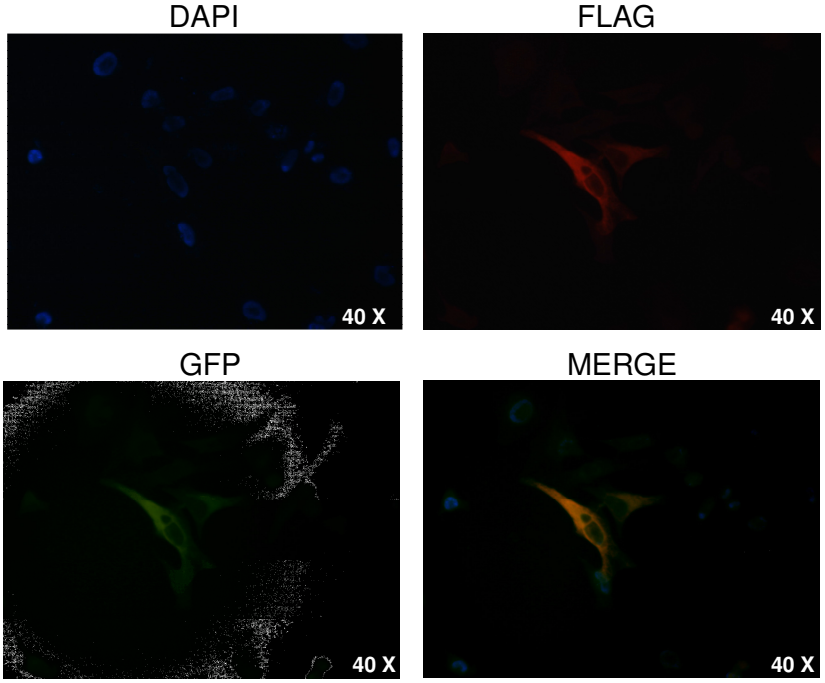

Figure 4.20b: Immuno-fluorescence staining results performed on HeLa cells transiently transfected with NT-3XFLAG-FAM134B-2 vector and pEGFP-N1 vector (to mark transfected cells) **using anti-FLAG mouse monoclonal antibody.**

The above immuno-fluorescence experiment revealed an asymmetrical, perinuclear staining pattern for FAM134B isoform 2. We noticed immediately that this staining pattern is very reminiscent of proteins that localize to the ER (Endoplasmic Reticulum). If this was the true sub-cellular localization of FAM134B, then it would have to co-localize with an ER-resident protein, like calnexin. Therefore we designed our next experiment as a FLAG-calnexin co-immuno-fluorescence staining on Huh7 cells transfected with all FAM134B-encoding constructs.

4.6.2 FAM134B protein co-localizes with calnexin, an ER resident protein

Following transient transfection of Huh7 cells with FAM134B-encoding constructs, as outlined in section 4.4.2, cells were incubated in a 5% CO_2 (carbon dioxide) chamber at 37°C for 48 hours to allow time for protein expression. At the end of this time, immuno-fluorescence staining was performed on these cells and N-terminal and C-terminal FLAG tagged FAM134B isoform 1 and isoform 2 were tracked using anti-FLAG mouse monoclonal antibody, anti-calnexin

rabbit polyclonal antibody and using DAPI for counterstaining. The images obtained at the end of this staining are given in Figure 4.21:

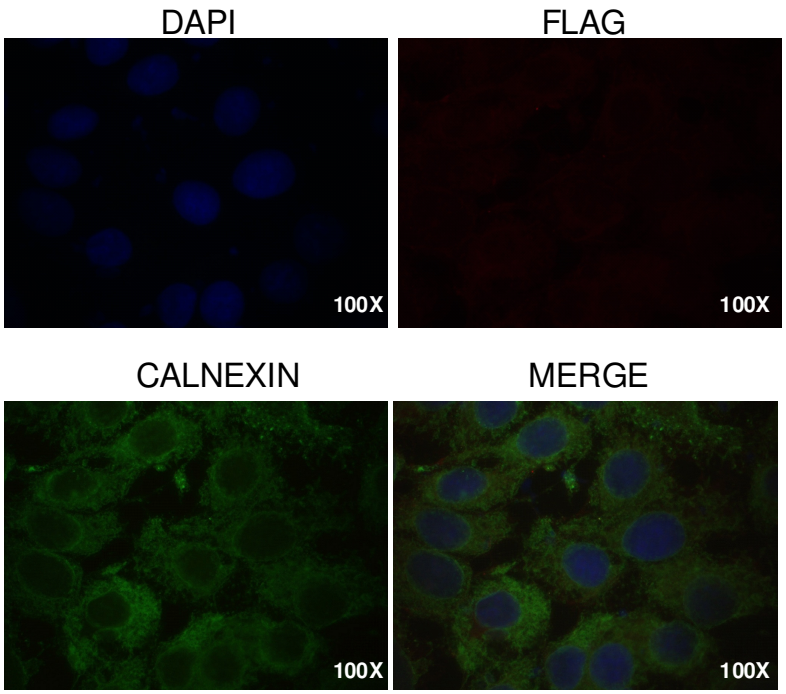

Figure 4.21a: Immuno-fluorescence images of Huh7 cells transfected with p3XFLAG-CMV10 control vector (used to detect the background signal from anti-FLAG primary antibody)

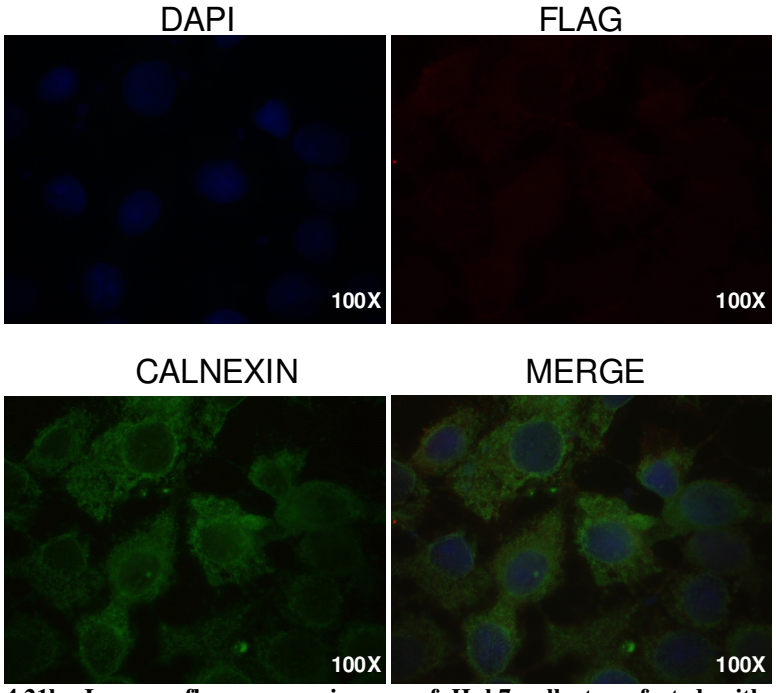

Figure 4.21b: Immuno-fluorescence images of Huh7 cells transfected with p3XFLAG-CMV14 control vector (used to detect the background signal from anti-FLAG primary antibody).

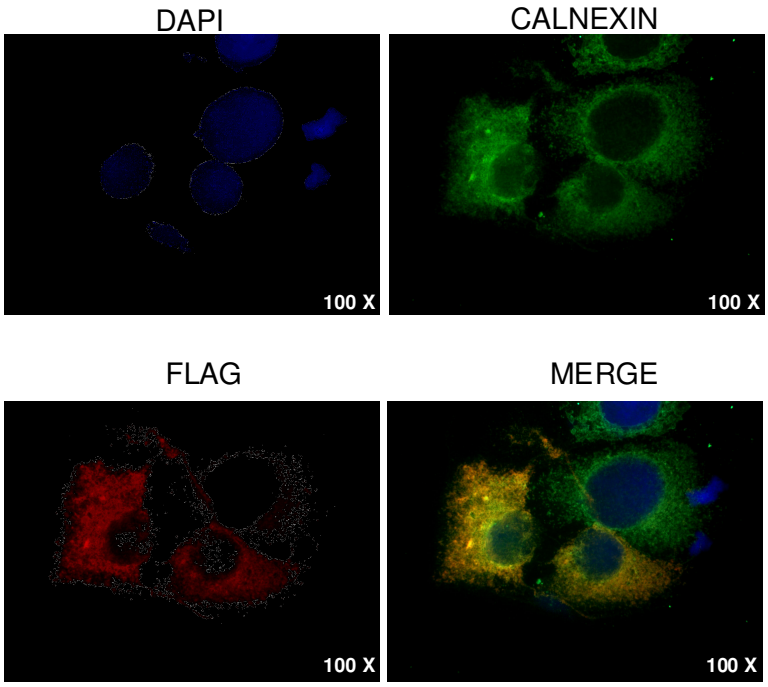

Figure 4.21c: Immuno-fluorescence images of Huh7 cells transfected with N-terminal FLAG-tagged FAM134B isoform 1 encoding vector.

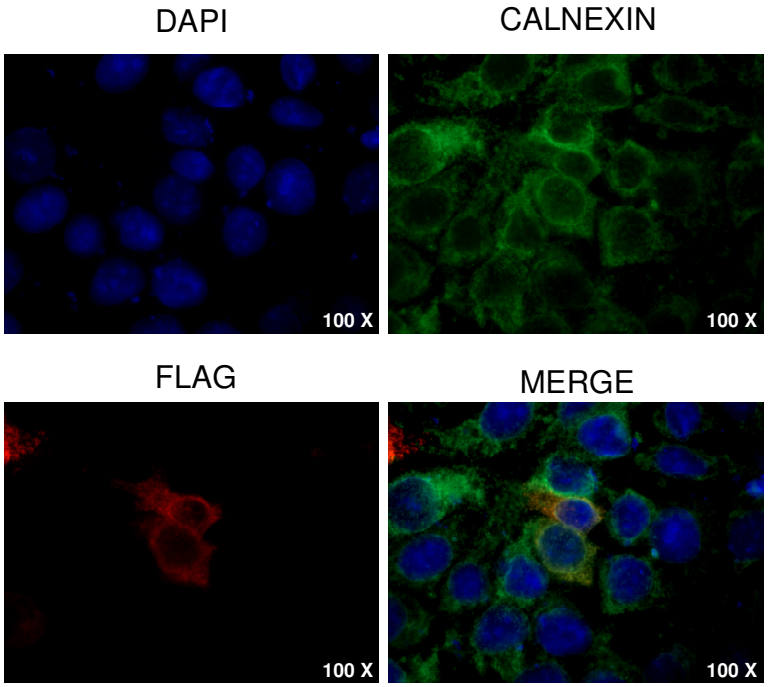

Figure 4.21d: Immuno-fluorescence images of Huh7 cells transfected with C-terminal FLAG-tagged FAM134B isoform 1 encoding vector.

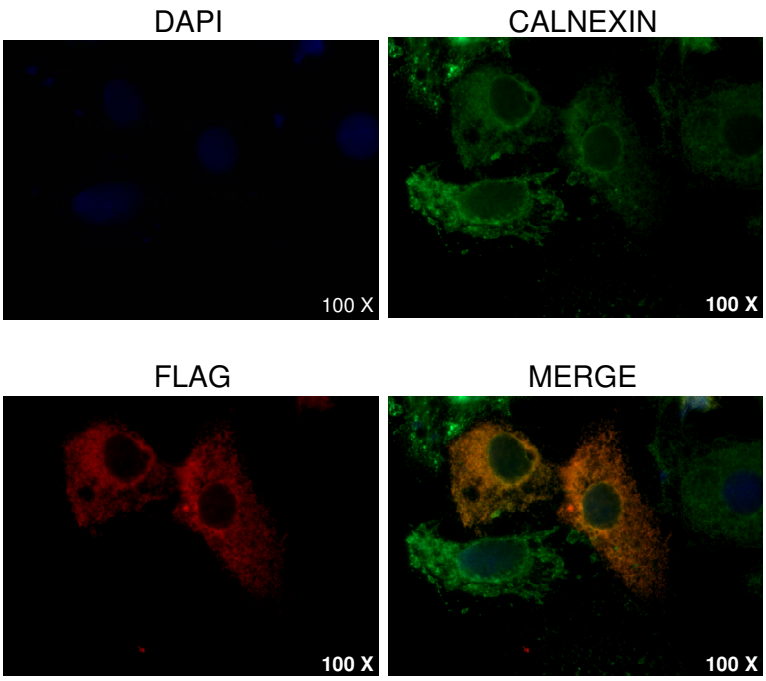

Figure 4.21e: Immuno-fluorescence images of Huh7 cells transfected with N-terminal FLAG-tagged FAM134B isoform 2 encoding vector.

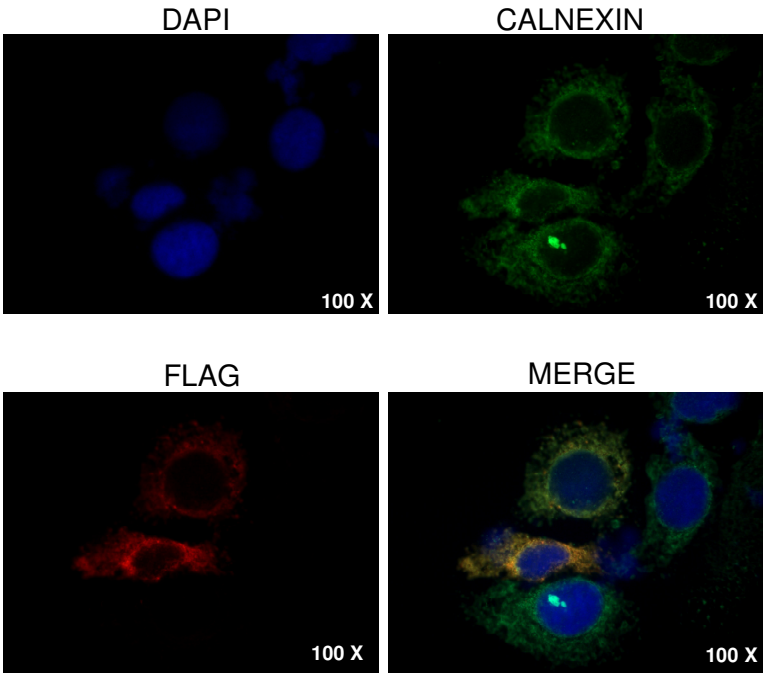

Figure 4.21f: Immuno-fluorescence images of Huh7 cells transfected with C-terminal FLAG-tagged FAM134B isoform 2 encoding vector.

In agreement with the results obtained from the FAM134B isoform 2 staining in the previous experiment, the asymmetrical, peri-nuclear staining is observed with all the other constructs. In addition, all FAM134B isoforms expressed display complete co-localization with calnexin, reinforcing the observation that FAM134B protein localizes to the ER.

4.7 Stable ectopic over-expression of FAM134B isoforms

For functional studies, we decided to over-express FAM134B in one of the liver cancer cell lines in our laboratory. We chose Huh7 cell line for this over-expression study as the basal expression level of both FAM134B transcript variants are very low in this cell line, as previously shown by RT-PCR experiments in Figure 4.17. As explained in the Methods section, Huh7-derived isogenic clones were generated that express one of the following vectors: NT-3XFLAG-FAM134B-1, NT-3XFLAG-FAM134B-2, CT-3XFLAG-FAM134B-iso-1, CT-3XFLAG-FAM134B-iso-2, p3XFLAG-CMV10 (control) and p3XFLAG-CMV14 (control) vectors.

4.7.1 Selection of positive Huh7 clones over-expressing FAM134B protein isoforms

For selection of positive over-expression clones, pellets were collected from cells as they were propagated in cell culture. Following lysis of the pellets for protein extraction, the clones were screened for positivity by a western blot experiment using FLAG mouse monoclonal antibody. The results of this screening are below:

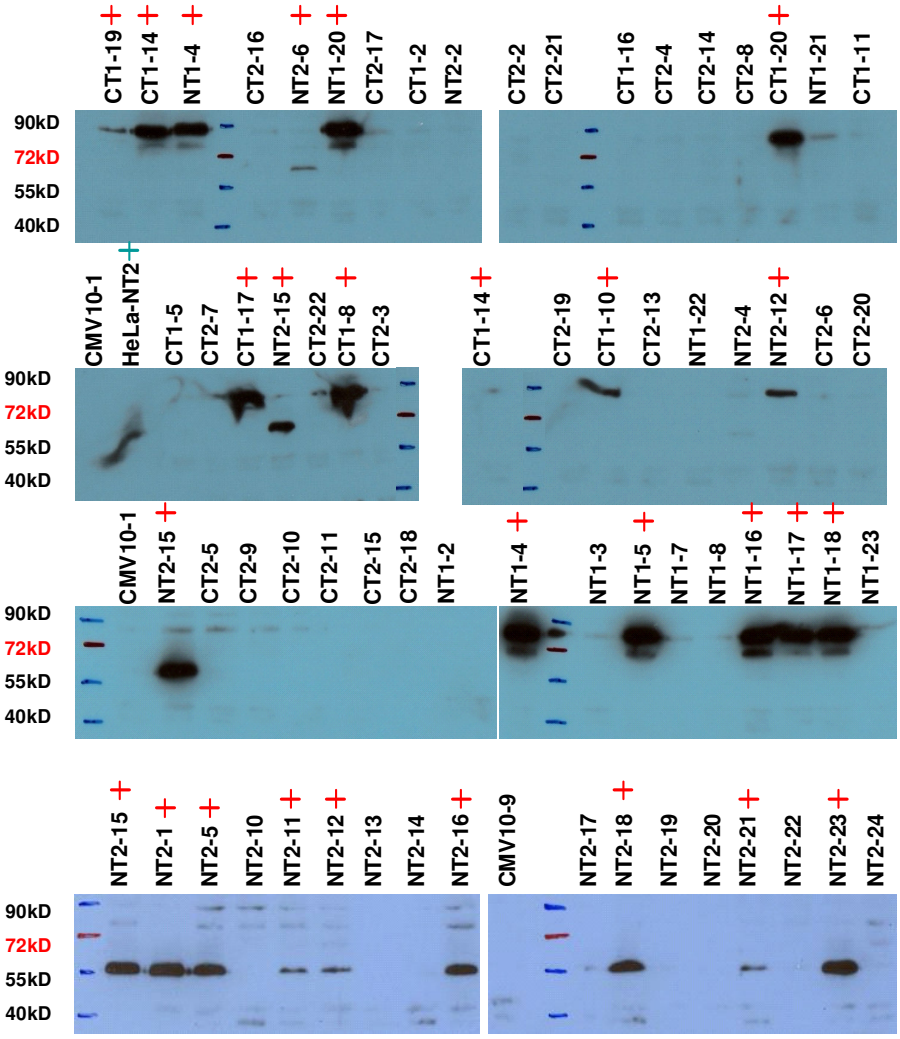

Figure 4.22: Selection of positive Huh7 clones over-expressing FAM134B protein isoforms
CMV10: colonies generated with p3XFLAG-CMV10 plasmid**,** NT1: colonies generated with NT-3XFLAG-FAM134B-1 plasmid**,** NT2: colonies generated with NT-3XFLAG-FAM134B-2 plasmid**,** CT1: colonies generated with CT-3XFLAG-FAM134B-1 plasmid**,** CT2: colonies generated with CT-3XFLAG-FAM134B-2 plasmid
+: positive control lysate of HeLa cells transiently transfected with NT-3XFLAG-FAM134B-2 plasmid
+ : indicates positive clones**.** The molecular weights corresponding to different bands of the standard molecular weight marker have been indicated at the right side of each blot.

4.7.2 Selection of positive Huh7 clones with genome-integrated empty vector

For clones generated with the empty control plasmids, screening was not possible by FLAG western blotting as there was no protein with a FLAG eptiope that could be recognized by the FLAG antibody. Instead, integration of the plasmids into the genome was assessed by screening through genomic DNA

extraction from the pellets of the empty control clones, followed by PCR analysis using the commercial CMV30 forward and CMV24 reverse sequencing primers of the p3XFLAG-CMV10/ p3XFLAG-CMV14 plasmids. The results of this PCR screening are given below:

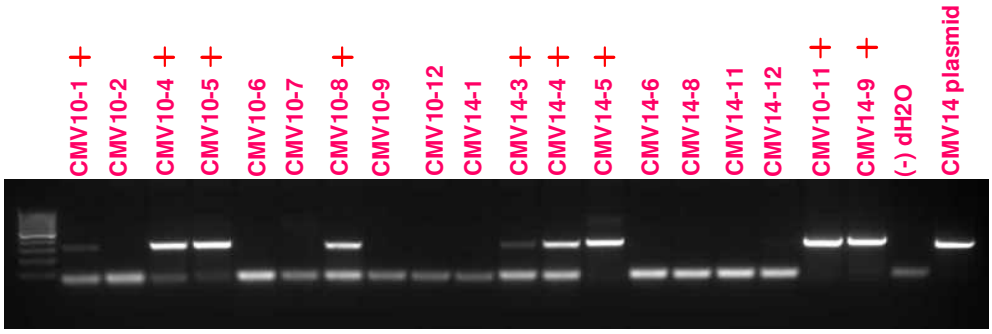

Figure 4.23: Selection of positive Huh7 clones with genome-integrated empty vector +: indicates positive clones. PCR was performed using 200ng of genomic DNA from each sample. The PCR reaction at the last lane of the gel named 'CMV14 plasmid' was performed using 200 ng of p3XFLAG-CMV14 plasmid as template to serve as a positive control reaction in this PCR screening protocol. The positive band appeared around 300bp, as expected.

As revealed by the screening protocols, not all the colonies tested yielded positive results. The ratios of total number of clones tested/number of positive clones for each construct are listed below:

- p3XFLAG-CMV10: 5/10

- p3XFLAG-CMV14: 4/9

- NT-3XFLAG-FAM134B-1 plasmid: 6/13

- NT-3XFLAG-FAM134B-2 plasmid: 10/20

- CT-3XFLAG-FAM134B-1 plasmid: 5/10

- CT-3XFLAG-FAM134B-2 plasmid: 0/20

Except for CT-3XFLAG-FAM134B-2 plasmid, positive clones were obtained from all constructs. For the next set of experiments, one positive colony was chosen from each construct: CMV10-11, CMV14-9, NT1-4, CT1-14 and NT2-15.

4.7.3 Testing of positive Huh7 FAM134B over-expressing stable clones for monoclonality

Prior to any functional studies, as a final step, the monoclonality of these five clones was checked by performing an immuno-peroxidase staining on them using a FLAG antibody, followed by hematoxylene counterstaining. Below are the results of this immuno-staining experiment:

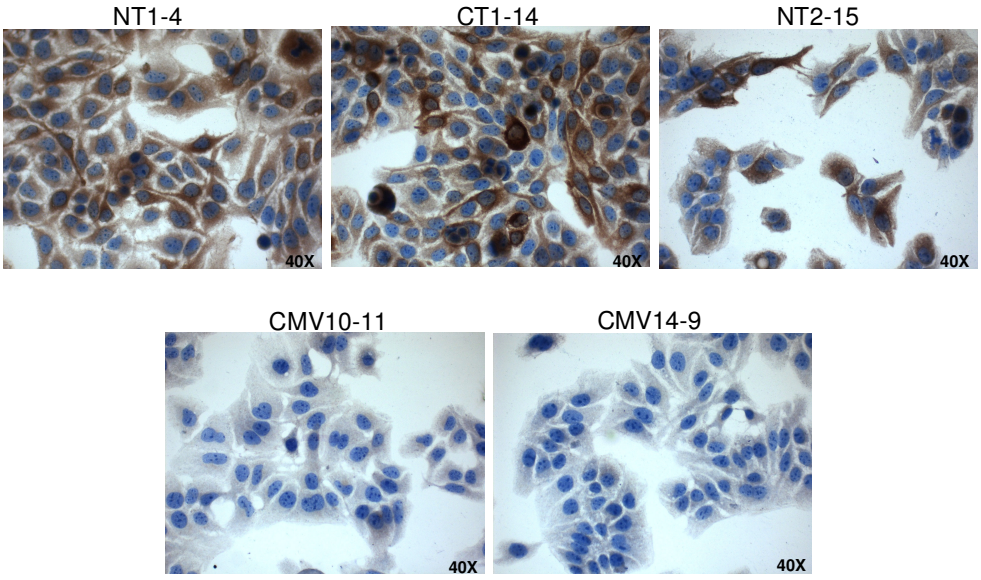

Figure 4.24: Anti-FLAG immuno-peroxidase staining on Huh7 stable FAM134B over-expressing stable clones. The brown staining indicates FLAG tagged FAM134B protein in cells. The faint staining from CMV10-11 and CMV14-9 clones represent the background staining from the FLAG antibody. Counterstaining was performed with hematoxylene.

As can be seen in the above images, the immuno-staining experiment revealed 100% positivity for the expression of the FLAG tagged FAM134B protein in the clones analyzed. The interpretation of this staining pattern is that they are monoclonal, meaning that each clone is single cell-derived.

4.8 Functional Studies performed with Huh7 FAM134B over-expressing stable clones

Having identified FAM134B as a protein localizing into the ER, we were now interested in elucidating its function in cells. For functional studies, we had the FAM134B over-expression clones as a system to use for testing our hypotheses on the function of this protein. Since FAM134B gene was identified as a senescence associated gene, our first hypothesis was that it had a causative role in senescence. In parallel to this, we hypothesized that it would change the proliferation rates of cells. Our final hypothesis was that this ER protein had a role in regulating the response of cells to ER-stress. Our rationale for forming each of these hypotheses as wells as or strategies for testing them will be discussed one by one below.

4.8.1 FAM134B over-expression does not induce senescence in Huh7 cells

Our starting point in choosing to concentrate on FAM134B protein was its significant up-regulation in senescent Huh7 clones compared to immortal Huh7 clones. Therefore, as a next step in our study, we asked the obvious question of whether FAM134B expression caused any changes in the parental Huh7 clone in terms of its senescence behaviour. In order find an answer to this question, we performed a SABG (Senescence-Associated Beta-Galactosidase) assay on the five different afore-mentioned clones, followed by FLAG immuno-peroxidase staining. Following fixation and subsequent X-gal incubation of the cells for 24 hours, they were subjected to immuno-peroxidase staining using a FLAG mouse monoclonal antibody. Figure 4.14 displays the results obtained at the end of this experiment:

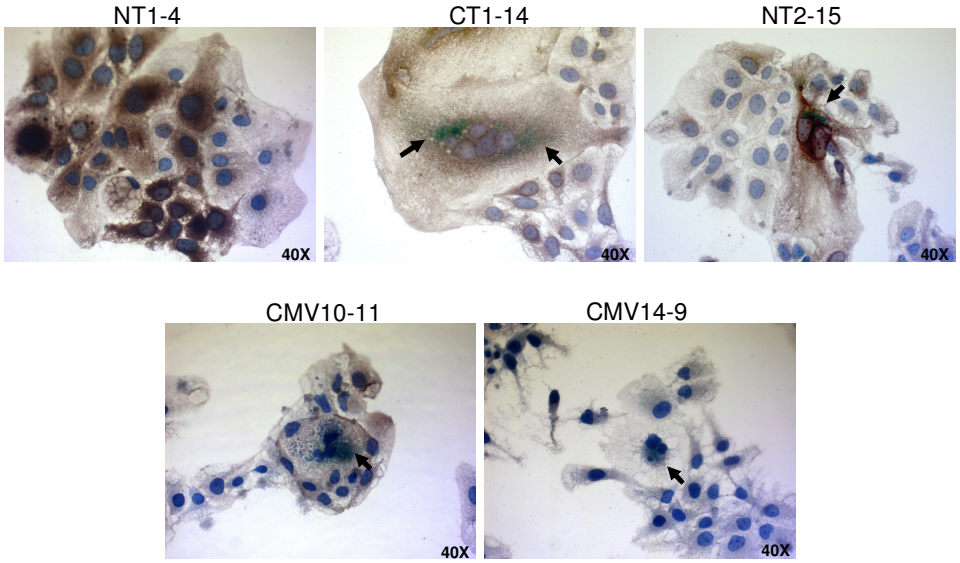

Figure 4.25: SABG-FLAG co-immuno-peroxidase staining of Huh7 stable FAM134B over-expression clones. The brown staining indicates FLAG tagged FAM134B protein in cells. Arrows indicate green cells displaying green SABG staining. Counterstaining was performed with hematoxylene.

This SABG-FLAG co-immuno-peroxidase experiment revealed a very low number of cells that stained positive for SABG activity. These few green cells displaying positive SABG index were observed both in clones over-expressing FLAG-tagged FAM134B protein and in clones expressing the empty control vectors and there wasn't any readily observable difference between the SABG indices of the FAM134B over-expressing clones versus the control clones. Furthermore, flat, enlarged and multi-nucleated cells reminiscent of the senescent cells could be observed both in the over-expression clones and in the control clones and not all of these cells displayed positive SABG index. The overall results of this experiment indicate that FAM134B overexpression does not induce senescence in Huh7 cells.

4.8.2 FAM134B over-expression has no effect on Huh7 cell proliferation rate

Having found out that FAM134B protein has no causative role in senescence, we asked the next question of whether it has any effect on the proliferation rate of cells. In seeking an answer to this question, we performed a BrdU incorporation assay on our FAM134B over-expressing clones. We incubated our clones with BrdU for 4 hours and performed immuno-peroxidase staining using a BrdU mouse monoclonal antibody. Cells that were positive as well as those that were negative for BrdU incorporation could clearly be distinguished under microscope light. The following figure presents the results of this BrdU incorporation assay:

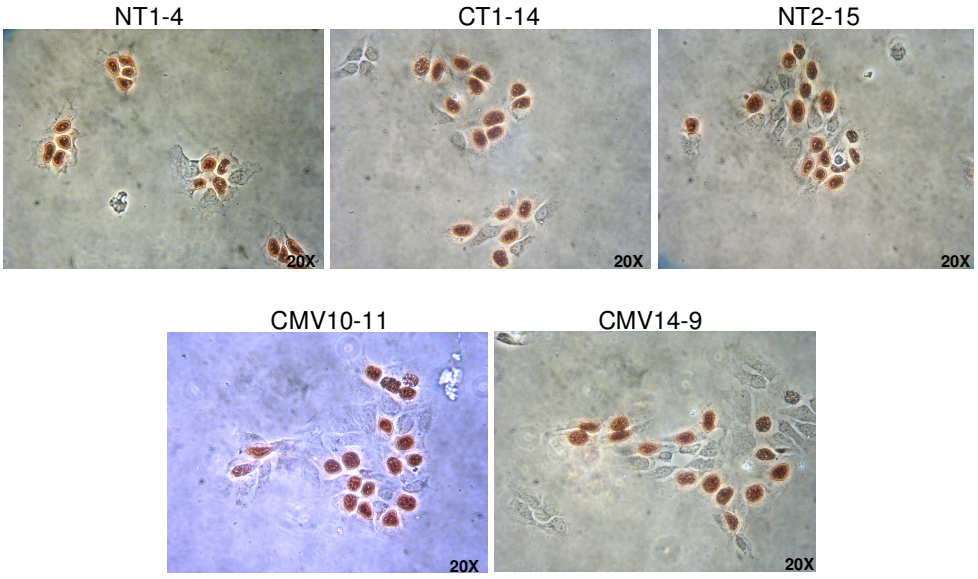

Figure 4.26: BrdU immuno-peroxidase staining on Huh7 stable FAM134B over-expression clones. The brown staining indicates BrdU incorporated into the nucleus.

As seen in Figure 4.26, there are a high percentage of cells with positive BrdU staining. To assess the difference between the BrdU incorporation rates of FAM134B over-expressing clones versus control clones, quantification was

performed through manual counting of cells under microscope light. For each slide representing one clone, 10 fields were randomly chosen and BrdU positive as well as BrdU negative cells were counted. For each field, a BrdU positivity percentage was calculated and the means and standard deviations of the percentages of these 10 fields were worked out. The resulting quantification data is presented below:

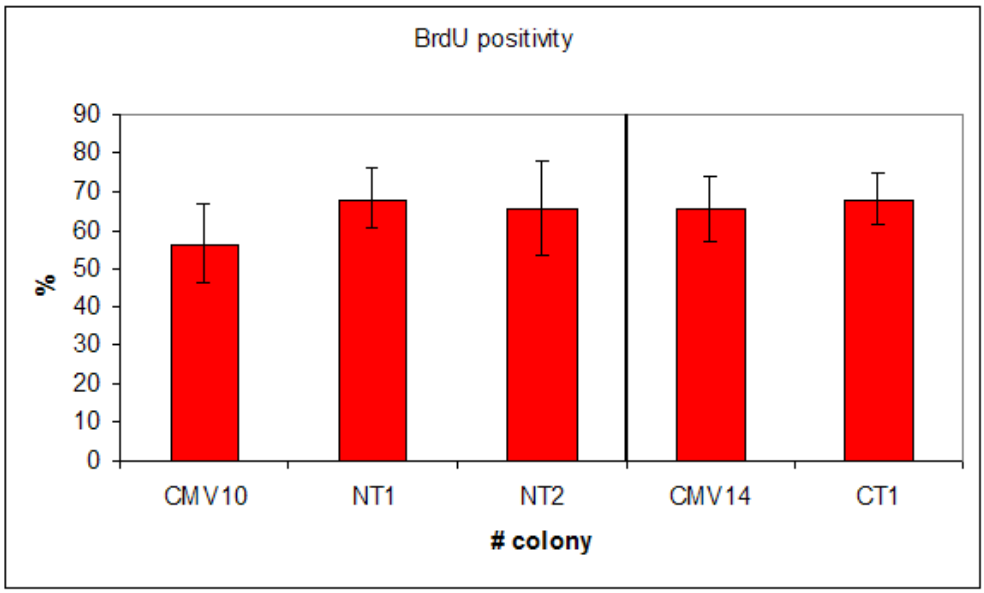

Figure 4.27: Quantification of BrdU immuno-peroxidase staining on Huh7 stable FAM134B over-expression clones.

As can be interpreted from the graph, the BrdU incorporation percentages of the different clones are close to each other, except for a slight difference between the N-terminal FLAG-tagged FAM134B over-expression clones and the corresponding CMV10-11 stable clone. The overall results imply that FAM134B over-expression doesn't have any significant effect on Huh7 cell proliferation.

4.8.3 FAM134B over-expression revealed no observable effect on response of Huh7 cells to ER-stress

Previous experiments have demonstrated that FAM134B protein localizes to the ER. It The function of ER is to provide an optimal environment for the synthesis, folding, and assembly of membrane and secreted proteins. The accumulation of unfolded or misfolded proteins in the ER under conditions of "ER stress" threatens the normal functioning of eukaryotic cells. It has been known for long that hepatocytes contain abundant endoplasmic reticulum (ER) which is essential for protein metabolism and stress signaling. It has also been known for quite some time that senescent cells have abundant ER activity and that secretive pathways undergo dramatic changes in these cells in order to meet the high demands of secretion of proteins like inflammatory cytokines, growth factors and other molecules that can alter the local tissue microenvironment (Campisi J., 2008).

Based on the above information and the fact that FAM134B expression is up-regulated in senescent Huh7 clones, we reasoned that the ERs of these senescent cells could be acquiring a new organization with FAM134B protein being employed somewhere in this process and that FAM134B over-expression could change the response of Huh7 cells to ER-stress. To test this hypothesis, we took the approach taken by Delom F. *et al.* (2007) and treated our FAM134B over-expressing Huh7 clones with various doses of tunicamycin, an antibiotic that induces ER stress through prevention of formation of N-acetylglucosamine lipid intermediates and glycosylation of newly synthesized glycoproteins. Huh7 FAM134B over-expression clones were seeded into 96 well-plates as triplicate and incubated for 24 hours with various doses of tunicamycin. Following this treatment, dis-attached cells were washed off with 1X PBS and the extent of cell survival was quantified by performing an SRB (Sulforhodamine B) assay on the remaining attached cells. Using the Elisa reading values from each well, the percent of surviving cells was calculated for each well by dividing the Elisa reading of that well to that of the untreated control well. The graph obtained from this calculation is given below:

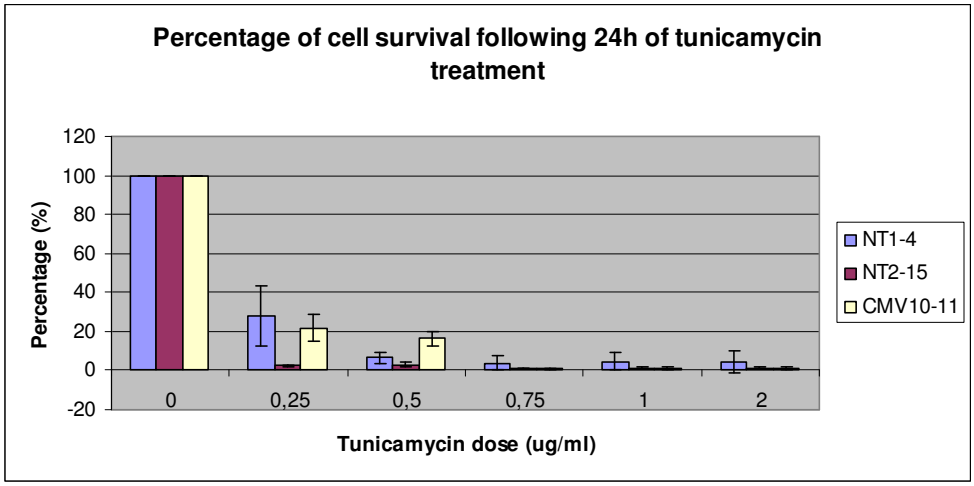

Figure 4.28a: Graph representing percentage of cell survival of NT1-4, NT2-15 and their control CMV10-11 clone following 24 hour of tunicamycin treatment at different doses. Data is derived from triplicate experiment**.** 0mg/ml cells have been treated with DMSO only.

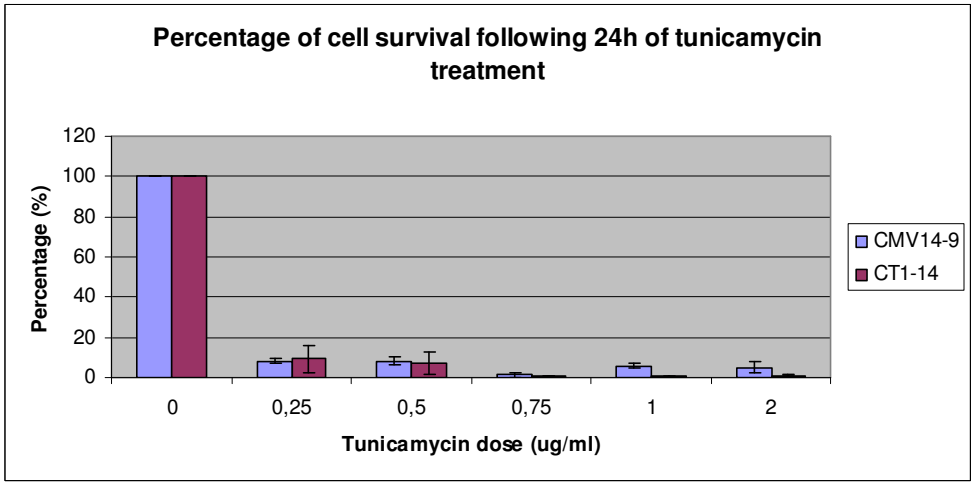

Figure 4.28b: Graph representing percentage of cell survival of CT1-14 and its control CMV14-9 clone following 24 hour of tunicamycin treatment at different doses. Data is derived from triplicate experiment. 0mg/ml cells have been treated with DMSO only**.**

According to the above graphs, there doesn't seem to be a major difference between the different clones' response to ER-stress induced through tunicamycin. According to Figure 4.28a, the sensitivity of NT1-4 clone to

tunicamycin is not changed compared to that of the CMV10-11 control clone. Compared to this same clone, however, the sensitivity of NT2-15 clone to tunicamycin shows a slight increase, as revealed by a decrease in cell survival percentage.

According to Figure 4.28b, there isn't a significant difference between the sensitivities of CT1-14 clone and its control CMV14-9 clone to tunicamycin treatment. All in all, these experiments indicate that FAM134B over-expression has no overall significant effect on the response of Huh7 cells to ER-stress induced through tunicamycin treatment. The over-expression of N-terminal FLAG-tagged FAM134B isoform 2 causes a slight decrease in the sensitivity of Huh7 cells to tunicamycin, which needs to be verified by further experiments.

CHAPTER 5. DISCUSSION AND CONCLUSION

In this study, we focused our attention on a novel gene named FAM134B, the protein product of which had previously not been studied in any detail. Our starting point for concentrating on this protein is the result of a microarray study that was performed by our group (Ozturk M. *et al.*, unpublished data) for identifying the gene expression profiling differences between the senescent and the immortal Huh7 stable clones established previously (Ozturk N. et al, 2005). In the significant gene list representing the most differentially expressed genes between these clones, FAM134B appeared as a gene that was significantly (p-value = 1.097E-06) up-regulated in senescent clones with respect to immortal clones. Therefore, we decided to characterize the protein product of FAM134B gene in terms of sub-cellular localization and function and in doing so, assess any causative role that this protein may have in the senescence programming induced in Huh7 cells.

We started off by verifying the differential expression data of FAM134B in our clones. The RT-PCR performed on the cDNA of these clones showed that both FAM134B transcript variants displayed down-regulation in immortal clones as compared to the parental Huh7 clones and up-regulation in the senescent clones as compared to the immortal clones. We carried on with meta-analysis of FAM134B mainly in HCC microarrays and identified FAM134B gene in several HCC microarray databases as an HCC significant gene that displayed progressive down-regulation in liver disease. It's not hard to notice that the features listed on FAM134B in these databases (progressive down-regulation in liver disease, genomic location near a LOH region, down-regulation in HCC accompanied by metastasis) are reminiscent of the features a tumor suppressor gene.

As mentioned earlier in the text, there has only been one report published on FAM134B protein so far and this report focuses on FAM134B isoform 2 under the name of 'JK-1'. In this report, the researchers claim that their results indicate that JK-1 is commonly over-expressed in ESCC and has a prominent

capacity to transform normal cells. They present their overall results as the first evidence that the over-expression of JK-1 and its transforming capacity in normal cells may play a critical role in the molecular pathogenesis of ESCC. This conclusion is interesting from the point of view that while one protein can act as a 'tumor-suppressor' in one system, it can conversely act as an 'oncogene' in another, reflecting the complexity of functional protein organization of cells.

Our next step in this study was to check the expression of FAM134B transcript variants in HCC and breast cancer cell lines, as well as in a mouse cDNA tissue panel. In the cDNA panel expression study, highest expression was observed in brain, kidney, ovary and testis tissues and a low level of expression was observed in liver tissue, in agreement with the GNF Expression Atlas human data in Figure 4.9 and Figure 4.10. At this point, there comes a question of why FAM134B expression is not detected in normal liver, although it's proposed as a potential tumor suppressor. One possible answer to this question is that FAM134B expression goes up as cells undergo aging, becoming higher at senescence arrest stage. So, we do not detect it easily in young mouse liver. Another possible answer is that its expression in humans is different from that of mice. In our cDNA panel expression study, for some tissues differences were observed between the expression levels from the cDNAs of different genders. These expression differences between the two genders in some tissues may be due to differential RNA degradation in samples or may reflect differential physiological transcriptional regulation events.

In the sub-cellular localization studies that we performed with Huh7 cells transiently over-expressing FAM134B isoforms, we observed an asymmetrical, perinuclear staining for FAM134B protein. Subsequent FLAG-calnexin-co-staining experiments identified FAM134B as an ER protein. Proteins localized to the ER usually have a signal sequence that directs them to the ER during intracellular protein transport at or near their N-terminus. Analysis of the FAM134B isoform sequences didn't reveal any such known ER-targeting motifs. Such signal peptide motifs are usually cleaved off proteins once they enter the ER. Suspecting that FAM134B protein could possess a novel signal

peptide for ER targeting and that this peptide could be cleaved off the protein once inside the ER, we were worried that the N-terminal flag tag that we fuse to this protein could mask such a signal peptide and consequently change the protein's final sub-cellular destination. Therefore, during vector construction, the cloning strategy was designed such that FAM134B transcript variants were fused to both N-terminal and C-terminal flag tags. In the sub-cellular localization experiments, however, no difference was observed between N- and C- terminal tagged isoforms, implying that the FLAG tag doesn't block the proper functioning of any ER-targeting signal peptide present in the FAM134B protein or doesn't interfere with the overall folding pattern of the protein to the extent at which it changes its final sub-cellular destination.

Another interesting detail was the observed molecular weights of the two FAM134B protein isoforms when they were ran through an SDS-Polyacrylamide gel. Whereas the predicted molecular weight of FAM134B isoform 1 is 55kD, the band it produced in the western blot represents (by comparison to the pre-stained molecular weight marker) a molecular weight of over 80 kDa. Likewise, FAM134B isoform 2 appeared to have a molecular weight of around 60 kDa, whereas its predicted molecular weight is only 39kDa. The FAM134B proteins in our over-expression vectors are FLAG-tagged; however, this huge discrepancy between the predicted and the observed molecular weights cannot be explained merely by the presence of such a small moiety as the FLAG tag. The 3X-FLAG tag that is present in our vectors is only 24 amino acids long, corresponding to a molecular weight of 2.7 kDa. This discrepancy between protein molecular weight and SDS-gel electrophoretic mobility can instead be explained by the possible presence of several protein modifications on FAM134B protein as predicted by protein analysis tools and databases. Post-translational modifications like acetylation, myristoylation and glycosylation could be adding an extra weight on the protein and also changing its migration pattern through an SDS-Polyacrylamide gel. A more plausible explanation is the presence of a high number of negatively charged residues on these protein isoforms. As mentioned earlier, the isoelectric points of these protein isoforms are around 4, which make them unusually acidic. Already carrying an excess negative charge, it maybe the case that these protein isoforms cannot bind SDS

under the SDS-PAGE conditions and thus, their electrophoretic mobilities can only determined by their electrostatic charge and hydrodynamic properties (Garcia-Ortega L. *et al.*, 2005).

As a next step, we established stable cell lines that express FAM134B isoforms. Unfortunately, no positive clones could be obtained that stably over-express the C-terminal FLAG-tagged FAM134B isoform 2. Of the 20 clones tested, none gave a positive band in the western blot experiment performed with FLAG antibody. We suspected whether there was something wrong with the construct that we had generated. However, this was unlikely as all constructed vectors were verified through sequencing. Moreover, this construct was used in the transient transfection studies of Huh7 cells and produced positive staining in the FLAG-calnexin-co-immuno-fluoresence experiment as seen in Figure 4.21. Since stable over-expression clones could be obtained with all the remaining constructs, this ruled out any possibility that FAM134B over-expression was potentially growth restraining and thus was not tolerated by Huh7 cells. Possibly, the lack of any positive clones in the 20 clones tested was a pure event of luck, meaning that positive clones could be identified if more clones were picked and tested. Another possible explanation is that the vector was probably stably integrated into the genomes of some of the tested clones; however, since the transfected plasmids were delivered in circular format, the integrity of this specific plasmid was disrupted inside the cells so that it failed to express the desired protein. This problem could be counter-acted by delivering the plasmid in an appropriately pre-linearized format. However, due to time constraints, the experiments were carried out with the positive clones that were already established.

Next, prior to any functional studies, the monoclonality of the stable Huh7 FAM134B over-expression clones was checked because working with polyclonal cells could deviate our results. To test this, we performed FLAG immuno-peroxidase staining on the clones and observed that all of them displayed 100% positive staining pattern, a hallmark of monoclonal cells. In this staining experiment, it was apparent that although all cells expressed the FAM134B protein, some cells expressed it strongly while others expressed it

more weakly. This difference doesn't reflect polyclonality of these cells but it's rather because the cells are not all in the same phase in their cell cycle. If the same staining was performed on previously synchronized cells, a more homogeneous staining pattern would be observed in terms of the intensity of the FAM134B expression signal.

In the SABG experiments that were carried out, it was observed that FAM134B protein over-expression does not induce senescence in Huh7 cells. This finding indicates that over-expressed FAM134B protein does not 'cause' immortal cells to revert to senescence merely by itself, but also does not rule out the possibility that this protein could still be important in the senescence program. The up-regulation of FAM134B in the senescent Huh7 clones in the study of Ozturk *et al.* (2005) compared to the immortal clones could be a 'consequence' of the initiated senescence program rather than its 'cause' and the FAM134B protein could still be performing an important function somewhere downstream in this program. Another possible explanation for no observation of increased senescence positivity in the stable FAM134B over-expression clones is that over-expression of a single protein may not be enough to initiate the senescence program and possible partners of FAM134B missing in our experimental system and other key players of senescence may be serving here as limiting factors.

Another observation made during the imaging of the FAM134B over-expression clones was that occasionally enlarged, flattened and multi-nucleated cells were seen but that such cells also appeared in the empty vector clones. This observation was also recorded for SABG positivity of the clones and both observations reflect the normal spontaneous senescence of Huh7 cells, reinforcing the conclusion that FAM134B over-expression does not have any 'causative' role in the initiation of the senescence program. Striking here was the extremely low number of green (SABG activity positive) cells detected, so low that it did not allow any proper quantification study. The low extent of SABG positivity in these clones stems from the fact that throughout the antibiotic-mediated colony selection process, we had specifically been selecting for proliferating clones and so that senescent clones were either eliminated from the

culture in time or that they were not preferred in the colony picking process because of their limited colony size (unless the over-expressed FAM134B protein had a strong senescence inducing capacity to make the majority of colonies senescent, which was not the case). To complement the SABG staining experiment, we also subjected the FAM134B over-expression clones to BrdU incorporation assay and found that FAM134B over-expression has no significant effect on cell proliferation rates. Taken together, these findings indicate that FAM134B over-expression does not induce immediate replicative senescence in Huh7 cells. If FAM134B over-expression clones are kept in cell culture for a year, however, theoretically SABG staining will display that spontaneous senescent cells appear more frequently.

The final set of experiments compared the responses of FAM134B over-expression clones and empty vector clones to ER-stress. In these experiments, we could not observe an overall effect of FAM134B over-expression on the response of Huh7 cells to ER-stress when induced through tunicamycin treatment. The over-expression of N-terminal FLAG-tagged FAM134B isoform 2 caused a slight increase in the sensitivity of Huh7 cells to tunicamycin, but this finding needs to be verified by further experiments. In many instances, deregulation of endoplasmic reticulum (ER) homeostasis has been correlated with pathologic states and particularly with cancer (Moenner M. *et al.*, 2007). Therefore, the increase in the sensitivity of this clone to ER-stress could mean that FAM134B isoform 2 signals downstream to a cell death pathway in case of too much ER stress and it provides tumor suppression through such a regulation of ER stability.

The lack of any change in the overall response of FAM134B over-expressing Huh7 cells to ER-stress could be a true finding or it could stem from the nature of the agent, tunicamycin, used for induction of ER-stress in our experimental system. Since tunicamycin is an antibiotic that induces ER stress through prevention of formation of N-acetylglucosamine lipid intermediates and glycosylation of newly synthesized glycoproteins and that among the few number of motifs that are predicted in protein databases for FAM134B are three N-glycosylation sites, there is the possibility that this antibiotic may be affecting

the proper folding and final maturation of the FAM134B protein itself. This would imply that a high amount of immature FAM134B protein would be synthesized by ribosomes but these proteins would fail to become mature, functional FAM134B proteins since they would lack the required post-translational modifications. Therefore, if this were the case, it would not be possible to test the true effect of FAM134B over-expression on ER-stress induced through tunicamycin since the protein would not be functional in cells. To overcome such a potential limitation, the effect of FAM134B over-expression on the response of Huh7 cells to ER stress could be tested by employing other known ER-stress inducers that have a less dramatic effect on ER and that act through rather more indirect ways. Unless these additional experiments prove otherwise, the possibility that FAM134B protein isoforms are employed in tumor suppression through the maintenance of ER stability still exists.

One interesting aspect of our findings is that FAM134B protein isoforms do not possess any known ER localization sequences *per se*, yet they can successfully be imported into the ER, probably into the ER membrane, to be more specific. This implies that these protein isoforms employ alternative ways for their intra-cellular import. A search for proteins that can locate to the ER without a signal peptide sequence returned a protein family named 'Reticulon family'. This family of proteins have been shown to associate with the ER membrane through a motif called a 'reticulon motif'. Reticulon motif contains two large hydrophobic regions separated by a 66 residue hydrophilic segment. The hydrophobic portions are supposed to be membrane-embedded and the hydrophilic 66 residue localized to the lumenal/extracellular face of the membrane, acting as a loop in between the two transmembrane domains. (Van de velde HJ. *et al*., 1994; Roebroek AJ. *et al*., 1996; Roebroek AJ. *et al*., 1998; GrandPre T. *et al*., 2000). A single reticulon homology domain (RHD) hydrophobic region was shown to be sufficient to target an enhanced green fluorescent protein–reticulon fusion protein to the ER, wheras deletion of the RHD abolished association with the ER (Chen MS. *et al*., 2000; Iwahashi J. *et al*. 2007).

Interstingly, reticulon motif was predicted by MotifScan in the protein sequence of FAM134B protein isoform 1, and also predicted by KEGG SSDB when searched among Pfam domains. This predicted motif appears to span the protein from amino acid number 82 to amino acid number 279, as shown in Figure 5.1.

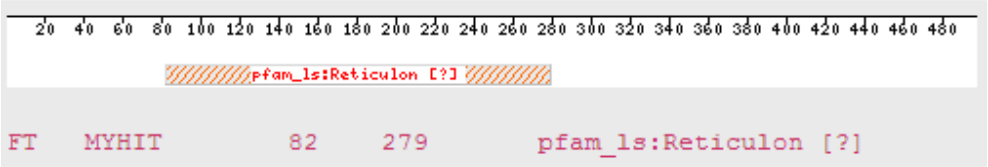

Figure 5.1: MotifScan prediction of 'reticulon motif'on FAM134B isoform 1 protein sequence.

The extent of homology between reticulon motif and the 82-279 amino acid region of FAM134B isoform is not very strong. The e-value of the alignment as predicted by MotifScan is 0.0015. Although much amino acid identity has been lost over the course of evolution, the overall structure of the reticulon homology domain has been preserved from plants to yeasts to humans. This suggests that three-dimensional protein structure is of greater importance than individual residues for reticulon homology domain function (Yang Y. and Strittmatter SM., 2007). Therefore, the reticulon homology motif predicted in FAM134B isoform 1 sequence may be a true and functional motif, even though it does not display exact sequence conservation with the hyper-conserved residues within the reticulon homology domain. Figure 5.2 illustrates an alignment between the 82-279 amino acid region of human FAM134B isoform 1 and a selection of vertebrate reticulons from rat, mouse, human and also a reticulon from C.elegans.

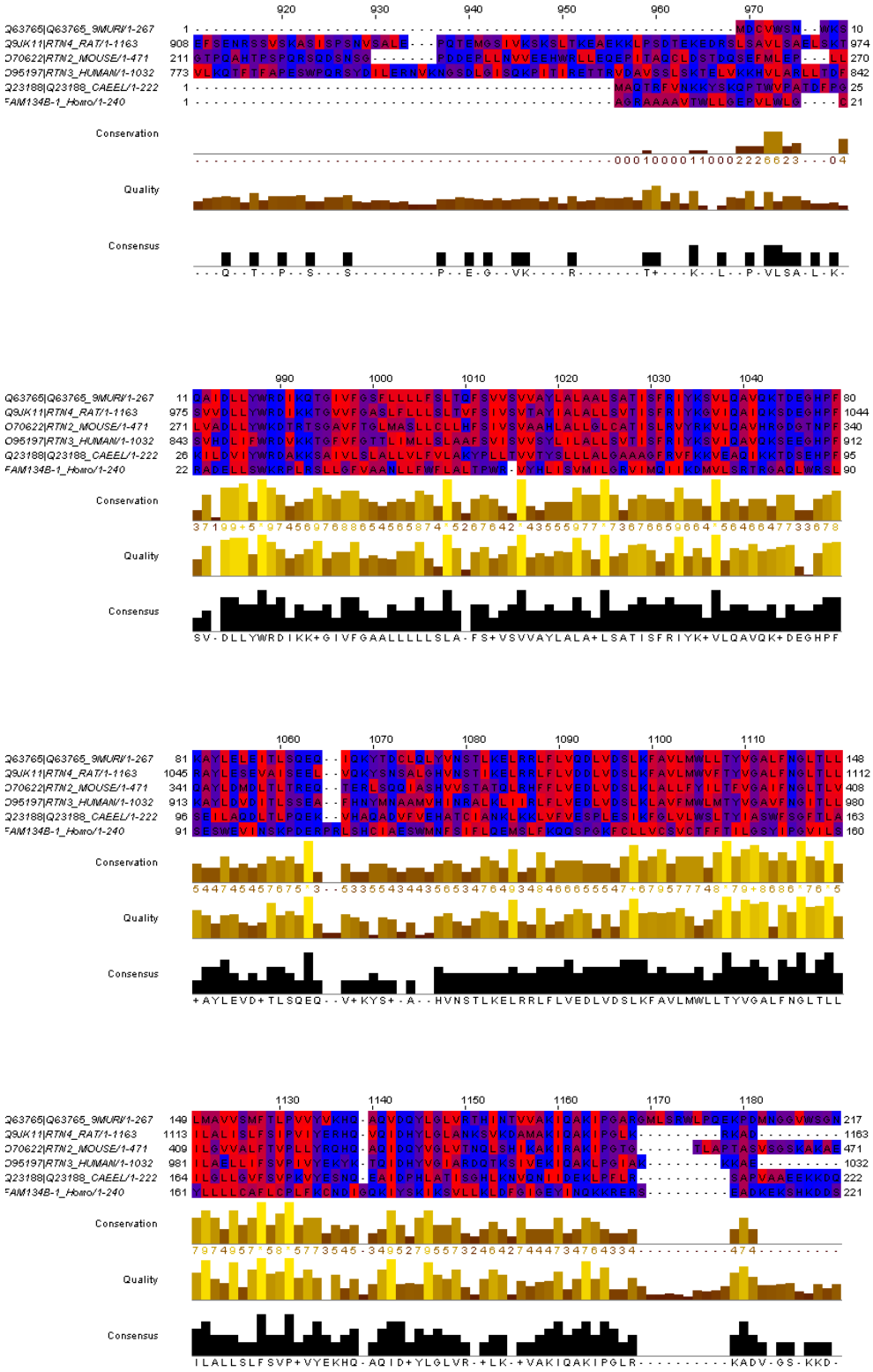

Figure 5.2: The ClustalW 2.0.8 multiple sequence alignment of vertebrate reticulons and FAM13B isoform 1 predicted reticulon homology domain.

In this alignment, the amino acid residues have been coloured by their hydrophobicity, where hydrophobic residues are coloured with red and hydrophilic residues are coloured with blue. This allows to visualize the first hydrophobic (red) region which shows a high degree of conservation and corresponds to the first transmembrane region, followed by the hydrophilic (blue) region which shows a low degree of conservation and corresponds to the loop region and finally the second hydrophobic (red) region which shows a very high degree of conservation and corresponds to the second transmembrane domain. This is in agreement with the information that across phyla, the second hydrophobic region of the reticulon homology domain is the most highly conserved, followed by the first hydrophobic region, with the carboxy terminus the least conserved (Yan R. *et al.*, 2006). Reticulon motif is located at the very C-terminus of reticulon family of proteins. FAM134B isoform 1 differs from the reticulon family in this respect, as the reticulon motif is located rather closer to the N-terminus, between amino acids 82 and 279 of the full-length 497 amino acid sequence (Figure 5.2).

Since the alternatively spliced form FAM134B isoform 2 lacks the initial 141 amino acids of FAM134B isoform 1, it does not possess the entire RHD domain. It contains only the second hydrophobic region of the RHD domain and it is predicted as a single-pass transmembrane protein. In our experiments, it was shown that this isoform localizes to the ER as well, indicating that the single hydrophobic region of the RHD domain is sufficient to embed this isoform into the ER membrane.

In an attempt to verify the membrane association of the potential RHD predicted on FAM134B isoforms, we used the DAS transmembrane prediction server (Cserzo M. *et al.*, 1997) publicly available at *http://www.sbc.su.se/~miklos/DAS/* and determined the overall hydrophobic properties of both FAM134B isoform 1 and isoform 2. These hydrophobicity plots are given in Figure 5.3:

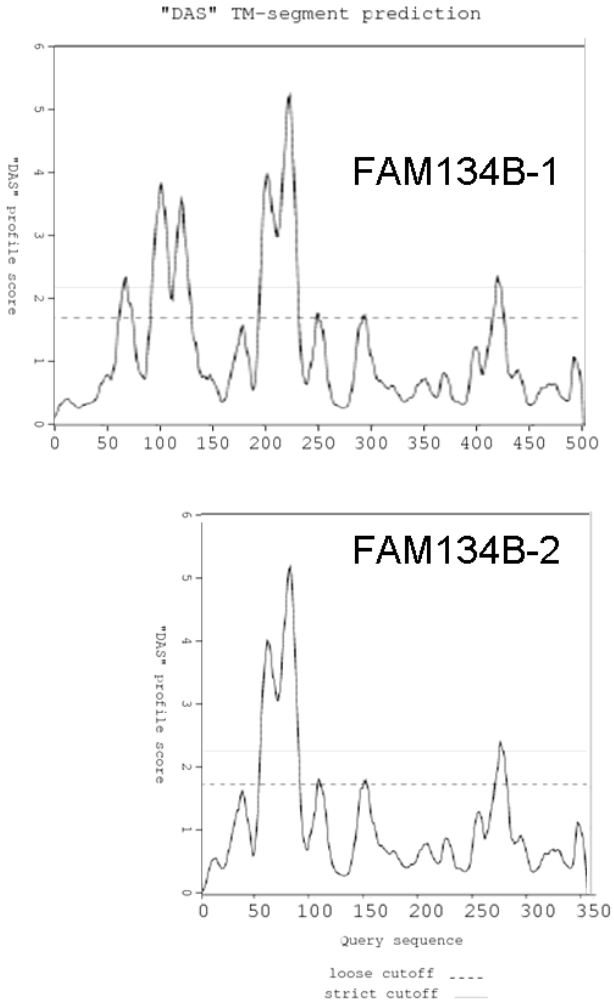

Figure 5.3: Predicted hydrophobicity plots of FAM134B isoform 1 and isoform 2. The x-axis represents the amino acid residues in the protein sequences. The y-axis represents each residue's probability of being embedded in the membrane or its hydrophobicity. The dashed line and the straight line are loose and strict cutoffs, respectively.

The hydrophobicity plots given above indicate that FAM134B isoform 1 has two hydrophobic regions, the amino acid positions of which correspond to the predicted reticulon motif. The plot given for FAM134 isoform 2 illustrates that this isoform possesses a single hydrophobic region, which corresponds to the second hydrophobic region of the reticulon homology domain. It is clear from the two plots that the two isoforms differ in their hydrophobicity at their N-terminus sequence, where they are alternatively spliced from a common mRNA, and they are totally identical starting form amino acid number 151 in isoform 1 and amino acid number 11 in isoform 2.

The membrane topologies of reticulon proteins are so far only partially defined. In parallel to this partial information, we predicted the membrane topologies of FAM134B isoform 1 and isoform 2. These predicted topologies are given in Figure 5.4:

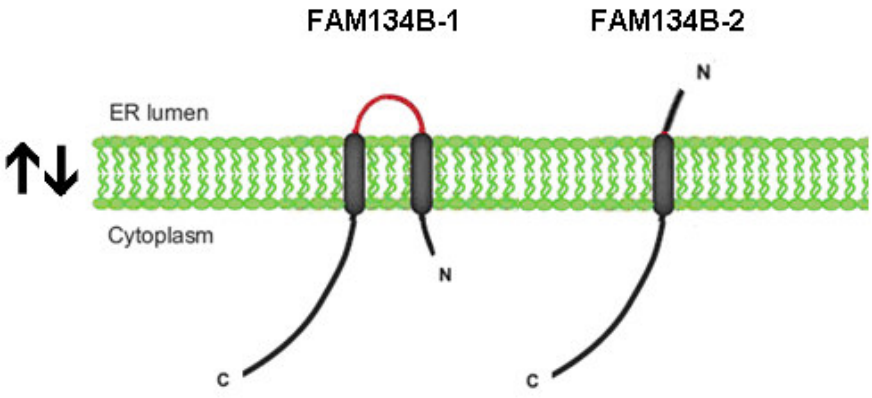

Figure 5.4: Possible membrane topologies of FAM134B isoform 1 and isoform 2.
The double arrows mean that ER lumen and cytoplasm can switch places, indicating that there are actually two conformations possible for each isoform. The illustration has been modified from Yang YS. and Strittmatter SM. (2007).

It is also noteworthy to mention that isoelectric points of reticulon family of proteins are around 4, meaning that, like the FAM134B protein isoforms, they are unusually acidic. Another similarity between reticulon family of proteins and FAM134B protein is that both are alternatively spliced, generating multiple isoforms with different N-terminal sequences and identical C-terminal sequences. In contrast to the highly conserved carboxy terminal RHD, the amino-terminal regions of reticulons display no sequence similarity at all, even among paralogs within the same species. The divergent reticulon amino-terminal domains appear to carry out species-and cell-specific roles, whereas the RHD may carry out more basic cellular functions (Yan R. *et al*., 2006).

The functional motif of reticulon proteins is the reticulon motif (Oertle T. *et al,* 2003). There is growing evidence that reticulons are involved in bending and shaping of the ER membrane, in trafficking of material from the ER to the Golgi apparatus, and in apoptosis. Reticulons interact with proteins involved in

vesicular formation and fusion such as SNAREs and SNAPs, pointing to a role in intracellular trafficking (Yang YS. and Strittmatter SM., 2007). Reticulon 1C (RTN1C) was found to inhibit Bcl-X_L and reticulon 4A (RTN4A) was found to inhibit both Bcl-X_L, and another apoptosis inhibitor, Bcl-2, demonstrating a pro-apoptotic role for reticulons (Tagami S. *et al.*, 2000). Furthermore, reticulon 3 (RTN3) was shown to mediate Bcl-2 accumulation in mitochondria and its expression was shown to be up-regulated in response to endoplasmic stress (Wan Q. *et al.*, 2007). The reticulon gene family is based on a cellular component ontology i.e. proteins are considered to be members of the family if they contain at least part of an identifiable reticulon homology domain (Oertle T. *et al,* 2003). Since FAM134B isoform 1 contains such a homology domain, it can be speculated that FAM134B is employed in cellular functions similar to those attributed to reticulons. Roles in apoptosis and maintenance of ER stability have already been proposed for FAM134B based on the results of this study. Whether FAM134B is involved in such functions and whether it can be classified as a novel reticulon family member can only be concluded in the light of additional biological evidence.

All in all, our results shed light on many aspects of the novel FAM134B protein and provide the first evidence that both isoforms of this protein localize to the Endoplasmic Reticulum. The up-regulation of FAM134B expression upon the initiation of the senescence program in Huh7 cells has been described for the first time in our study, adding to the chains of indirect evidence reported for the expression changes of FAM134B in numerous micro-array studies mentioned earlier in the text. The expression levels of FAM134B protein isoforms have been checked in several HCC and breast cell lines and mouse tissues and the function of FAM134B protein has been tested through several experiments in the stable over-expression clone system, making this the only study that ever focuses on the characterization of both isoforms of FAM134B protein. Our results are important in terms of addressing and understanding the basic differences between the senescent and immortal Huh7 clones, which need to be worked out in detail before they can be manipulated for designing therapeutic applications of senescence programming in HCC.

CHAPTER 6. FUTURE PERSPECTIVES

Our work has identified FAM134B as a senescence up-regulated gene encoding two ER protein isoforms. As a short-term follow-up of our study, experiments that should be performed for confirmation of preliminary data are summarized below:

- Firstly, verification of the ER localization of FAM134B protein isoforms is required. This can be done by performing ER fractionation on FAM134B over-expression clones, followed by anti-FLAG western blotting on the ER fraction.

- For confirmation of the ER localization, tracking of the endogenous protein is also a necessity. FAM134B antibody is now commercially available and it can be used in immuno-fluorescence or immuno-peroxidase experiments to track the exact sub-cellular localization of FAM134B protein isoforms.

- Our findings on the response of Huh7 cells over-expressing FAM134B isoforms to ER-stress need to be confirmed. Due to the direct and drastic affects of tunicamycin on protein modification and maturation, the ER-stress experiments need to be repeated with other stress inducers such as MG132 (a proteasome inhibitor), methanesulfonic acid methyl ester (MMS) (a DNA alkylating agent), A23187(an ER Ca^{2+}-ATPase inhibitor) or thapsigargin (a lumenal Ca^{2+} mobilizing agent).

- The functional tests performed with FAM134B over-expression clones need to be checked with FAM134B shRNA-mir down-regulation clones.

The long-term follow- up experimental strategy to be taken for this work is summarized below:

- The apparent tumor-suppressor features of FAM134B in HCC can be checked by testing the expression of FAM134B isoforms in HCC tumors and adjacent non-tumor tissues.

- Since the functions of FAM134B isoforms have yet not been assessed, additional functional assays for detecting altered growth characteristics *in vitro* of tumor features can be performed and the results from over-expression and control clones can be compared. These assays include, but are not limited to, anchorage-independent growth assay as colony formation in soft agar and contact inhibition growth assay as foci formation.

- The *in vivo* tumorigenicity of FAM134B over-expression can be assessed by injection of over-expression and control clones into nude mice.

- Possible protein partners of FAM134B protein isoforms can be identified by performing an IP (immuno-precipitation) or a Yeast-2-hybrid assay

- The existence of the predicted transmembrane domains, motifs and modification sites can be verified by using deletion and point mutation constructs and modification-specific antibodies

- FAM134B was shown to be re-activated in invasive cervical cancer cell lines in response to treatment with 5-aza-2'-deoxycytidine and trichostatin A (Sova P. *et al.*, 2006). Whether this possible epigenetic control mechanism of

FAM134B expression exists also in the liver cancer cell line system can be checked.

- In one microarray study, the expression of FAM134B was shown to be significantly up-regulated in response to estradiol in MDA-MB-231 cells that have been engineered to re-express ER-alpha. Furthermore, through *in silico* analysis, three putative ERE (Estrogen Response Element) motifs were identified in the promoter of FAM134B (Moggs JG. *et al.*, 2005). The response of FAM134B expression to estradiol in the breast cancer cell line system can be studied in detail and the existence of these putative ERE sites can be tested by deletion constructs.

REFERENCES

American Cancer Society. Cancer Facts and FIGS (2005). *American Cancer Society* [online], http://www.cancer.org/docroot/home/index.asp

Adams LA. and Angulo P. (2005) Recent concepts in nonalcoholic fatty liver disease. *Diabet. Med.* **22**, 1129–1133

Aguilar F., Harris CC., Sun T., Hollstein M. and Cerutti P. (1994) Geographic variation of p53 mutational profile in nonmalignant human liver. *Science* **264**, 1317–1319

Anthony P. in *Pathology of the Liver* (eds MacSween R., Burt A., Portmann B., Ishak K., Scheuer P., Anthony P.) 711–775 (Churchill Livingstone, London, New York, Sydney, Toronto, 2002).

Badvie S. (2000) Hepatocellular carcinoma. *Postgrad. Med.J.* **76**, 4–11

Bairoch A. and Apweiler R. (1998) The SWISS-PROT protein sequence data bank and its supplement TrEMBL in 1998. *Nucleic Acids Res.* **26**:38-42

Ben-Porath I., Weinberg RA. (2004) When cells get stressed: an integrative view of cellular senescence. *J Clin Invest* **113**(1):8-13

Bergsland EK. (2001) Molecular mechanisms underlying the development of hepatocellular carcinoma. *Semin Oncol* **28**: 521-531

Block TM., Mehta AS., Fimmel CJ., Jordan R. (2003) Molecular viral oncology of hepatocellular carcinoma. *Oncogene* **22**:5093-5107

Blum Hubert E. (2005) Hepatocellular carcinoma: Therapy and prevention. *World J Gastroenterol* **11**(47) :7391-7400

Braig M., Lee S., Loddenkemper C., Rudolph C., Peters AH., Schlegelberger B., Stein H., Dorken B., Jenuwein T., Schmitt CA. (2005) Oncogene-induced senescence as an initial barrier in lymphoma development. *Nature* **436**(7051):660-665.

Brechot C. (2004) Pathogenesis of hepatitis B virus-related hepatocellular carcinoma: old and new paradigms. *Gastroenterology* **127**: S56-61

Bressac B., Galvin K. M., Liang TJ., Isselbacher KJ., Wands JR., Ozturk M. (1990) Abnormal structure and expression of p53 gene in human hepatocellular carcinoma. *Proc. Natl. Acad. Sci. USA* **87,** 1973–1977.

Bressac B., Kew M., Wands J. & Ozturk M. (1991) Selective G to T mutations of p53 gene in hepatocellular carcinoma from southern Africa. *Nature* **350**, 429–431

Cagatay T, Ozturk M. 2002. P53 mutation as a source of aberrant beta-catenin accumulation in cancer cells. *Oncogene* **21**:7971-80

Campisi J. (2005) Senescent cells, tumor suppression, and organismal aging: good citizens, bad neighbors. *Cell* **120**(4):513-522

Campisi J. (2005) Suppressing cancer: the importance of being senescent. *Science* **309**(5736)**:**886-887.

Campisi J. (2008) New tricks for dealing with old cells? Poster abstract from *Understanding Aging: Biomedical and Bioengineering Approaches* Conference on June 27-29, 2008 at UCLA.

Chen MS., Huber AB., van der Haar ME., Frank M., Schnell L., Spillmann AA., Christ F., Schwab ME. (2000) Nogo-A is a myelin-associated neurite outgrowth inhibitor and an antgigen for monoclonal antibody IN-I. *Nature* **403**:434-439

Chen X. *et al*. (2002) Gene expression patterns in human liver cancers. *Mol. Biol. Cell* **13**(6):1929-39

Chen Z., Trotman LC., Shaffer D., Lin HK., Dotan ZA., Niki M., Koutcher JA., Scher HI., Ludwig T., Gerald W., Cordon-Cardo C., Pandolfi PP. (2005) Crucial role of p53-dependent cellular senescence in suppression of Pten-deficient tumorigenesis. *Nature* **436**(7051)**:**725-730.

Chisari FV. (2005) Unscrambling hepatitis C virus-host interactions. *Nature* **436**, 930–932

Bowen DG. & Walker CM. (2005) Adaptive immune responses in acute and chronic hepatitis C virus *Nature* **436**, 946–952

Collado M., Gil J., Efeyan A., Guerra C., Schuhmacher AJ., Barradas M., Benguria A., Zaballos A., Flores JM., Barbacid M., Beach D., Serrano M. (2005) Tumour biology: senescence in premalignant tumours. *Nature* **436**(7051):642

Combet C., Blanchet C., Geourjon C. and Deléage G. (2000) NPS@:Network Protein Sequence Analysis *TIBS 25, No 3* **291**:147-150

Crosti P., Malerba M., Bianchetti R. (2001) Tunicamycin and Brefeldin A induce in plant cells a programmed cell death showing apoptotic features. *Protoplasma* **216**, 31-8

Cserzo M., Wallin E., Simon I., von Heijne G., Elofsson A. (1997) Prediction of transmembrane alpha-helices in procariotic membrane proteins: the Dense Alignment Surface method. *Prot. Eng.* **10**(6):673-676

Dawson RMC., Elliot DC., Elliot WH., Jones KM. (1986) Data for Biochemical Research, 3rd ed., p. 335., *Oxford University Press,* New York

Delom F., Emadali A., Cocolakis E., Lebrun JJ., Nantel A., Chevet E. (2007) Calnexin-dependent regulation of tunicamycin-induced apoptosis in breast carcinoma MCF-7 cells. *Cell Death & Diff.* **14**:586-96

Dimri GP. (2005) What has senescence got to do with cancer? *Cancer Cell* **7**:505-12

Duret L., Perrière G. and Gouy M. (1999)HOVERGEN: database and software for comparative analysis of homologous vertebrate genes. *In Bioinformatics Databases and Systems*, Letovsky, S. (ed.), Kluwer Academic Publishers, Boston, pp. 13-29.

Edmondson HA., Peters RL. (1983) Tumors of the liver: pathologic features. *Semin Roentgenol.* **18**:75-83

El-Serag HB., Tran T., Everhart JE. (2004) Diabetes increases the risk of chronic liver disease and hepatocellular carcinoma. *Gastroenterology* **126**:460–468

Encyclopædia Britannica. Retrieved July 10, 2008, from Encyclopædia Britannica Online: http://www.britannica.com/EBchecked/topic/479680/protein

Falquet L., Pagni M., Bucher P., Hulo N., Sigrist CJ., Hofmann K., Bairoch A. (2002) The PROSITE database, its status in 2002. *Nucleic Acids Res.* **30**:235-238

Farazi PA., DePinho RA.. (2006) Hepatocellular carcinoma pathogenesis: from genes to environment. *Nat Rev Cancer* **6**:674-687

Farrell GC. and Larter CZ. (2006) Nonalcoholic fatty liver disease: from steatosis to cirrhosis. *Hepatology* **43**:S99–S112

Fujita E., Jimbo A., Isoai A., Maruyama K., Momoi T. (2002) Caspase-12 processing and fragment translocation into nuclei of tunicamycintreated cells. *Cell Death Differ.* **9**: 1108-14

Garcia-Ortega L., De Los Rios V., Martinez-Ruiz A., Onaderra M., Lacadena J. ; Martinez Del Pozo A.; Gavilanes JG. (2005) Anomalous electrophoretic behavior of a very acidic protein : Ribonuclease U2. *Electrophoresis* **26**(18):3407-3413

GrandPre T., Nakamura F., Vartanian T., Strittmatter SM. (2000) Identification of the Nogo inhibitor of axon regeneration as a Reticulon protein. *Nature* **403**:439-444

Guermeur Y., Geourjon C., Gallinari P., Deleage G. (1999) Improved Performance in Protein Secondary Structure Prediction by Inhomogeneous Score Combination. *Bioinformatics* **15**(5):413-421

Hannemann J., Velds A., Halfwerk JBG., Kreike B., Peterse JL, van de Vijver MJ. (2006) Classification of ductal carcinoma *in situ* by gene expression profiling. *Breast Cancer Res.* **8**(5)

Heifetz A., Keenan RW., Elbein AD. (1979) Mechanism of action of tunicamycin on the UDP -GlcNAc: dolichylphosphate transferase. *Biochem.*, **18**:2186-92

Herbig U., Sedivy JM. (2006) Regulation of growth arrest in senescence: telomere damage is not the end of the story. *Mech Ageing Dev* **127**(1):16-24.

Hoek K., Rimm DL., Williams KR., Zhao H., Ariyan S., Lin A., Kluger HM., Berger AJ., Cheng E., Trombetta ES., Wu T., Niinobe M., Yoshikawa K.,

Hannigan GE., Halaban R. (2004) Expression profiling reveals novel pathways in the transformation of melanocytes to melanomas. *Cancer Res.* **64**(15):5270-82

Hsu I. C. *et al.* (1991)Mutational hotspot in the p53 gene in human hepatocellular carcinomas. *Nature* **350**:427–428

International Human Genome Sequencing Consortium (2004) Finishing the euchromatic sequence of the human genome. *Nature* **431**(7011):931-945

Iwahashi J., Hamada N., Watanabe H. (2007) Two hydrophobic segments of the RTN1 family determine the ER localization and retention. *Bichem Biophys Res Commun.* **355**:508-512

Ji C., Kaplowitz N. (2006) ER stress: Can the liver cope? *Journal of Hepatology* **45**:321–333

Jou *et al.* (2007) OncoDB.HCC: an integrated oncogenomic database of hepatocellular carcinoma revealed aberrant cancer target genes and loci. *Nucleic Acids Research* **35** (Database issue):D727-D731

Kanehisa M. *et al.* (2004) The KEGG resource for deciphering the genome. *Nucleic Acids Research* **32**(Database issue):D277-80

Kaufman RJ. (1999) Stress signaling from the lumen of the endoplasmic reticulum: coordination of gene transcriptional and translational controls. *Genes Dev.* **13:**1211–1233

King RD., Sternberg MJ. (1996) Identification and application of the concepts important for accurate and reliable protein secondary structure prediction. *Protein Sci.* **5**(11):2298-310

Kluger HM., Chelouche Lev D., Kluger Y., McCarthy MM., Kiriakova G., Camp RL., Rimm DL., Price JE. (2005) Using a xenograft model of human breast cancer metastasis to find genes associated with clinically aggressive disease. *Cancer Res.* **65**(13):5578-87

Kokame K., Kato H., Miyata T. (2001) Identification of ERSE-II, a new cis-acting element responsible for the ATF6-dependent mammalian unfolded protein response. *J. Biol. Chem.* **276**:9199–9205

Kubica S., Trauwein C., Niehof M., Manns M. (1997) Target gene modulation in hepatocellular carcinomas by decreased DNA-binding of p53 mutations. *Hepatology* **25:**867–873

Lavanchy D. (2004) Hepatitis B virus epidemiology, disease burden, treatment, and current and emerging prevention and control measures. *J. Viral. Hepat.* **11**:97–107

Libbrecht L., Desmet V., Roskams T. (2005) Preneoplastic lesions in human hepatocarcinogenesis. *Liver Int* **25**:16-27

Limdi JK. and Crampton JR. (2004) Hereditary haemochromatosis. *Qjm* **97**:315–324

Marrogi AJ. *et al*. (2001) Oxidative stress and p53 mutations in the carcinogenesis of iron over load-associated hepatocellular carcinoma. *J. Natl Cancer Inst.* **93**:1652–1655

McMillan DR., Gething MJ., Sambrook J. (1994) The cellular response to unfolded proteins: intercompartmental signaling. *Curr. Opin. Biotechnol.* **5:**540–545

Michaloglou C., Vredeveld LC., Soengas MS., Denoyelle C., Kuilman T., van der Horst CM., Majoor DM., Shay JW., Mooi WJ., Peeper DS. (2005) BRAFE600-associated senescence-like cell cycle arrest of human naevi. *Nature* **436**(7051)**:**720-724

Mishra G. *et al.* (2006) Human Protein Reference Database - 2006 Update. *Nucleic Acids Research* **34**:D411-D414.

Moenner M., Pluquet O., Bouchecareilh M., Chevet E. (2007) Integrated Endoplasmic Reticulum Stress Responses in Cancer. *Cancer Res.* **67**(22):10631–4

Moggs JG., Murphy TC., Lim FL., Moore DJ., Stuckey R., Antrobus K., Kimber I., Orphanides G. (2005) Anti-proliferative effect of estrogen in breast cancer cells that re-express ERalpha is mediated by aberrant regulation of cell cycle genes. *J Mol Endocrinol.* **34**(2):535-51

Mori K. (2000) Tripartite management of unfolded proteins in the endoplasmic reticulum. *Cell* **101:**451–454

Nakagawa T., Zhu H., Morishima N., Li E., Xu J., Yankner B. A., and Yuan J. (2000) Caspase-12 mediates endoplasmic-reticulum-specific apoptosis and cytotoxicity by amyloid-beta. *Nature* **403:**98–103

Narita M., Lowe SW. (2005) Senescence comes of age. *Nat Med* **11**(9)**:**920-922

Oertle T., Klinger M., Stuermer CA., Schwab ME. (2003) A reticuolar rhapsody: phylogenetic evolution and nomenclature of the RTN/Nogo gene family. *Faseb Journal* **17**(10): 1238

Okuda K. (2000) Hepatocellular carcinoma. *J. Hepatol.* **32**:225–237

Oshimure M., Barrett JC. (1997) Multiple pathways to cellular senescence : Role of telomerase repressors. *European Journal of Cancer* **33**(5):710-715

Osna NA., Clemens DL. and Donohue TM., Jr. (2005) Ethanol metabolism alters interferon-gamma signaling in recombinant HepG2 cells. *Hepatology* **42**:1109–1117

Ozturk M. (1991) p53 mutation in hepatocellular carcinoma after aflatoxin exposure. *Lancet* **338**:1356–1359

Ozturk M. (1999) Genetic aspects of hepatocellular carcinogenesis. *Semin Liver Dis* **19**: 235-242

Ozturk N., Erdal E., Mumcuoglu M., Akcali KC., Yalcin O., Senturk S., Arslan-Ergul A. *et al.* (2005) Reprogramming of replicative senescence in hepatocellular carcinoma-derived cells. *PNAS* **103**(7):2178–2183

Parfrey H., Mahadeva R., Lomas DA. (2003) (1)-antitrypsin deficiency, liver disease and emphysema. *Int. J. Biochem. Cell Biol.* **35**:1009–1014

Postigo A.A., Depp JL., Taylor JJ., Kroll KL. (2003) Regulation of Smad signaling through a differential recruitment of coactivators and corepressors by ZEB proteins. *EMBO J.* **22:**2453–2462

Puisieux A, Lim S, Groopman J, Ozturk M. (1991). Selective targeting of p53 gene mutational hotspots in human cancers by etiologically defined carcinogens. *Cancer Research* **51**:6185-9

R Development Core Team (2008) R: A Language and Environment for Statistical Computing R Foundation for Statistical Computing, Vienna, Austria. ISBN: 3-900051-07-0, http://www.R-project.org

Ramilo O., Allman W., Chung W., Mejias A., Ardura M., Glaser C., Wittkowski KM., Piqueras B., Banchereau J., Palucka A.K., Chaussabel D. (2007) Gene expression patterns in blood leukocytes discriminate patients with acute infections. *Blood* **109**(5): 2066–2077

Rebhan M., Chalifa-Caspi V., Prilusky J., Lancet D. GeneCards: integrating information about genes, proteins and diseases. (1997) *Trends in Genetics* **13**: 163

Rebhan M., Chalifa-Caspi V., Prilusky J., and Lancet D. (1998) GeneCards: A novel functional genomics compendium with automated data mining and query reformulation support. *Bioinformatics* **14**: 656-664

Rhodes DR. *et al* (2004) ONCOMINE: a cancer microarray database and integrated data-mining platform. *Neoplasia* **6**:1-6

Rost B., Sander C. (1994) Combining evolutionary information and neural networks to predict protein secondary structure. *Proteins* **19**(1):55-72

Roebroek AJ., Ayoubi TA., Van de Velde HJ., Schoenmakers EF., Pauli IG., Van de Ven WJ. (1996) Genomic organization of the human NSP gene, prototype of a novel gene family encoding reticulons. *Genomics* **32**:191-199

Roebroek AJ., Contreras B., Pauli IG., Van de Ven WJ. (1998) cDNA cloning, genomic organization, and expression of the human RTN2 gene, a member of a gene family encoding reticulons. *Genomics* **51**:98-106

Roncalli M., Bianchi P., Bruni B., Laghi L., Destro A., Di Gioia S., Gennari L., Tommasini M., Malesci A., Coggi G. (2002) Methylation framework of cell cycle gene inhibitors in cirrhosis and associated hepatocellular carcinoma. *Hepatology* **36:**427–432

Ruan *et al.* (2008) Tree display perl modules by Li Heng. TreeFam: 2008 Update. *Nucleic Acid Res.* **36** (Database issue):D735-40

Safran M., Solomon I., Shmueli O., Lapidot M., Shen-Orr S., Adato A., Ben-Dor U., Esterman N., Rosen N., Peter I., Olender T., Chalifa-Caspi V., Lancet D. (2002) GeneCards 2002: towards a complete, object-oriented, human gene compendium. *Bioinformatics* **18(11)**: 1542-1543

Safran M., Solomon I., Shmueli O., Lapidot M., Shen-Orr S., Adato A., Ben-Dor U., Esterman N., Rosen N., Peter I., Olender T., Chalifa-Caspi V., Lancet D. (2002) GeneCards 2002: An Evolving Human Gene Compendium. *Proceedings of the IEEE Computer Science Bioinformatics Conference CSB2002*, p. 339

Sarkany RP. (2001) The management of porphyria cutaneatarda. *Clin. Exp. Dermatol*. **26**:225–232

Satyanarayana A, Manns MP., Rudolph KL. (2004) Telomeres and telomerase: a dual role in hepatocarcinogenesis. *Hepatology* **40**: 276-283

Schmutz,J., Martin,J., Terry,A., Couronne,O., Grimwood,J., Lowry,S., Gordon,L.A. *et al.* (2004) The DNA sequence and comparative analysis of human chromosome 5. *Nature* **431**(7006):268-274

Shamu C., Cox J., Walter P. (1994) The unfolded-protein-response pathway in yeast. *Trends Cell Biol.* **4:**56–60

Sharpless NE., DePinho RA. (2005) Cancer: crime and punishment. *Nature* **436**(7051)**:**636-637

Shay JW., Wright Woodring E. (2004) Senescence and immortalization: role of telomeres and telomerase. *Carcinogenesis* **26**(5):867-874

Shay JW., Bacchetti S. (1997). A survey of telomerase activity in human cancer. *Eur J Cancer* **33**:787-91

Sherman M. (2005) Hepatocellular carcinoma: epidemiology, risk factors, and screening. *Semin. Liver Dis.* **25**:143–154

Sherr CJ., McCormick F. (2002) The RB and p53 pathways in cancer. *Cancer Cell* **2**:103-112

Suriawinata A., Xu R. (2004) An update on the molecular genetics of hepatocellular carcinoma. *Semin Liver Dis* **24**: 77-88

Sherwood SW., Rush D., Ellsworth JL., Schmike R.T. (1988) Defining cellular senescence in IMR-90 cells: A flow cytometric analysis. *PNAS* **85**(23): 9086–9090

Sova P., Feng Q., Geiss G., Wood T., Strauss R., Rudolf V., Lieber A., Kiviat N. (2006) Discovery of novel methylation biomarkers in cervical carcinoma by global demethylation and microarray analysis. *Cancer Epidemiol Biomarkers Prev.* **15**(1):114-23

Su AI., Cooke MP., Ching KA., Hakak Y., Walker JR., Wiltshire T., Orth AP., Vega RG., Sapinoso LM., Moqrich A., Patapoutian A., Hampton GM., Schultz PG., Hogenesch JB. (2002) Large-scale analysis of the human and mouse transcriptomes. *PNAS* **99**(7) :4465-4470

Su AI., Cooke MP., Wiltshire T., Batalov S., Lapp H., Ching KA., Block D., Zhang J., Soden R., Hayakawa M., Kreiman G., Cooke MP., Walker JR., Hogenesch JB. (2004) A gene atlas of the mouse and human protein-encoding transcripts. *PNAS* **101**(16) :6062-6067

Tagami S., Eguchi Y., Kinsohita M., Takeda M., Tsujimoto Y. (2000) A novel protein, RTN-XS, interacts with both Bcl-XL and Bcl-2 on endoplasmic reticulum and reduces their anti-apoptotic activity. *Oncogone* **19:**5736-5746

Tang WK., Chui CH., Fatima S., Kok SH., Pak KC., Ou TM., Hui KS., Wong MM., Wong J., Law S., Tsao SW., Lam KY., Beh PS., Srivastava G., Chan AS., Ho KP., Tang JC. (2007) Oncogenic properties of a novel gene JK-I located in chromosome 5p and its over-expression in human esophageal squamous cell carcinoma. *Int J Mol Med.* **19**(6):915-23

Tanguay RM., Jorquera R., Poudrier J., St-Louis M. (1996) Tyrosine and its catabolites: from disease to cancer. *Acta Biochim. Pol.* **43**:209–216

Thompson JD., Higgins DG., Gibson TJ. (1994) CLUSTAL W: improving the sensitivity of progressive multiple sequence alignment through sequence weighting, position-specific gap penalties and weight matrix choice. *Nucleic Acids Res.* **22**(22):4673-4680

Thorgeirsson SS., Grisham JW. (2002) Molecular pathogenesis of human hepatocellular carcinoma. *Nat Genet* **31**: 339-346

Urano F., Wang X., Bertolotti A., Zhang Y., Chung, P., Harding H. P., Ron D. (2000) Coupling of Stress in the Endoplasmic Reticulum to Activation of JNK Protein Kinases by Transmembrane Protein Kinase IRE1 *Science* **287:**664–666

Van de velde HJ., Roebroek AJ., Senden NH., Ramaekers FC., Van de ven WJ. (1994) NSP-encoded reticulons, neuroendocrine proteins of a novel gene family associated with membranes of the endoplasmic reticulum. *J. Cell Sci.* **107**:2403-2416

Verschueren K., Remacle JE., Collart C., Kraft H., Baker BS., Tylzanowski P., Nelles L., Wuytens G., Su MT., Bodmer R. *et al.* (1999) SIP1, a novel zinc finger/homeodomain repressor, interacts with Smad proteins and binds to 5'-CACCT sequences in candidate target genes. *J. Biol. Chem.* **274:**20489–20498

Vichai V. and Kirtikara K. (2006) Sulforhodamine B colorimetric assay for cytotoxicity screening. *Nature Protocols* **1**:1112 - 1116

Volkmann M., Hofmann WJ., Muller M., Rath U., Otto G., Zentgraf H., Galle PR. (1994) p53 over-expression is frequent in European hepatocellular carcinoma and largely independent of the codon 249 hot spot mutation. *Oncogene* **9:**195–204.

Wan Q.; Kuang E.; Dong W.; Zhou S.; Xu H.; Qi Y.; Liu Y. (2007) Reticulon 3 mediates Bcl-2 accumulation in mitochondria in response to endoplasmic reticulum stress. *Apoptosis* **12** (2): 319-328

Wiemann SU., Satyanarayana A., Tsahuridu M., Tillmann HL., Zender L. *et al.* (2002) Hepatocyte telomere shortening and senescence are general markers of human liver cirrhosis. *Faseb J* **16**:935-42

Wilson BJ., Giguère V. (2008) Meta-analysis of human cancer microarrays reveals GATA3 is integral to the estrogen receptor alpha pathway. *Mol Cancer* **7**: 49

Wright LS., Li J., Caldwell MA., Wallace K., Johnson JA., Svendsen CN. (2003) Gene expression in human neural stem cells: effects of leukemia inhibitory factor. *J Neurochem.* **86**(1):179-95

Wurmbach E., Chen YB., Khitrov G., Zhang W., Roayaie S., Schwartz M., Fiel I., Thung S., Mazzaferro V., Bruix J., Bottinger E., Friedman S., Waxman S., Llovet JM. (2007) Genome-wide molecular profiles of HCV-induced dysplasia and hepatocellular carcinoma. *Hepatology* **45**(4):938-47

Yan R., Shi Q., Hu X., Zhou X. (2006) Reticulon proteins: emerging players in neurodegenerative diseases. *Cell Mol Life Sci.* **63**:877-889

Yang YS. and Strittmatter SM. (2007) The reticulons: a family of proteins with diverse functions. *Genome Biology* **8**:234

Yau C., Fedele V., Roydasgupta R., Fridlyand J., Hubbard A., Gray JW., Chew K., Dairkee SH., Moore DH., Schittulli F., Tommasi S., Paradiso A., Albertson DG., Benz CC. (2007) Aging impacts transcriptomes but not genomes of hormone-dependent breast cancers. *Breast Cancer Res.* **9**(5)

Yu MC., Yuan JM. (2004) Environmental factors and risk for hepatocellular carcinoma. *Gastroenterology* **127**: S72-78